Fatigue Damage Sensor

Improving fatigue lifetime predictions of aluminium high speed craft

J. C. C. de Korte

TU Delft

Fatigue Damage Sensor

Improving fatigue lifetime predictions of aluminium high speed craft

by

Jan Cornelis Coen de Korte

Performed at

Damen Shipyards Group

&

Faculty of Mechanical, Maritime and Materials Engineering, 3mE
Delft University of Technology
The Netherlands

to obtain the degree of

Master of Science
in Marine Technology

to be defended publicly at the Delft University of Technology on
Monday December 3, 2018 at 15:15.

Supervisor:	Prof. dr. ir. M. L. Kaminski,	TU Delft
Thesis committee:	Dr. ir. J. H. den Besten,	TU Delft
	Dr. ir. O. Morales Napoles,	TU Delft
	Ir. E. Huiskamp,	Damen Shipyards Group

This thesis is confidential and cannot be made public until December 3, 2023.

TU Delft

Abstract

At the Research & Development department of the Damen Shipyards Group, research is performed on six main topics: Mechanical Systems, Noise and Vibrations, Ship Structures, Hydromechanics, Human Factors and electrical & automation systems. In the ship structures section one of the main issues is improving the fatigue lifetime predictions of aluminium high speed craft. This research has two distinct components. One of them is the fatigue loading, for example the improvements on the prediction of operational profiles and wave conditions to be encountered during the lifetime of the vessel. The other part is to improve the fatigue resistance predictions of structural details. The ultimate goal of the fatigue research at Damen Shipyards is to build lighter ships in a responsible way.

The problem with fatigue research on board of ships is the time it takes before a structural detail fails. Ship and offshore structures are typically designed for a minimum lifetime of twenty years. Because of the built-in safety in the fatigue analyses, cracks are expected to occur even later than twenty years. One of the main reasons to start this research, was the demand for a low-cost and fast method to gain fatigue damage data from in-service high speed craft. Current feedback methods are expensive and cumbersome and can therefore not easily be used for a whole fleet.

The main goal of this research was to get early feedback on the fatigue damage in the aluminium high speed craft built by Damen Shipyards. Therefore an innovative sensor is developed during this research to indicate damage in the underlying structure in an accelerated manner. Using the knowledge on the total stress concept gathered in the development of this novel fatigue damage sensor, the feasibility and effects of implementing the total stress concept in Damen's fatigue prediction methods is studied. The totals stress concept developed by Henk den Besten in the VOMAS joint industry project captures the fatigue resistance of all aluminium welded joint details in one single SN curve: The fatigue master curve.

The main requirements for developing a novel fatigue sensor is that it should it give a mechanical output and have characteristics regarding fatigue damage mechanisms similar to aluminium welded joints. Since a mechanical output is required it should be able to operate effectively without electronics, and the output (cracked sensor) must be able to be translated to a remaining lifetime of a corresponding structural detail. After a number of concepts, the design shown in figure 5.16 is chosen because of its expected similarity with a double sided cruciform joint. Since the total stress concept is adopted one can, when fatigue resistance similarity is demonstrated with a double sided cruciform joint, translate this to any structural detail. To test the hypothesis of similarity between the fatigue resistance characteristics of the sensor and the total stress concept fatigue tests are performed at the TU Delft in the material science laboratory. The results of the experiments indicate that the fatigue resistance data of the sensor corresponds with the fatigue resistance described by the Random Fatigue Limit model from the Total Stress Concept. Simultaneous to the laboratory tests, the sensor is tested on full scale aboard the USCGC 'Bertholf'. Because the analysis of the previous tests on board of the 'Bertholf' showed that the encountered stresses are very low, the expectation was not that the sensor would fail within the period of this research. However the full scale trials are a good experiment to test the bonding method and the procedures involved in the installation and inspection of the sensor. The result after six months is that there did not occur a crack in the sensor and the adhesive layer was still intact. Finally a method is presented to calculate for a structural detail a probability of exceeding a certain lifetime based on a failed sensor. This is done by performing a Monte Carlo simulation to obtain the joint probability distribution of the sensor lifetime and the structural lifetime.

For the feasibility study on the implementation of the total stress concept at Damen, first the current practices are studied. It appeared that both for the loading and for the resistance, measures needed to be taken. Therefore a MATLAB script is made, where the total stress curve can be translated to a nominal stress based SN curve for any structural detail. There are different approaches possible regarding the total stress curve. After consideration the Random Fatigue Limit model is adopted as the most suitable option for design purposes. The study showed that by implementing the total stress concept, lifetime extensions of a factor ten can be reached, or corresponding section modulus reductions.

Preface

This research gave me the opportunity to learn more about fatigue and doing laboratory experiments. But it also taught me the importance of planning and keeping yourself motivated which is very important when you are working for nine months on a topic. In addition it gave me a nice view at Damen as a company.

The goals set at the start of this research would have been even more difficult to reach without the help and support of some people or companies. First I would like to thank Henk den Besten for his feedback, discussions and his sharing of knowledge about the subjects regarding my research during the progress meetings and for his help setting up the fatigue experiments. Secondly I owe a lot to my daily supervisor Ewoud Huiskamp from Damen Research, who was very much involved in this topic, gave great feedback and helped me a lot by showing me different points of view on the topic. I also have to thank Ton Riemslag of the material science lab, during the tests he pointed me on an important calibration error which I therefore could fix without having lost test results or delay in the process.

I am very grateful that MARIN gave me the opportunity to include the fatigue damage sensor in an early design stage in their test campaign aboard the US coast guard cutter 'Bertholf'.

Furthermore I would like to thank my girlfriend Miriam Eykelboom for her helpful feedback on my report concerning the English grammar. I also would like to thank her for her patience with me, especially in the last months of this thesis. My parents who supported me for the last seven years throughout my study but especially the last nine months I would also like to thank for the interest they showed in the topic and the daily supporting phone calls. I know that they are very happy and proud that I finally finished my study at the TU Delft. Finally I want to thank all the colleagues at Damen Shipyards for the enjoyable time I had during my graduation.

J. C. C. de Korte
Delft, December 2018

Contents

List of Figures

List of Tables

Nomenclature

List of Abbreviations

BV	Bureau Veritas
CA	Constant Amplitude
DS	Dual Slope
FDS	Fatigue Damage Sensor
FEA	Finite Element Analysis
FEM	Finite Element Method
FE	Finite Element
FSS	Full Scale Specimen
GL	Germanischer Lloyd
HAZ	Heat Affected Zone
HCF	High Cycle Fatigue
HSC	High Speed Craft
JIP	Joint Industry Project
LCF	Low Cycle Fatigue
LSS	Large Scale Specimen
LTF	Lifetime Factor
MCF	Medium Cycle Fatigue
mSC	Microscopic Stress Concentration
NSIF	Notch Stress Intensity Factor
PDF	Probability Density Function
RAO	Response Amplitude Operator
RFL	Random Fatigue Limit
RMS	Root Mean Square
SCF	Stress Concentration Factor

SIF	Stress Intensity Factor
SSS	Small Scale Specimen
SS	Single Slope
TS	Total Stress
USCGC	United States Coast Guard Cutter
USCG	United States Coast Guard
VA	Variable Amplitude
WSD	Wave Scatter Diagram

1 Introduction

"Nothing in life is to be feared, it is only to be understood. Now is the time to understand more, so that we may fear less."

Marie Curie

Because of their reliability and their constantly improving sea keeping behaviour. More and more high speed craft are used in the oil and gas industry and in the offshore wind industry. High speed craft (HSC) are subject to wind and waves, typical cyclic loadings and therefore suffer from metal fatigue.

In the VOMAS joint industry project, the total stress (TS) concept has been developed, in which fatigue resistance of all aluminium welded joint details is combined in a single *SN* curve. It was found that with the total stress concept, fatigue resistance of welded joints is significantly higher than in current fatigue design methods. To use the total stress concept in design, it should be integrated in the Damen fatigue design tool *Alufastship*, which currently uses design SN-curves from Germanisher Lloyd (GL). By calculating fatigue resistance for standard Damen details, Damen FAT classes with corresponding SN curves can be calculated.These new *SN* curves can be integrated in the Damen fatigue design tool.

If fatigue damage in ship structures is monitored, it can be used to ensure structural reliability of the vessel at any time, and improve fatigue design methods. However monitoring fatigue damage is complex because ships are designed in a way that no cracks are tolerated within the first 20 year of the ship's lifetime. For proper designed vessels, cracks will only occur after a long time.

A novel fatigue damage sensor has to be invented to indicate damage in the underlying structure in an accelerated manner. Fatigue damage can, among other, be accelerated by introducing a stress concentration in the structure.

In this research the feasibility of such a sensor will be investigated. In the future all Damen built high speed craft can be equipped with this damage sensor to get early feedback on accumulated fatigue damage. With this feedback the fatigue prediction methods can be improved and next to that the current condition of the corresponding structural detail can be assessed and a prediction of the expected lifetime can be made based on the lifetime of a cracked sensor.

In chapter 2 a description of the problem, and necessary background information will be given.

Chapter 3 gives the boundaries of the research, the objectives and limitations and concludes with the research questions to be answered and the plan to come to these answers.

In chapter 4 an overview of the available literature and research already done is presented with a brief description of the most relevant information.

The concept designs made for the fatigue damage sensor will be discussed in chapter 5 and a final concept will be chosen where a more detailed design will be made for.

The necessary knowledge about the total stress concept to understand the fatigue behaviour of the sensor will be discussed in chapter 10.

The preparations and the results of the fatigue laboratory tests performed at the TU Delft will be discussed in chapter 7.

In chapter 8, the practical application and testing of the sensor aboard of the *USCGC 'Bertholf'* will be presented.

The translation of a cracked sensor to a prediction of remaining lifetime of the underlying structural detail will be presented in chapter 9.

Chapter 10 will discuss the feasibility and effects of implementing the TS concept in *Alufastship*.

Finally the conclusions and recommendations will be described in the last chapter. And the appendices where will be referred to throughout the thesis are located in the end of the document.

2

Problem description

"All structures will be broken or destroyed in the end – just as all people will die in the end. It is the purpose of medicine and engineering to postpone these occurrences for a decent interval."

James Edward Gordon

In this chapter the problem where the research is created for will be explained. To do this there will be started by giving general background information about the company which gave the incentive for the research. Next the general problems arising with fatigue in ship and offshore structures will be presented, hereafter there will be zoomed in on the specific problems regarding high speed craft.

2.1. Damen Shipyards Group

Damen Shipyards Group operates more than 32 shipbuilding and repair yards, employing nearly 12000 people worldwide. Damen has delivered more than 5000 vessels in more than 100 countries, and delivers some 160 vessels annually to customers worldwide. Based on its unique, standardised ship-design concept, Damen is able to guarantee consistent quality. Damen's focus on standardisation, modular construction and keeping vessels in stock leads to short delivery times, low 'total cost of ownership', high resale values and reliable performance. Furthermore, Damen vessels are based on thorough R&D and proven technology. Damen offers a wide range of products, including tugs, work boats, naval and patrol vessels, high speed craft, cargo vessels, dredgers, vessels for the offshore industry, ferries, pontoons and super yachts. For nearly all vessel types Damen offers a broad range of services, including maintenance, spare parts delivery, training and the transfer of (shipbuilding) know-how. Damen also offers a variety of marine components, such as nozzles, rudders, anchors, anchor chains and steel work. In addition to ship design and shipbuilding, Damen Shiprepair & Conversion has a worldwide network of 15 repair and conversion yards with dry docks ranging up to 420 x 80 metres. Conversion projects range from adapting vessels to today's requirements and regulations to the complete conversion of large offshore structures. DSC completes around 1500 repair and maintenance jobs annually.

The R&D department provides specific technical support for the product groups (project / proposal and project / management departments), Engineering Services and affiliates in the fields of naval and mechanical engineering. R&D undertakes specific studies for the development of ships for the Product Groups and to expand the knowledge base. This research can be divided into six categories, that is to say: Mechanical Systems, Noise and Vibrations, Ship Structures, Hydromechanics, and Electrical & Automation Systems. [25]

2.2. Fatigue

In general, structural calculations on ships are based on the elasticity theory. When the yield stress of a material is exceeded, the more complex plasticity theory has to be used. Therefore in normal engineering practice a structure is assumed to be failed when the stresses reach the yield stress of the material. Fatigue is a phenomenon which occurs typically at a much lower stress than the yield stress where elastic theory is applicable.

The main ingredient for fatigue damage is cyclic loading. On board of ships the cyclic loading is due to the wave induced bending moments and local loads like for example slamming.

There is a need for the monitoring of fatigue damage. This is complex because ships are designed to crack after 20 year, and typically cracks will only occur after a long time. Feedback is required to improve design methods and know the state of the structure. Current feedback methods are expensive and cumbersome and can therefore not easily be applied to a whole fleet of HSC. Strain gauges for example are indirect and do not measure damage but strain. Therefore there is a need for a device to give early feedback on fatigue damage based on the same fatigue damage mechanisms as aluminium welded joints on board of HSC.

In the VOMAS joint industry project the total stress concept has been developed in which fatigue resistance of all aluminium welded joint details is combined in a single SN curve. It was found that with the total stress concept, resistance of welded joints is significantly higher than used in current fatigue design methods. To use the total stress concept in design the corresponding fatigue resistance curves should be integrated in the Damen fatigue design tool which currently uses the design SN curves of Germanischer Lloyd (GL). By calculating fatigue resistance for standard Damen details, Damen FAT classes with corresponding SN curves can be calculated that can be integrated in the Damen fatigue design tool. This research will have serious impact on the weight of the ships build by the Damen Shipyards Group.

2.3. High speed craft

A considerable part of the vessels sold by Damen Shipyards are high speed craft. The vessels are mostly used for crew and payload transfers to offshore locations. To be able to reach high speeds with an as low as possible energy consumption aluminium is often chosen as material for the hull structure. This has a few reasons. From a material selection point of view it is known that the performance indices for both tension and bending, respectively $\frac{\sigma_y}{\rho}$ and $\frac{\sqrt{\sigma_y}}{\rho}$ are higher for aluminium. This means that for the same weight, one can achieve a stronger construction by using aluminium. The same applies to the stiffness index $\frac{E^{1/3}}{\rho}$ which is more favourable for aluminium. By designing HSC where construction weight is an important factor, it can therefore pay off to use aluminium because it significantly lowers the total mass of the vessel compared to the use of steel. Aluminium has a Young's modulus of approximately 69 GPa, where steel typically has a Young's modulus of approximately 209 GPa. From a fatigue point of view this is concerning, since the Young's modulus is the governing parameter in crack growth [28].

Since Damen started to focus on the fatigue strength of HSC in the early design stage, almost no fatigue cracks have been reported. This is an indicator that there is room for improvement in the designs by doing more reliable and less conservative fatigue predictions. Recently the design of a whole new aluminium fast crew supplier began; a full aluminium ship of 70x11m reaching a top speed of 40 kts. See figure 2.1. For aluminium ships of this length, reaching these high speeds, fatigue and weight are real points of concern and a lot can be won by doing less conservative fatigue predictions.

Figure 2.1: Concept design of the full aluminium FCS7011 (Source: Damen Shipyards Group)

There is thus a need to receive early feedback on the fatigue damage of the in service HSC to be able to make later designs more reliable / less conservative from a fatigue perspective.

Another big uncertainty in the prediction of fatigue damage is the loading. In the predictions, assumptions are made for the operational profile and sailing area of the vessels, together with corresponding wave spectra. This can deviate heavily in real life. To get good feedback on the fatigue damage predictions, the sensor data and GPS data with corresponding weather and waves, should be combined to build a database for making better predictions in the future. The latter is part of parallel ongoing research.

2.4. Conclusion

The commercial new build of HSC is an important business of the Damen Shipyards Group. One of the main research topics of Damen's R&D department is the research on fatigue of aluminium HSC. A problem with the research on fatigue is that feedback on the designs comes in slowly because the designs are made to start cracking not earlier than twenty years. Since HSC are typically build with aluminium and they are getting bigger and bigger and have to reach ever increasing sailing speeds fatigue becomes even more of an issue.

3

Study definition

"Though this be madness, yet there is method in it."

William Shakespeare

In this chapter the goals of this graduation project are defined. Also the boundaries of the research will be discussed here, in order to be able to come up with the research question and the corresponding sub questions. The chapter will be concluded with a working plan.

3.1. Objectives

The main objectives of this research are:

- To develop a low cost and simple to produce and install sensor which accelerates fatigue damage with respect to a welded joint in order to give early fatigue damage information.
- The verification and validation of the sensor by doing laboratory tests for similarity in the fatigue mechanisms using the total stress concept.
- To describe how to make a reliable prediction of the remaining lifetime of the vessel, based on one or multiple sensors with a fully developed crack.
- To investigate the implementation of the total stress concept in the Damen fatigue prediction methods

The first objective is to develop a low-cost sensor which is able to measure fatigue damage in a relative short period of time. The sensor and its installation have to be financial attractive enough to install on the whole fleet of HSC. The fatigue mechanisms of both the sensor and the welded joints on board have to be similar.

The goal of the second objective is mainly to test the hypothesis of similarity in the fatigue characteristics of both the sensor and corresponding aluminium welded joints. This is necessary to in the end be able to relate the lifetime of the sensor to the lifetime of a corresponding structural detail. To meet this goal, experiments have to be performed to test the hypothesis that the fatigue resistance of the sensor behaves according to the TS concept.

Being able to make reliable predictions and give probabilities of survival of the ship based on one or multiple sensors with a crack is the goal of the third objective. The desired output of the sensor is a through width crack combined with a corresponding time observed by one of the crew members. this objective is also about defining practical procedures for using the sensor. For example how often the sensor should be inspected, when the sensor is considered to be failed and has to be reported to Damen research. Also what should be done with the fatigue damage data received from the fleet.

The last objective is to look into the current practice at Damen of predicting the fatigue lifetime and to investigate what the effects on the fatigue analysis and thus on the engineering of HSC will be when the fatigue resistance curves from the TS concept will be adopted.

3.2. Research boundaries

The boundaries in this project are:

- Only fatigue of aluminium welded joints is considered. The majority of the built HSC are constructed of aluminium, which makes this a valid limitation. In addition, the TS concept is only valid for aluminium welded joints, when this will be expanded the methods described in this thesis can also be expanded to use in steel structures.

- Only stress due to the global bending moment will be taken into account in the modelling process. Slamming and the corresponding structural response whipping can induce an increase of fatigue damage, however due to the slender design of Damen's HSC with small bow flare the effect is assumed to be little. When there is a not to be neglected effect of whipping on the fatigue damage the choice can be made to introduce a whipping factor. According to [9] the contribution of whipping on the fatigue damage of the USCGC 'Bertholf' is around 6%. Similar research can be performed on typical HSC designs to be able to neglect for convenience dynamic responses in the modelling process.

3.3. Research questions

Based on the problem description in chapter 2 and the previous defined objectives the main research question of this project will be:

- *"How can fatigue damage be measured on board of aluminium high speed craft, in a mean time frame of two years, with a low cost sensor giving a mechanical output"*

In order to have some handles to answer the main question, some sub-questions are defined here:

- *"What are the requirements of the fatigue damage sensor and subsequently; what are the different possibilities for concept designs?"*

- *"How can the sensor be joined to the ship's hull with as little as possible interference on the results?"*

- *"What fatigue tests should be performed to obtain confidence in the design? I.e. to test the hypothesis that the fatigue performance of the sensor is behaving similar to the fatigue resistance characteristics according to the TS concept."*

- *"How can the fatigue damage data received from the sensors be matched to fatigue lifetime predictions on aluminium welded joints on board high speed craft?"*

- *What effect does the implementation of the total stress concept have on the fatigue designs of high speed craft?*

3.4. Working plan

With the research questions formulated above, the working plan to be able to answer them will be explained here.

3.4.1. Literature review

The literature review will be performed for a few reasons, on one hand to investigate what research already has been done in this specific field, on the other to synthesise the needed information to get a summary for future reference during the project.

There will be looked into the literature of the following topics: Fatigue in general, different fatigue concepts and in particular the total stress concept. Finally the current state of the art regarding fatigue sensors will be investigated.

3.4.2. Concept design crack sensor

Using the theoretical frame work obtained from the above mentioned literature review, conceptual designs for the sensor will be made. To come up with these designs, first requirements are set. Next a morphological chart will be presented to provide insight in the different possibilities to meet these requirements. From the morphological chart a few concepts will be derived and analysed to have a first indication of the feasibility of the concept. From this analysis subsequently a choice for a final concept will be made to further develop during this research. Using the knowledge gathered in all the steps of the research, a final design will be made. This final design is preferably generally applicable to all aluminium high speed craft for convenience. furthermore the sensitivity on the dimensions due to inaccuracy in the production or installation process must be recognised to know and account for the effects.

3.4.3. Practical testing sensor

The United States Coast Guard (USCG) has contracted MARIN to carry out fatigue structural maintenance validation work on a coast guard cutter. In order to assure the best possible result in terms of technical achievement, MARIN has involved other organisations in the project. For this reason MARIN has organised the Valid joint industry project (Valid JIP). Within the USCG the project has become known as the fatigue life assessment project (FLAP). The goals of the work are to forecast structural maintenance needs of USCG Cutters, to further improve the understanding of wave loading leading to fatigue damage, and to increase the confidence level in predicting wave loading leading to fatigue damage [7]. USCG and MARIN agreed on testing the fatigue damage sensor on board of the coast guard cutter 'Bertholf', see figure 3.3. The cutter's hull is made out of steel, so the results may not be accurate for predicting the lifetime of the vessel when the total stress concept is adopted. Since this research is based on Aluminium. However this full scale test can prove the joining concept and the workability of the installation and inspection procedures. Together with data from the installed strain gauges on board, conclusions can be drawn after a crack occurs in the sensor. It is mainly a test to validate the choice for the bonding method, to verify that the bonding will not fail due to the ship's environment and loading. The sensor for this application will preferably be made in such a manner that within a maximum time span of six months, it will fail given that the loadings allow it to receive the information before the end of this project.

Figure 3.3: The USCG Bertholf underway during sea trials in the Gulf of Mexico (Source: `http://media.globenewswire.com`)

3.4.4. Laboratory testing
Laboratory tests will be done to be able to test the hypothesis of similarity of the relevant fatigue mechanisms between the sensor concept and welded joints from the TS concept. This will give a good idea of feasibility of the concept. Knowing the large scatter band in *SN* curves a certain amount of tests have to be performed to get enough confidence in the concept. If the results of the tests are satisfying, the TS concept can be used to match the fatigue damage results of a sensor to predict the lifetime of fatigue sensitive details on board.

3.4.5. Matching the sensor to the vessel's welding details
The procedure to match the fatigue damage data to the lifetime predictions of the various welded joints on board should be made based on the total stress concept. Therefore there has to be looked into the probabilistic behind the fatigue in both the sensor and the aluminium welded joints to come up with joint probability distributions. When joint probability distributions can be calculated for the sensor and corresponding structural details, predictions can be made of the expected lifetime of the considered structural detail.

3.4.6. Feasibility study on the implementation of the TS concept in *Alufastship*
Currently the TS concept is not applied in the fatigue calculation at Damen Shipyards. One of the aims of the implementation is that it should be quick enough to be used by all engineers involved in fatigue analysis of HSC. To achieve this, first there will be looked into the current practice to use it as a basis for the extension to the TS concept. Secondly the consequences of implementing the fatigue resistance curves of the TS concept in *Alufastship* will be investigated. The hypothesis is that the implementation of the TS concept will have huge effects on the fatigue damage predictions and thus on the structural weight of the HSC.

3.5. Conclusion
The main objective of this research is to develop a low cost and simple to produce and install sensor which accelerates fatigue damage with respect to a welded joint in order to give early fatigue damage information. The research is aimed on aluminium welded joints since the majority of build HSC are made of aluminium. For convenience only stresses due to the global wave bending moment will be taken into account. To have handles to carry out this research, research questions are formulated. Based on these research questions a working plan is described.

4

Literature review

"The possession of knowledge does not kill the sense of wonder and mystery. There is always more mystery."

Anaïs Nin

In this chapter the results of the literature study are presented. This study is done throughout the whole project and constantly supplemented.

4.1. Fatigue in aluminium ([1], [28], [11])

Aluminium is a polycrystalline material, the size of the crystals are typically O(10^{-8} m). Although aluminium is considered as an isotropic material on macro scale, microscopically it is anisotropic. This is because of the random orientation of the grains within an atom. This microscopically anisotropic behaviour results in microscopic stress concentrations (mSC) at grain boundaries since the stress can differ from grain to grain. A second cause of the existence of mSC's is the fact that crystal dislocations start to move under a cyclic loading. This induces local plasticity. This locally induced plasticity typically concentrates in slip bands and the moving of those dislocations are called cyclic slip. Cyclic slip follows the path of least resistance i.e. the grain orientation that aligns with the maximum shear stress. This orientation is at $\pm 45^o$ for normal loading and at $0^o/90^o$ for torsion. See figure 4.5 for an overview of the different scales of physics involved in fatigue.

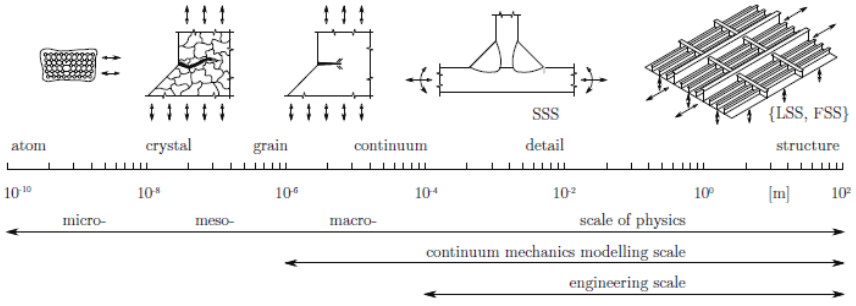

Figure 4.5: Different scales involved in fatigue assessment [4]

The fatigue damage process is typically divided in three main periods: crack initiation, crack growth and finally failure. The crack initiation period starts due to the existence of mSC's. This nucleation of microcracks starts very early in the fatigue life. The emergence of these microcracks typically happen at nominal stress amplitudes below the yield stress. The existence of mSC's is the reason for plasticity on microscale and thus the emergence of these microcracks. Crack initiation is a (near) surface phenomenon, therefore corrosion, manufacturing defects and inclusions, voids and pores in the material contribute to the initiation of cracks.

Especially the last three are something that is introduced by welding. In general the crack initiation period is highly random due to the randomness of the input parameters. For example the size and number of weld defects.

The direction of crack growth is dominated by the far field stress. As well as to crack initiation, it also applies to crack growth that the path of the least resistance is followed. In fracture mechanics there are three types of crack propagation to distinguish, namely: Mode I, II and III. Respectively an opening mode, in-plane shearing, and out-of-plane shearing. See figure 4.6.

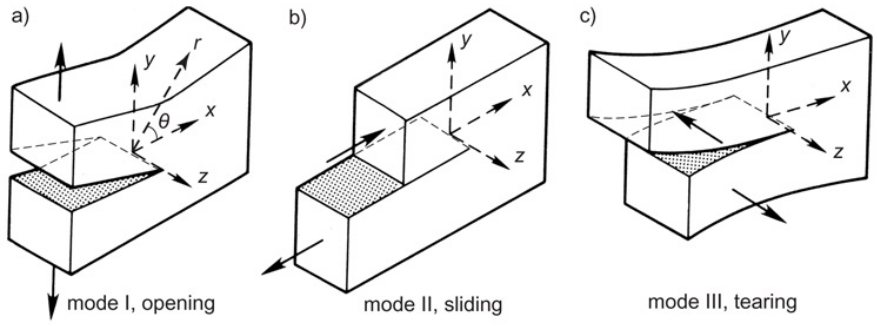

Figure 4.6: Modes of crack propagation [17]

Fatigue occurs under a long term cyclic loading. In general, the highest fatigue damage will occur at locations with the highest stress ranges due to the longitudinal bending moment. Not only the global bending moment contributes, but also local loadings do. These local loadings, mostly around the water line due to the cyclic wave impact, mostly affect the penetrations of the longitudinal stiffeners trough the webs. The fatigue crack initiates almost always in a welded joint. The governing factor regarding fatigue damage on the loading side is the stress range and the number of cycles per specific stress range. These two factors $\Delta\sigma$ and N in general are plotted against each other on a logarithmic scale. It appears that when both plotted on a logarithmic scale, the so-called SN curve is a straight line regarding fatigue resistance. For very low stress ranges there is a theoretical fatigue limit, where no fracture will occur for any number of cycles. In practice 10^8 cycles for a certain stress range without crack is defined as the fatigue limit. In general the fatigue curve is constructed following equation 4.1.

$$log(N) = log(C) - m \cdot log(\Delta\sigma) \tag{4.1}$$

A typical value for m, which is the inverse of the slope of the line, is $m = 3$ for ship and offshore structures. There is always a certain threshold value regarding the stress range, so not all cycles the vessel endures contribute to the fatigue damage of the structure. Since obtaining the whole SN curve by experiments is a very time consuming activity, normally the curve will be derived from 2 or 3 points. The SN curve assumes a certain life time for a certain constant stress range, this obviously is not usually the case for ship and offshore structures. To relate the SN curve to varying loading, Miner's rule can be used. Miner's rule states that when for a certain ΔS_i and corresponding N_i the structural detail is completely damaged. When the number of cycles is lower, say n_i, the damage will be proportional to the ratio n_i/N_i as in equation 4.2.

$$D_i = \frac{n_i}{N_i} \tag{4.2}$$

So the total damage is then equal to:

$$D = \sum_{i=1}^{k} \frac{n_i}{N_i} \tag{4.3}$$

If D reaches 1, the total fatigue damage is reached and the structural detail is considered to be failed.

For constant amplitude loading (CA) it is easy to count the cycles that accumulate the fatigue damage. When a variable amplitude loading (VA) is applied, which is typically the case for ship and offshore structures, the counting of the stress cycles becomes much more complex. A random measured stress signal is not always

made up of a single peak between two zero crossings, it is not even uncommon that several peaks often appear between two zero crossings [19]. There are various approaches to deal with this, however a commonly applied method in the assessment of fatigue in marine structures, is the rainflow counting method. One of the reasons for this is that the extracted cycles from this method comply with those obtained from CA tests where *SN* curves are based on. More about this method in [19] and [20].

Welding has a huge effect on the fatigue behaviour of structures. The heat affected zone (HAZ) is affected by the heat of the welding, this yields to material with bigger grains. That has a negative influence on the fatigue strength of the material. The welding also has the effect of introducing micro cracks in the weld toe, which induces microscopic stress concentrations.

Since stiffness attracts loading, the shape of the weld also has an effect on the local stress. In figure 4.7 the stress lines through a few welded details are shown. This attracted loading induces stress concentrations at the weld toe and weld root for partially penetrated welds where the density of stress lines become larger. This stress concentration is highly depending on the angle between the plate and the weld defined in figure 4.8. The higher the angle the lower the stress concentration.

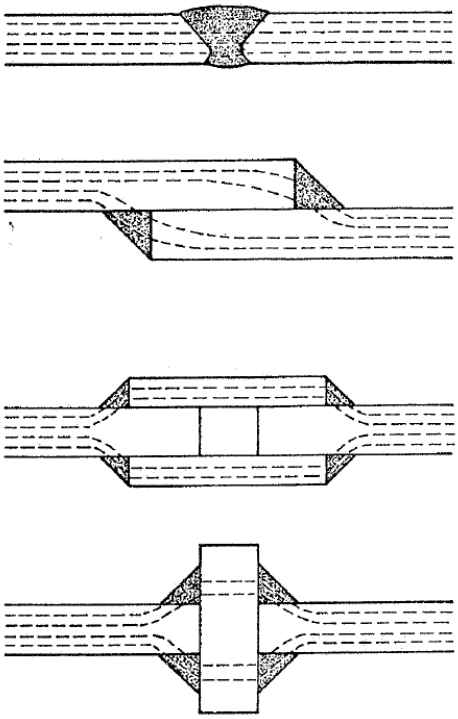

Figure 4.7: Stress lines through weld [1]

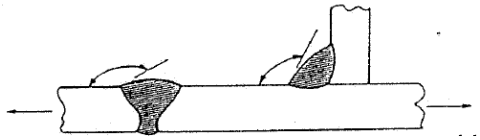

Figure 4.8: Weld angle [1]

4.2. Fatigue concepts ([26])

Different methods to predict fatigue damage will be discussed in this section.

4.2.1. Nominal stress concept

This method uses dedicated SN curves for representative structural details based on nominal stress. One difference between small scale specimen (SSS) and large- and full scale specimen (LSS, FSS) is the influence of residual stresses. In SSS these stresses are of the self-equilibrating type, since there are almost no displacements constraints involved, while for the LSS/FSS there are. These are of the equilibrium equivalent type. Fatigue test data has to be corrected to satisfy welded joint similarity. Also size effects play a role in welded joint similarity, for increasing t_p the absolute notch affected zone size increases. For plate thicknesses $t_p > 20$ all dimensions should be scaled according to equation 4.4 to prevent this. For smaller t_p these dimension variations are usually not covered, this pays out in scatter and reduced accuracy of the N estimate. On the other hand it also pays out in a low complexity of the method and low computational power is needed.

$$\left(\frac{S_0}{S_n}\right) = \left(\frac{t_{p0}}{t_p}\right)^k \tag{4.4}$$

4.2.2. Structural hotspot stress concept

If structural details deviate more from the details used in the dedicated SN curves, it can be necessary to use the structural hotspot stress concept. This concept can only be used for weld toe induced fatigue damage. For weld root induced damage it cannot. The structural hotspot stress concept gives the opportunity to include more geometrical details in the calculation. The structural hotspot stress S_h is a non measurable fictitious stress. S_h can be derived by extrapolating the stress from certain extrapolation points depending on the plate thickness.

4.2.3. Notch stress intensity factor (NSIF) concept

When the notch radius goes to zero ($\rho \rightarrow 0$), the local stress at the notch becomes asymptotic and has no unambiguous solution. Therefore the notch stress intensity factor (NSIF) is introduced based on William's asymptotic solution, see [33]. Unlike the regular stress intensity factor K_I, which is a cracked geometry parameter, the NSIF is an intact geometry parameter. By curve fitting a general solution is found for the NSIF, depending on, among others, the curve fitted parameter k_1. See equation 4.5. Where the eigenvalue λ is weld angle depending. According to [21] a Basquin type of relation is possible based on the NSIF. However this is only possible for welded joints with same weld angle since the unit of the NSIF is depending on the eigenvalue λ and λ is depending on the weld angle.

$$K_1^N = k_1 \sigma_n t^{1-\lambda_1} \tag{4.5}$$

4.2.4. Total stress concept

From the industry the demand came for a practical, efficient methodology to predict fatigue in an early design stage for aluminium HSC. The aim was to develop a design method concerning high-cycle fatigue of arc-welded joints in high speed aluminium ships [6]. In this research a generic fatigue damage model is developed where the multiple SN curves necessary in the nominal stress concept are reduced to one master curve. The total stress concept is based on an equivalent structural response parameter rather than on the nominal stress. The equivalent structural response parameter S_T, see equation 4.6, incorporates for weld toe notches an effective structural stress range $\Delta\sigma_s/(1-r_l)^{1-\lambda}$ and a notch crack growth integral I_N including the size effects [4]. In chapter 10 the application of the total stress concept on the fatigue damage sensor design will be discussed more in detail.

$$S_T = \frac{\Delta\sigma_s}{t_p^{(\prime)\frac{2-m}{2m}} \cdot I_N(r_s, n, m)^{\frac{1}{m}} \cdot (1-r_l)^{1-\gamma}} \tag{4.6}$$

4.3. Fatigue damage sensors

A lot of fatigue damage sensors are developed in the past, mainly in aviation but also for civil and marine applications. A typical fatigue damage indicator for aviation for example is described in [16]. The Kawasaki fatigue damage sensor is one example of a sensor suitable for marine applications, see [32]. There are some general disadvantages in the fatigue damage sensors found in literature for the application on a fleet of HSC. Firstly the analysis is mostly very complex. For both [16] and [32] specialists have to inspect the sensor to be able to make a statement about the accumulated fatigue damage. This is what one typically finds about fatigue damage sensors mentioned in literature. Secondly, the sensors found in literature are not representative of ship structures, in for example, material, failure mode and stress distribution. In most cases a translation has to be performed to be able to say something about the fatigue damage in a representative structural detail. The goal of this thesis is to come up with a sensor which is representative

5

Concept design sensor

"At its heart, engineering is about using science to find creative, practical solutions. It is a noble profession."

Queen Elizabeth II

At the end of this chapter a detailed design is made of the fatigue damage sensor. To come up with a final design for the sensor the requirements will first be set. Next a morphological chart will be made to make the requirements and its physical solutions insightful. From the morphological chart a short list of concepts will be extracted to proceed with in the next phase. The next phase consist of doing analysis and feasibility studies on a conceptual level. From these analysis a final concept will be derived to proceed with and design and analyse in more depth.

5.1. Requirements

To come up with concepts for a fatigue damage sensor (FDS) requirements should be met. To have a good understanding of the requirements it is a good idea to make clear why there is a need for such a sensor. In software engineering the requirements exist of three levels, see figure 5.10. It appears that this approach of describing the requirements is also applicable on the development of the sensor. On the top level are the business requirements, these requirements show the business needs and give in essence the core of the problem. The business requirements only present a problem and a preferable outcome. Then on the second level are the stakeholder requirements. The stakeholder requirements give in essence what information stakeholders need to get from the system to be able to meet the business requirements. In this case the stakeholders are the people at Damen who are responsible for the analysis of the feedback from the sensor. Lastly there are the system requirements on the lowest level. These system requirements describe what the system must exist of to meet the stakeholders requirements.

Figure 5.10: Three requirement levels

Before a design is made it is important to know what problem the design should solve. The problem with fatigue predictions is that feedback of the design comes in slowly/ fatigue cracks typically occur most of the time after twenty years. To be able to improve the fatigue prediction methods it is important to obtain feedback of fatigue life of a large number of ship structures within a reasonable time frame. When this feedback shows with great certainty that the current prediction methods are unnecessary conservative, aluminium

HSC can be build in a responsible manner using less material. The influence of this on the design spiral can be huge. A lighter ships needs less power to reach a certain speed, this can induce a reduction of installed power what again induces a saving on weight. Additionally, lighter ships consume less fuel which is positive for both the environment and the business of the ship owner. To have a lucrative business case, the sensor and its installation should cost less then €100 so that it can be installed on a whole fleet of HSC.

It is desired to get feedback on fatigue life in a mean time frame of two years. The sensor should be designed in such a way that a crack occurs after approximately two years. When a crack is detected in the sensor, there must be a quick analysis available to make a reliable prediction of the expected lifetime of the corresponding structural detail. The production method of the sensor must be accurate enough to have reproducible fatigue resistance characteristics. The deviations due to the production tolerances should have a minimal effect on the fatigue resistance characteristics of the sensor. The sensor must be easy and quick to be installed, inherent to that is that the sensor should be small of size. The fatigue life output of the sensor may not be influenced by the joining method. On the other hand sensor and the joining method may not have a significant influence on the stress state of the underlying structure. I.e. the sensor should not introduce a fatigue sensitive location in the underlying structure. Also the structure or the conservation may not be permanently damaged by the presence of the fatigue damage sensor.

In order to meet all above stated requirements the sensor needs to have certain characteristics. To be able to accelerate fatigue damage in the sensor with respect to the underlying structure a representative fatigue sensitive location will be introduced. This can for example be a weld or a local stress change which reduces the fatigue lifetime of the sensor. Since the fatigue mechanisms of the sensor must be similar to the fatigue damage mechanisms of the corresponding structural detail and the postmortem analysis of the sensor must be as quick and easy as possible a mechanical output is desired rather than an output in the form of electronic data. The fatigue sensitive location has to be physically similar to a fatigue sensitive location of a corresponding structural detail in order to have similarity in the fatigue damage mechanisms. The design of the sensor has to be in such a way that fatigue is the governing failure mode. To be able to install the sensor on a remote location, an engineer must be able to transport the sensor in its hand luggage. To have enhanced confidence in the design it is desired to have the possibility to install several sensors in parallel.

Below, the above mentioned requirements are summarised:

- Business requirements:
  - Get more accurate fatigue prediction methods
  - Build ships using less material in a responsible manner
  - Total cost per sensor should be less than €100
- Stakeholder requirements:
  - Get fatigue damage data from the vessels in a mean time frame of two years
  - Fatigue damage data must be transformable to lifetime predictions of welded joints of HSC
  - It should be possible to produce within set tolerances
  - Sensor should be easily transportable
  - Method of joining sensor to hull should have minimal influence on the fatigue resistance of the sensor
  - The sensor should not damage the vessel or affect the structural integrity
- System requirements:
  - Accelerate fatigue damage
  - Output should be mechanic
  - Sensor should be representative to fatigue sensitive location on board
  - Fatigue should be the governing failure mode
  - Sensor should be possible to fit in hand luggage
  - Low sensitivity regarding production and installation flaws
  - Possibility to connect several sensors in parallel

5.2. Morphological chart

To provide insight in the different possibilities of a sensor, a morphological chart is made see figure 5.13. This chart is made based on the requirements defined in section 5.1. In section 5.2.1 the different options in the chart will be qualitatively discussed. By combining the most suitable options from the chart, concepts are generated.

5.2.1. Generating concepts

Sensor material

Since the mechanical sensor has to accelerate fatigue damage with respect to welded joints and has to be representative for metal fatigue in aluminium HSC, the material choices are limited to steel and aluminium. In the limitations of the research in section 3.2 is stated that this research will focus on the fatigue prediction of aluminium welded joints. One of the requirements is that the fatigue damage mechanisms have to be same for the sensor as for the corresponding welded joint. Since aluminium is the preferred material for the hulls of HSC the most suitable sensor material is aluminium.

Initial defect

Since information about fatigue damage of welded joints is the desired output of the sensor, the most logical choice appears to be having a weld on the concerned fatigue sensitive location of the sensor. However, welds are typically showing a wide scatter of quality differences along the weld seam. Since the weld seam on the sensor will be very small, this could give a great uncertainty on the fatigue life. To avoid this uncertainty it would be more convenient to overcome this by not using a weld, but still have similarity from a fatigue perspective with welded joints. When not using a weld there should be something introduced to have similarity with a weld. It is shown in figure 5.11 that even though the fatigue resistance of weld material (WM) and base material (BM), in this case aluminium, have different fatigue resistance characteristics. Introducing a stress concentration eliminates this difference in fatigue resistance.

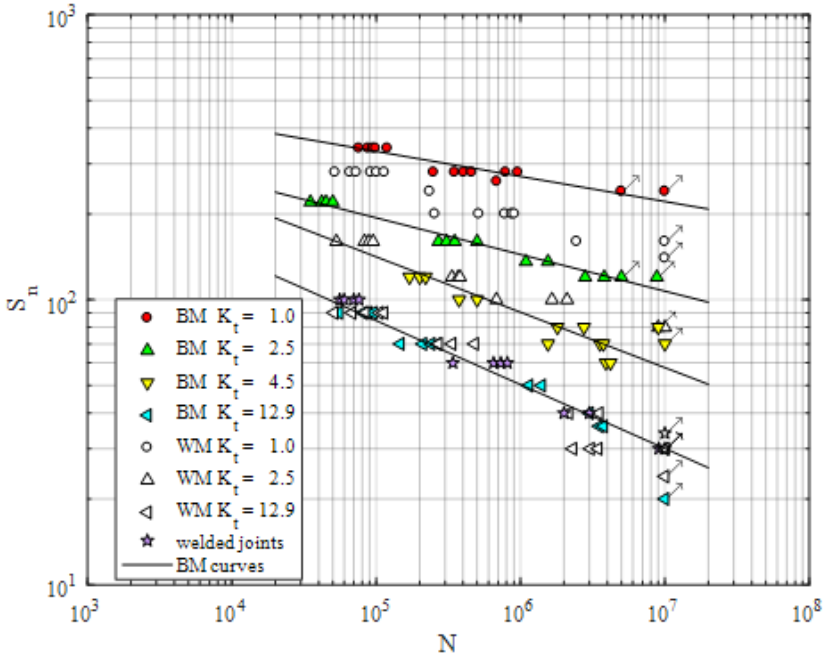

Figure 5.11: Effect of stress concentration of fatigue resistance base material w.r.t. weld material *(Source: Henk den Besten)*

Similarity in fatigue resistance characteristics between a sensors and a corresponding welded detail can be obtained by for example, creating a notched geometry similar to a weld toe notch. When the radius in this notch goes to zero in the limit, the stress concentration will be $K_t >> 12.9$ and thus will the fatigue resistance

of the notched geometry behave as weld material, see figure 5.11. Beside the stress concentration, milling the weld geometry and/or introducing an artificial weld defect is an option to get similarity with a corresponding welded joint. Another option can be to make an artificial weld defect in the notched geometry. The presence of an artificial defect has the additional benefit that the defect size is known for every sensor, unlike the welded option. According to the company SLV in Rostock, specialised in laser technology the process development of an artificial weld defect costs around €1000. Once the process has been developed, the cost per sensor will be around a few Euro.

Governing far field loading

The governing loading has a great influence on the way of accelerating the fatigue damage in the sensor. From a fatigue perspective the remote mechanical mode-I far field stress can be assumed to be the governing loading [4]. Since mode-I is the governing mode from a fatigue perspective, the tensile component of the stress contributes the most to the fatigue damage. Therefore only the axial component of the structural stress will be taken into account in the modelling process.

Governing fatigue life period

The lifetime of a weld is crack growth dominated; the crack will spend the majority of its lifetime in the notch affected zone [4]. Therefore crack growth is preferred to be the governing fatigue life period for the sensor.

Stress raising method

The sensor will be attached in the hull and with FEM calculations it will be verified that the sensor does not influence the stress distribution on the hull. This means that there is a forced displacement situation. Remember Hooke's law being $\sigma = E\epsilon$, the stress in the sensor will be proportional to the elongation. From that perspective there will be no stress raise in the sensor compared to the hull. However a stress concentration can be made by geometry. Notches in general cause a inhomogeneous stress distribution [28]. This can, for example, be done by removing the right material, or by introducing sharp notches. A few concepts are given in the chart.

The concept with in the centre a hole can be made of various geometries. A circular hole, an ellipse, a diamond shape etc. In figure 5.12 the stress distribution around a circular notch is shown. The governing stress concentration factor (SCF) is defined as $SCF = \frac{\sigma_{peak}}{\sigma_{nominal}}$. The lifetime decrease, which is the goal of the SCF in the sensor, is approximately proportional to the nominal stress increase due to the reduced sectional area as shown in equation 5.1. The lifetime decrease is then: K_S^m, where m is the SN curve slope which is 3.78 for the MCF range in the total stress concept [4].

$$K_S = \frac{A_{wide}}{A_{small}} \tag{5.1}$$

Besides the stress concentration, a notch shall be introduced to obtain welded joint similarity. For the concept with in the centre an hole, this could be a butt joint at the height of the centre of the hole. The butt joint introduces a singular point in the stress distribution (assuming $\rho \rightarrow 0$). To be sure the crack will not start at the edge of the hole, because this will introduce a HS type B, the edges have to be finished to locally lower the stress levels. This allows the crack to start in the weld as a HS type C.

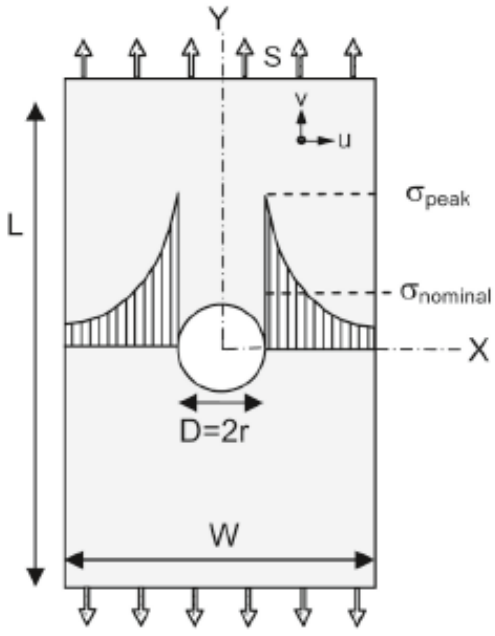

Figure 5.12: Stress distribution around circular centre notch [28]

The attachment is a representative detail since it is commonly applied in HSC. Since stiffness attracts loading, the abrupt increase of stiffness due to the attachment will cause a local stress raise however this

stress raise is equal to the stress raise on the weld of an attachment in the hull and there is aimed for a higher stress raise in order to accelerate fatigue damage in the sensor.

A thickness/width reduction will raise the stress because of the reduced area as shown in the concept with the hole in the centre. However there should be a weld like notch introduced for welded joint similarity.

Also a bending moment can be introduced with a weld on the most stressed part. A stress raise can be obtained by varying the arm. This idea has similarities with the Cognac fatigue experiment done by Shell in 1983 [24].

By welding a sensor on two fixed plates attached to the ship's hull, a sensor can be made with shear stress as a governing fatigue mode.

A concept with notches on the side, provides a local stress raise due to the reduced area. The notches can have any shape. Please note that there also should be a weld like notch introduced at the preferred crack location to achieve fatigue similarity with a welded joint.

Manufacturing method

One of the most important aspects is the ability to produce all sensors using the same procedure with as little as possible deviations due to the production process. This is mainly because this assures more consistency and reliability in the predictions and in the end this will result in less scatter. The choice of manufacturing method strongly depends on the design of the sensor. The different options will be discussed here briefly and qualitatively.

Drilling is (if done properly) a process which gives repeatedly a sensor with similar building tolerances.

Flame cutting heats the material and makes a rough cut by burning the material. Due to the low melting point of aluminium, flame cutting is not suitable for aluminium. For steel it is possible but it has some big disadvantages. Firstly, it does not give a clean cut and secondly the material properties can be affected since the material has to be heated before cutting. This makes a consistent product impossible.

Laser cutting is a more precise alternative. The manufacturing tolerances are lower, around $\pm\frac{t_p}{10}$, and it provides a relative clean cut with the right settings and well maintained equipment. The change in material properties due to the heat supply are assumed to be low since the heat input is very local.

Waterjet cutting is another manufacturing method suitable for aluminium. With the right settings a clean cut can be achieved. A limiting factor in waterjet cutting is the size of the waterjet. The diameter of the jet is O(1mm). This means that it is not possible to produce very sharp notches which can be a requirement when there is opted for high local stress raise to overcome the difference in fatigue resistance characteristics between aluminium and weld material.

For some geometries milling will be a good method. Since most of this work is done manually, it should be verified that the sensors do not deviate too much from each other. Since it is labour intensive, producing sensors in relatively large quantities makes this production process less lucrative.

Finishing

Particularly in the crack initiation period, which is a (near) surface phenomenon, surface treatment can be important. Small manufacturing defects, in general the surface roughness, induces microscopic stress concentrations (mSC's). The same applies to sharp edges. Investigated will be if surface treatment is necessary for this purpose, because it is not desired since it will raise the complexity and costs of the sensor. On the other hand, if the surface roughness can be controlled by the production method and is consistent for different sensors it can even be beneficial and necessary to initiate a crack in the sensor.

Sensor installation

In the requirements in section 5.1 is mentioned that the joining method should not influence the measurements. There are a various possibilities:

The major benefit of welding is the stiff connection with the hull, which makes sure that the loads can be well transferred through the sensor. One of the drawbacks is the necessity of hot work on board, this makes the installation complex and expensive. In addition to that, it will damage the paint job and it possibly introduces a fatigue sensitive location in the hull. These drawbacks do not meet the stakeholders requirements and therefore make it a not preferred method.

The second option is bonding. From aerospace it is known that there are bonding methods available which can survive in a highly stressed area. Advantages of this method are the simplicity of installing the sensor and the fact that it will not affect the underlying structure. Since the bonding probably has a significant

lower stiffness than the metal sensor, FEA should be performed to investigate the load transfer through the sensor.

Lastly bolting is mentioned as a method of sensor installation. This is a very stiff method that ensures that all displacements will be transferred through the sensor. One can reason that the bolting introduces large stress concentrations at the point of attachment, since all the loads have to be transferred there. This induces the change that the fatigue crack occurs somewhere else than the preferred location. A second reason to ignore this installation method is the amount of work involved in it since the bolts have to be welded on the hull after building the vessel or during the outfitting of the vessels installed.

Enhanced confidence

To get more confidence in the outcomes of the sensor, a choice can be made to carry out the sensor in a parallel version. The advantage is that one increases the sample size. From a statistic point of view this is a very practical way to decrease the error margin and get a more precise prediction of the remaining lifetime. In chapter 9 the effects of multiple sensors on the prediction of the expected lifetime of the structure will be explained.

Measuring method

The desired output of the sensor has to be determined. As mentioned before it is assumed that a considerable part of the fatigue life is spent in the notch affected zone. This means that a big amount of time, the fatigue crack cannot be seen by the human eye. The analysis of the output of the sensor can also be a combination of below described measuring methods.

A criterion can be that the desired output of the sensor is when a crack is noticeable (i.e. 1 mm for example or smaller when optical devices specialised for crack detection are used). Note that the inspections are performed by the ship's crew and that it has to be as easy and as quick as possible.

A desired output of the sensor can be when it has cracked completely. This can of course be easily seen by the crew and is a good standard, since fatigue methods consider a structure failed when the damage $D = 1$. Which means complete failure of the structural detail.

Strain is an output that the sensor cannot give. However it can be useful (especially for the first few ships equipped with the sensor) to measure strains to validate the effectiveness of the sensor.

Also environmental data through GPS position and wave data is obviously not something that the sensor can give as an output. GPS data through the AIS system can be purchased at companies like Marinetraffic or can be gathered by vessel monitoring programs. Global wave data can be downloaded from the internet. Together with the fatigue sensor, this data can be used to improve fatigue prediction methods both on the loading as on the response side.

Preferred lifetime

Different seasons have different weather and wave conditions. To let all seasons contribute to the fatigue damage, it is convenient to prefer a lifetime of at least one year. Beside the weather condition, the operational profile also plays a role in the preferred lifetime. When the expected lifetime of a structural detail is based on the observation of a cracked sensor, one assumes that the conditions during the lifetime of the sensor are representative of the complete lifetime of the vessel. The same applies to whether the sailing area during the lifetime of the sensor is a representative area for the lifetime of the vessel.

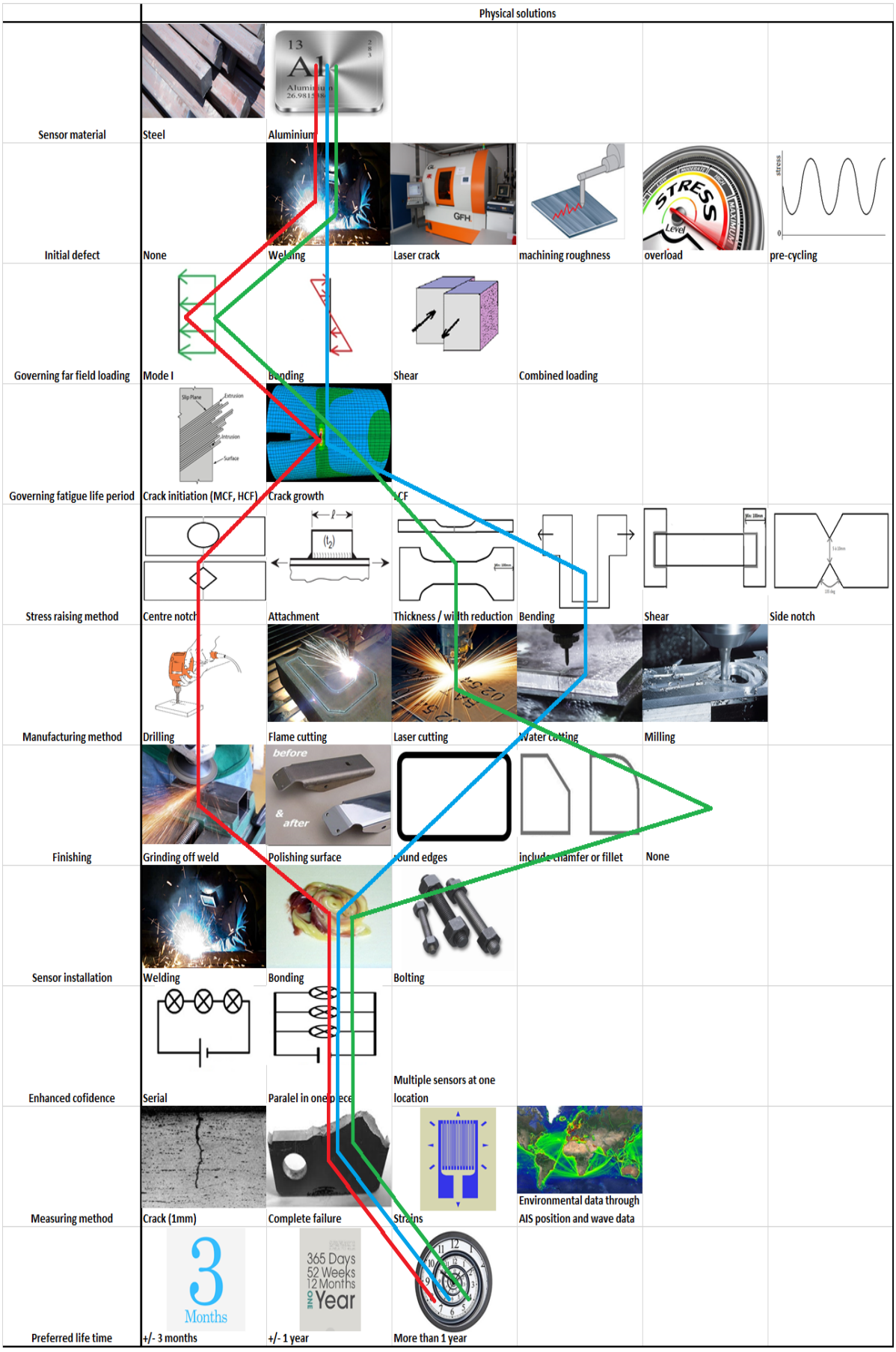

Figure 5.13: Morphological chart

5.2.2. Short list

Three possible concepts are extracted from the morphological chart to further investigate.

The centre hole concept is chosen because it raises the stress due to the reduced sectional are on one hand, and on the other a weld like geometry can be introduced in order to have geometrical similarity with a corresponding welded joint.

The bending concept is a potential concept, mainly because very high stress concentrations can be achieved by adopting a longer arm. There has to be investigated in what way geometrical similarity with a welded joint can be achieved to have similar fatigue resistance behaviour.

The side notch concept is very promising, mostly because the same reasons of the centre hole concept. An additional advantage of the side notch concept is that because of the open geometry, in contrast to the closed geometry of the centre hole concept, any weld like geometry can be produced.

Summarised, the following potential concepts are chosen:

- Centre hole concept (Red line)
- Bending concept (Blue line)
- Side notch concept (Green line)

These concepts seem to be very promising. To come up with a final concept to proceed with, and analyse in more depth, these concepts will be investigated on feasibility below. On a conceptual level calculations will be performed.

Centre hole concept

Figure 5.14 shows a FE plot of the centre hole concept. An aluminium specimen with a centre hole of any shape, raises the stress on one hand because of the reduced area and on the other due to the geometry of the hole. The circular hole gives a stress concentration at the edges, see figure 5.12. The nominal stress raising factor K_s can be varied by the ratio diameter/width to adjust the preferred lifetime. In addition to the hole there should be a weld or weld-like geometry to achieve geometrical welded joint similarity with a butt joint. The inside of the hole should be smoothed to avoid getting a HS type B, which is not desired since a HS type C is more common in welded joints on board of HSC. In case of a circular hole it can be drilled. If another shape is used, different possible manufacturing methods should be considered.

Bending concept

A bending moment can be created to locally raise the stress in the specimen. In the cognac experiment of Shell [24], a fatigue specimen based on this principle is used, see figure 5.15. The stress raising factor is very sensitive to the arm of the bending moment, a small elongation can increase the stress concentration significantly. Since the specimens thought of are all relatively large and use a lot of volume, which is undesirable in a ship's hull, the decision is made not to proceed with this concept.

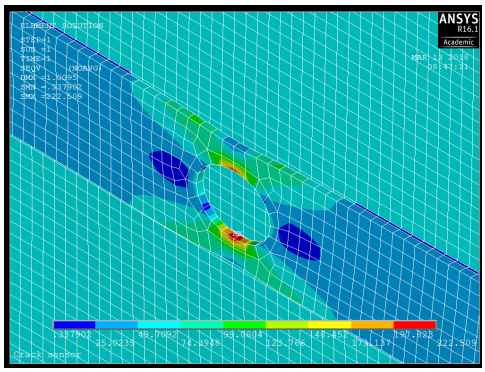

Figure 5.14: FEA of centre notch concept

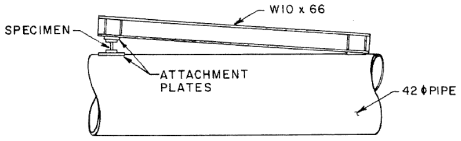

Figure 5.15: Bending beam specimen [24]

Side notch concept

The last concept discussed here is the side notch concept. For this concept one or two notches in the side of the specimen will be made. This leads to a stress raise due to the reduced area. Furthermore a weld-like geometry necessary. This can be achieved by choosing the right geometry for the side notches. Therefore a geometry was invented as presented in figure 5.16. The driver behind this design is that the hypothesis is that the fatigue characteristics of this sensor will be similar to that of a double sided cruciform joint. The smallest width of the sensor is assumed to be equivalent to the thickness t of the DS cruciform joint shown in figure 5.22b. The notch angle of the sensor in figure 5.16 corresponds with the 135^o weld angle 2α shown in figure 5.22b.

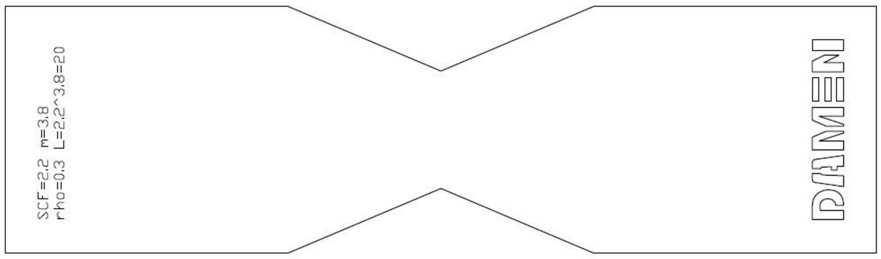

Figure 5.16: Side notch concept

Analysis of concepts

Like mentioned earlier, on a conceptual level analysis are performed on the feasibility of the different concepts. Since the found designs for the bending concept are all very voluminous will this concept not further be elaborated.

FEM calculations are performed on the geometries with a forced displacement loading. This is mainly done to get an idea what the maximum stresses will be at a known forced displacement loading. Since it is on a conceptual level it has merely a comparative character than aiming for exact values. Secondly the models are expanded with a stiffener with a high stiffness compared to the sensor. The sensor is joined to the flange of the stiffener with a bonding layer, this made it possible to also see the effect of the bonding layer on the load transfer.

In figure 5.17 and 5.19 various plots obtained from the FEM analysis are shown. For the analysis solid elements of the type SOLID186 are used.

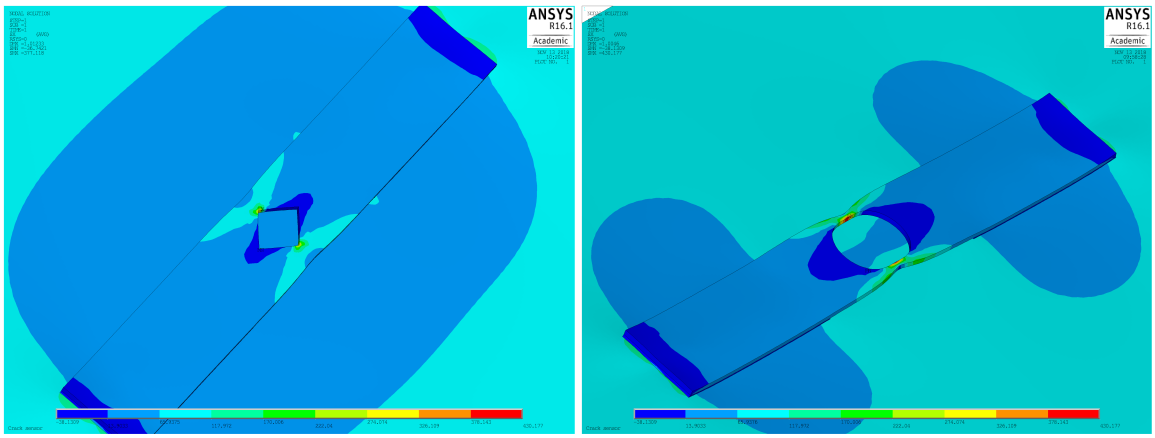

(a) Diamond notch (b) Ellipse concept

Figure 5.17: FEM plots centre hole concept

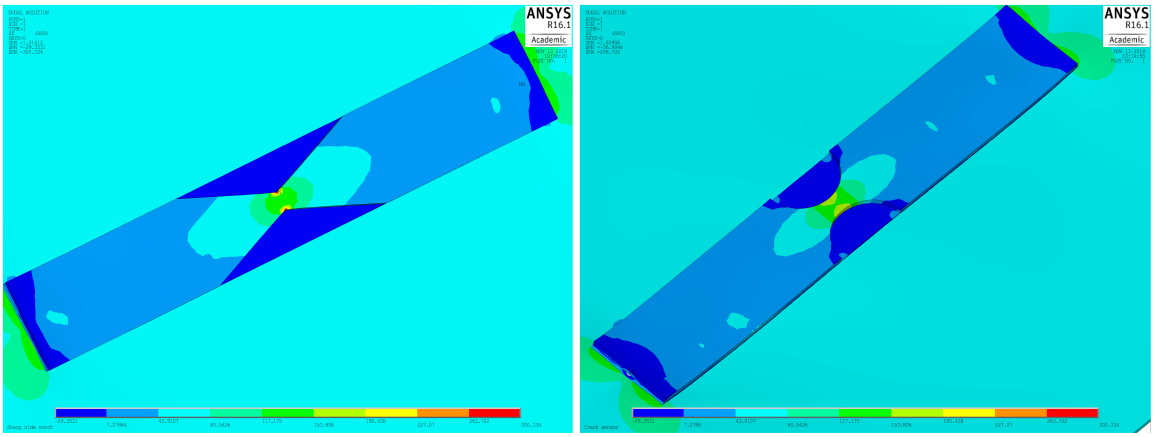

(a) Sharp side notch (b) Rounded side notch

Figure 5.18: FEM plots side notch concept

The FEM calculations are done to gather knowledge about the stress distributions in the sensor, but also to test the effects of the various input variables. Sensitivity analysis is done with both the notched geometry as the unnotched geometry. The latter is done to test the effects of certain parameters without the influence of the notch. For both the side notch concept as the centre notch concept the sensitivity of the thickness of the bonding layer is analysed. In figure 5.19 the influence of the bonding thickness on the stress raising factor for respectively the centre notch concept and the side notch concept is shown. It has been found that for arbitrary dimensions of the sensor there is an optimum in load transfer for the different concepts.

From a production perspective the most desirable way is to apply the adhesive over the full length of the sensor. Therefore the effect on the stress distribution through the sensor having an adhesive layer with a length equal to the sensor length is tested in comparison to a bridge like structure where only the ends of the sensor are bonded. From the FEM analysis it became clear that the difference is negligible and therefore the choice is made to apply an adhesive layer on the total area of the sensor. An additional benefit is that risk of peeling off is strongly reduced by applying the layer to the total length.

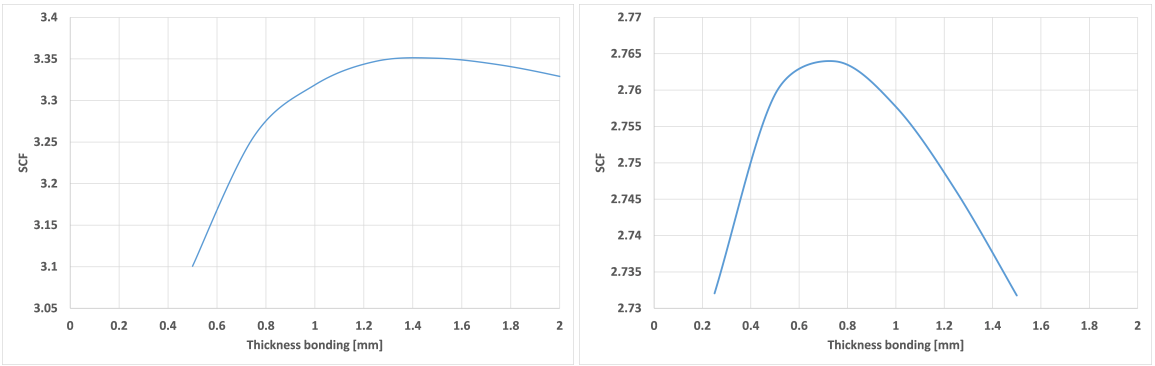

(a) Centre hole concept (b) Side notch concept

Figure 5.19: Influence of bonding thickness on stress raising factor

As stated, there is also sensitivity analysis done with an unnotched geometry to investigate the effects of various parameters and to eliminate the effect of the notch. To do this a rectangular plate with the main dimensions of a sensor is modeled with a bonding layer on the flange of a big stiffener. In this analysis the influence of the length of the sensor plating on the load transfer from the plating into the sensor is looked into. In figure 5.20 the effect of the sensor length on the load transfer is shown. It becomes clear that a certain run-up length is necessary to let the stress be transferred through the bonding layer into the sensor plate. Since a sensor of 1 m is from a practical perspective undesired a workable alternative has to be found. Figure 5.20 shows that there is not a linear relationship between the sensor length and the stress transfer. A good compromise between length and load transfer is chosen to be where the graph becomes more flat at 200 mm.

Shorter than 200 mm would mean a disproportionate difference in load transfer and double the length means only a slightly better load transfer.

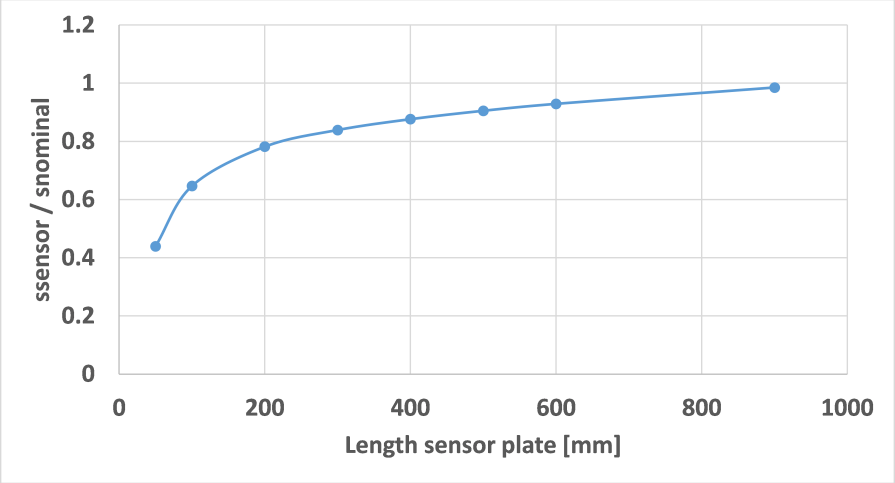

Figure 5.20: Influence length sensor on load transfer relative to applied loading

Trade-off concepts

An advantage of the concept with the circular hole is that it is a geometry frequently discussed in literature and easy to produce. A disadvantage is the necessity of a weld or weld like geometry. In case of a real weld, the hypothesis is; that because of the short welding length, the uncertainty of the quality will pay out in scatter. The production of a weld like geometry will raise the price and the complexity of the sensor significantly.

According to the FEA, the devised bending concept does not work as expected. Besides, the added value to proceed with this concept is not seen and therefore it will not be further investigated.

The most promising concept seems to be the side notch concept. For this concept similarity with a DS cruciform joint is assumed because of the physically similar notch geometry. Furthermore, due to the sharp notch the local stresses will be so high that any initial defect or weld will not be necessary since crack growth will dominate and also because the high notch stress will make the base material behave as weld material from a fatigue resistance perspective (recall figure 5.11). When there is not a weld present, this will pay off in reduced scatter. before this concept will be further elaborated, a more in depth analysis will be performed. This will be done to have more certainty in the design and in the assumption of similarity from a fatigue resistance perspective with a DS cruciform joint.

To have more certainty in the side notch concept the NSIF method will be adopted to calculate for both geometries the notch stress intensity factor (NSIF). According to [21] a Basquin type of relationship does exist for the fatigue resistance of welded joints based on the NSIF. In figure 5.21 this relationship is shown for both steel and aluminium structural details.

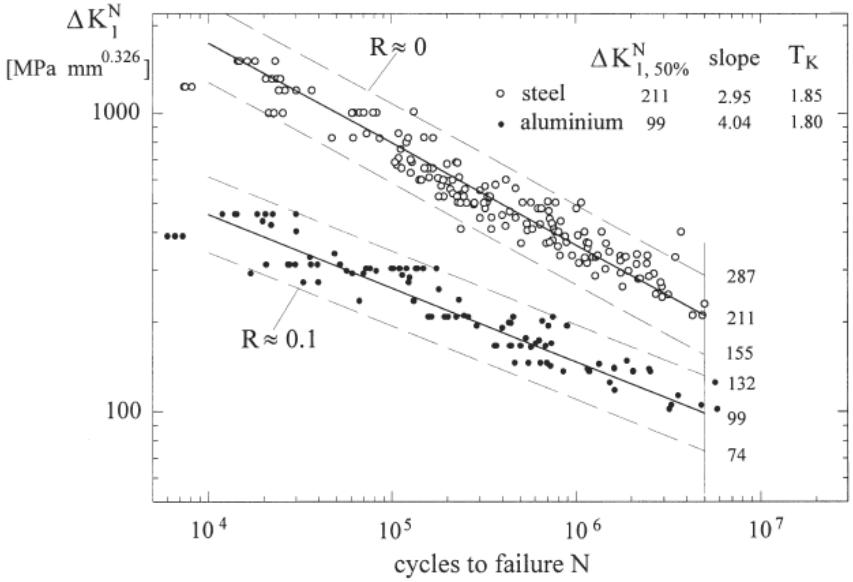

Figure 5.21: Fatigue strength of welded joints as a function of the mode-I NSIF [21]

The unit of the NSIF is $MPa \cdot mm^{1-\lambda}$, where the eigenvalue λ is depending on the angle 2α shown in figure 5.22b. Since the notch angle of the sensor is equal to the weld angle of the DS cruciform joint namely 135^o, the units of the NSIF are equal and a fair comparison can be made. A convenient expression for the NSIF of welded joints under a mode-I loading is according to [21]:

$$K_I^N = k_I \cdot \sigma_n \cdot t^{1-\lambda_I} \tag{5.2}$$

In [21] a curve fitted solution for the parameter k_1 is found for a DS cruciform joint. For a rectangular specimen with two edge V-notches, which is the geometry of the sensor, a curve fitted solution for the NSIF is presented in equation 5.3 obtained from [27].

$$K_I^V = f(\alpha,\gamma) \cdot \sigma_n \cdot w_I^\lambda \tag{5.3}$$

With the function f based on the notch angle 2α and the relative notch depth $\gamma = 2l/w$. Since the nominal stress σ_n can be assumed to be equal for both equation 5.2 and 5.3. Interesting is to calculate K_I^N/σ_n and K_I^V/σ_n for a combination of a sensor geometry and a welded joint geometry, if these values are comparable that indicates that the fatigue resistance characteristics are similar based on the relationship in figure 5.21. This calculation is done for a combination of a sensor and a DS cruciform joint with geometries defined in table 5.1. For the sensor, $2h$ is the length, w is the greatest width, 2β is the notch angle, and $w-2l$ is the smallest width. For the DS cruciform joint, t is the plate thickness, L is the cross plate thickness, and 2α is the weld angle. The weld reinforcement length and height, respectively l_w and h_w are defined as h for the DS cruciform joint. With the dimensions of the sensor as the basis, the dimensions of the DS cruciform joint are chosen in such a way that physical similarity can be assumed. The plate thicknesses of the welded joint are equal to the smallest width of the sensor, the weld angle is equal to the notch angle. The weld reinforcement length and width are calculated to be goniometric similar to a fictitious weld angle in the sensor. The calculation of the weld reinforcement is shown in equation 5.4. Performing the NSIF calculation gives the results presented in equation 5.5.

$$l_w = h_w = \frac{l}{\cos\beta} \cdot \sin 45^o \tag{5.4}$$

$$K_I^N \approx 12.52 \cdot \sigma_n \qquad K_I^V \approx 12.52 \cdot \sigma_n \tag{5.5}$$

The NSIF values stated in equation 5.5 together with the relation in figure 5.21 are a good indication that the sensor and the DS cruciform joint are similar from a fatigue resistance perspective. The goal in the end is to test the hypothesis that the fatigue resistance of the sensor behaves according to the TS concept. This analysis

based on the NSIF method indicates that the fatigue resistance of the sensor behaves according to the fatigue resistance of a DS cruciform joint, with the TS concept this can be translated to the fatigue resistance of any standard aluminium welded joint.

Table 5.1: Dimensions used in the NSIF calculation

Table 5.2: Sensor

Parameter	Value
h [mm]	100
w [mm]	50
2β [^{0}]	135
l [mm]	20

Table 5.3: DS cruciform joint

Parameter	Value
t [mm]	10
L [mm]	10
$l_w = h$ [mm]	37
$h_w = h$ [mm]	37
2α [^{0}]	135

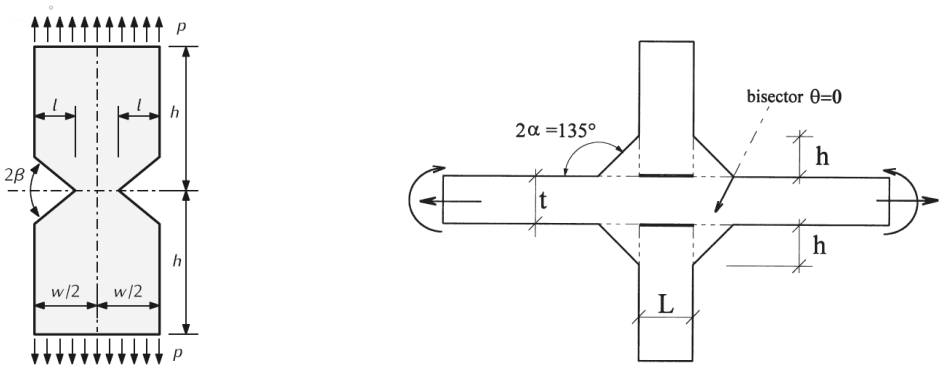

(a) DENT geometry [27]

(b) DS cruciform joint [21]

Figure 5.22: Definitions of dimensions

5.3. Detail design sensor

In this section the side notch concept will be further elaborated. There will be focused on the production of the sensor, the choice of the adhesive, and the interaction between the sensor, bonding, and the plate. Furthermore the mechanisms involved in the working of the sensor will be discussed.

5.3.1. Side notch concept further elaborated

The stress distribution in the sensor concept shown in figure 5.16 is established in two ways. On one hand the stress is raised by the reduction of the cross sectional area. This reduces the lifetime compared to the corresponding welded joint. On the other the stress will locally be raised due to the sharp notch ($\rho \rightarrow 0$), which should be similar to the notch of the DS cruciform joint with which similarity must be demonstrated. This superposition of stress raising by reduced sectional area and due to the sharp V-shaped notch will be discussed here. The stress raising factor on the far field stress due to the reduced area is described by:

$$K_s = \frac{A_1}{A_2} \tag{5.6}$$

With A_1 and A_2 defined as respectively the largest and the smallest cross sectional area. When the notch radius goes to zero ($\rho \rightarrow 0$), the local stress at the notch becomes asymptotic and singular, has no unambiguous solution and goes in theory to infinity ($\sigma \rightarrow \infty$). To deal with this, William's asymptotic solution [33] derived in 1952 is used to calculate the stress distribution at a sharp V-shaped notch. It can also be numerically approximated by performing a FEM calculation. Since K_S is known because of the geometry of the sensor, the contribution of the stress, due to the V-shaped notch is the superposition on the stress raising factor K_s. When performing this calculation for various notch depths, one can see the effect of the notch depth on the

maximum stress. The notch radius in the considered calculation is equal to 0.3 mm. In figure 5.23 the superposition of the notch stress, due to the reduced sectional area, and the singular notch stress can be seen in quantitative comparison. What can be observed from figure 5.23 is that although the notch stress raising factor is slowly decreasing for larger notch depths, it is virtually constant.

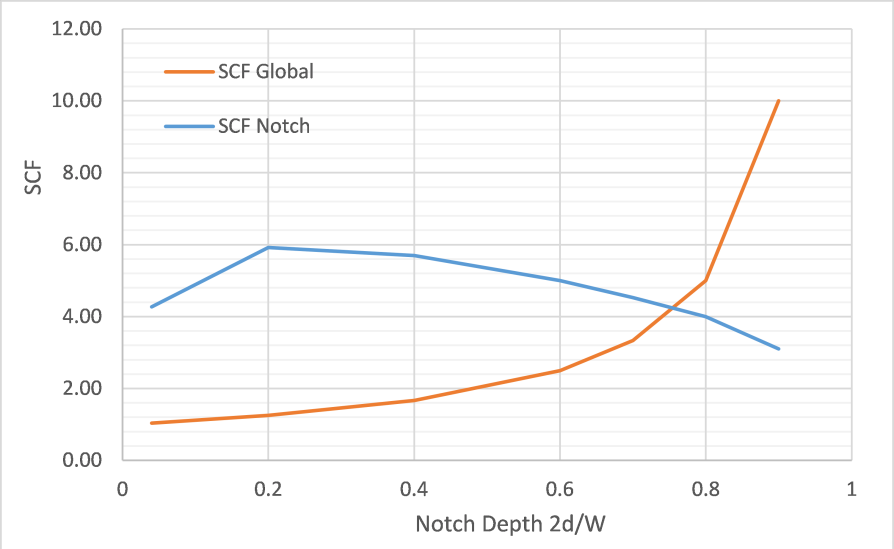

Figure 5.23: Superposition of notch stress

The factor on lifetime compared with the considered structural detail scales exponentially with the relevant fatigue resistance slope m. If at this stage the single slope fatigue curve from [4] is used $m = 3.78$, the factor on lifetime LTF compared with underlying structure can be calculated as follows:

$$LTF = K_s^m \tag{5.7}$$

As function of notch depth, the lifetime factor is shown in figure 5.24. Note that the SN curves are based on the nominal stress rather than the peak stress at the notch and therefore the lifetime factor is based on *SCF Global* in figure 5.23.

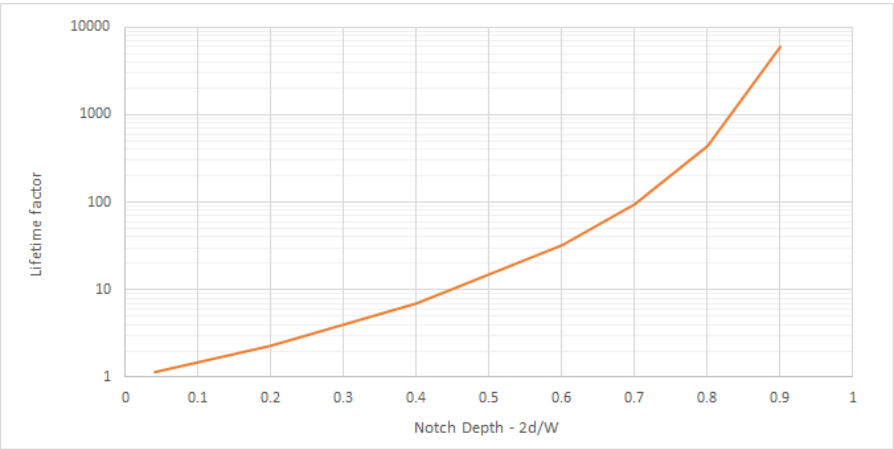

Figure 5.24: Factor on lifetime compared with underlying structure as function of notch depth

Because of the sharp notch, the local stress at the notch will exceed the yield stress at relatively low far field stresses. This is not an issue and is in fact one of the criteria to initiate a fatigue crack. It does become problematic if the nominal stress at the cross section exceeds the yield stress. The latter puts a limitation on the geometry of the sensor. The maximum expected stress in the sensor should be lower than the maximum expected stress multiplied with k_s during a mean time frame of two years.

About the sensor material a choice has to be made, there must be on the one hand similarity with the HSC structure and on the other, it must be strong enough to resist the increased stress in the sensor. The hull of the HSC are typically constructed from aluminium alloy 5083 H-111 which has both for the welded and unwelded situation a yield stress of 125 MPa. Aluminium 5083 H-321 has a yield strength of 215 MPa for unwelded material. Since it is not the yield stress but the Young's modulus which is governing the crack growth, both alloys can be used to manufacture the sensor. Note that the sensor will be placed at a high stressed area in the hull and that the stresses are raised due to the geometry. Since the governing failure mode has to be fatigue and the stress has to stay below the yield stress, the aluminium alloy with the highest yield stress: 5083 H-321 is preferred.

The HSC structures are designed to not exceed the yield strength. This means that it is safe to state that the maximum expected nominal stress at the considered sensor location in the worst case scenario, is equal to 125 MPa. In section 5.3.2 a negative stress raising factor $k_s = 0.85$ is mentioned due to the bonding. Taking this into account; the maximum stress raising factor is $K_s = \frac{215}{125 \cdot 0.85} = 2.0$. This yields to a factor on lifetime of approximately $LTF \approx 2.0^{3.78} = 14.4$. If there is more information about the expected far field stress at the sensor location, a higher k_s can be realized.

5.3.2. Production & installation

To achieve similarity between the sensor and the DS cruciform joint from the TS concept, it is important that $\rho \approx 0$. Therefore a production technique must be found with very small tolerances. Laser cutting is chosen as preferred production method. A notch radius of $O\left(\frac{t_p}{10}\right)$ can be achieved according to the manufacturer. In addition, laser cutting provides a clean cut when the right settings are used. There will be aimed on notch radii $\rho < 0.5$ mm, which means that the plate thickness has to be $t_p < 5$ mm. In table 5.4 the laser cutting settings used for the production are shown. The laser cutting machine used is the Trumpf trulaser 3030 6Kw. Not only the settings but also the state of maintenance of the machine plays a big role in the quality of the product.

Table 5.4: Laser cutting settings used for the Trumpf trulaser 3030 6Kw

Parameter	**Value**
Power [kW]	6
Cutting velocity [mm/s]	65

The structural adhesive selected for the bonding of the sensor to the ship's hull, is Araldite 2021, a two component toughened methacrylate adhesive system. This adhesive, based on a modified type of acrylic, is fast curing and offers high strength and toughness [15]. For a short summary of the technical specifications, see table 5.5. The choice for this specific bonding is made because it provides an excellent bond to aluminium and because of its good mechanical properties. In addition to that it has a very good resistance to chemicals and water, which is important because it has to withstand the harsh environment on board of ships. The preliminary FEM calculations indicated that the bonding layer can withstand the loading on the sensor. Since the displacements are typically very low, the stresses will also be low. In the practical tests of the sensor the bonding will be tested on full scale in the harsh environment of a ship's hull. In appendix A the installation procedure is presented.

Table 5.5: Summary of technical specifications Araldite 2021-1 [14]

Parameter	**Value**
σ_y [MPa]	42
τ_y [MPa]	25
ν [-]	0.3
E [MPa]	1800
G [MPa]	692

Beside the stress raising factor due to the geometry of the sensor, the stress will also be decreased because of the distribution of the stress through the bonding into the sensor plate. The effect and sensitivity of this phenomenon will be discussed further in this section.

Bonded joint design
The bonding can be seen as an composite with a layer metal, in the middle a layer adhesive and on top a layer metal. As expected has the adhesive layer the lowest stiffness of the three, the goal is therefore to make sure this layer will not fail under the forced displacement present in the ship's structure. Calculations will be performed to prove this. Figure 5.26 shows an FEM plot of the sensor bonded on a stiffened panel.

Influence thickness bonding and thickness control
To get to know the influence of the thickness of the bonding, a sensitivity analysis is done. The FEM calculations show a small sensitivity on the thickness of the bonding on the stress in the sensor, see figure 5.25. It must be noted that there is a optimum from a load transfer perspective.

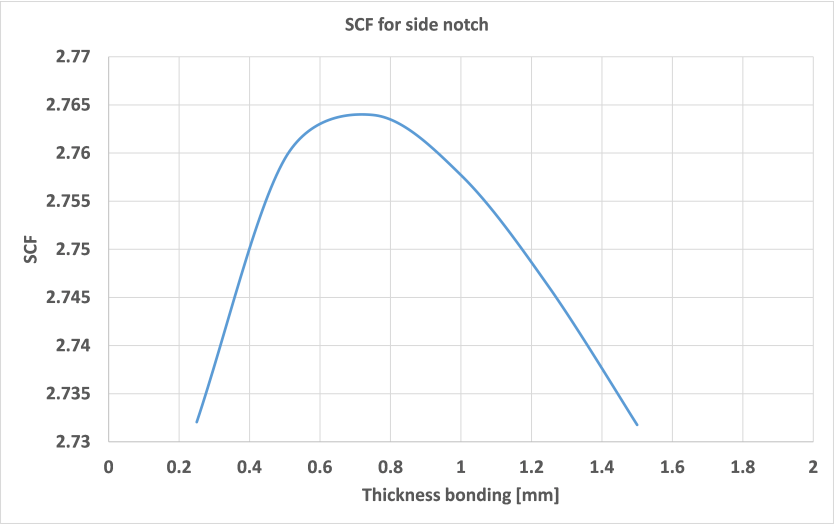

Figure 5.25: Factor on lifetime compared with underlying structure as function of notch depth

It can be seen that the load transfer is the most efficient around 0.7 mm. The bonding thickness will be controlled by sticking a few pieces of double sided tape of 0.5 mm thickness to the sensor. This is done to have more control on the adhesive thickness which reduces the uncertainties. By pressing the glued sensor to the desired location on the ship's hull, the thickness of the adhesive layer is known to be close to 0.5 mm. In the installation instruction, figure A.78, the method can be seen.
To know the stress decrease in the sensor due to the bonding an FE calculation is performed, with an unnotched sensor plate, on a 0.5 mm layer of adhesive attached to an aluminium plate, subjected to an axial loading. It is found that the stress in the sensor plate without the influence of a notch is 85% of the stress in the plating. This means that this has to be taken into account as a negative stress raising factor $k_s = 0.85$.

Design of adhesive joints
The maximum shear stress to overcome for the adhesive layer, occurs when the sensor starts to yield.

$$\tau_{mean} = \frac{\sigma_y \cdot t \cdot W_{small}}{A_{sensor}} \tag{5.8}$$

The mean shear stress at failure of adhesive consist, according to[18], of an adhesive factor K, a metal factor M, and a design factor f. See equation 5.9 till 8.2. The adhesive factor K With τ_{Bmax} as the maximum shear stress at failure of the adhesive joint, d is the thickness of the adhesive layer and G the shear modulus is defined as follows:

$$K = \tau_{Bmax} \cdot \sqrt{\frac{2d}{G}} \tag{5.9}$$

The metal factor M with E as the Young's modulus of the joint material:

$$M = \sqrt{E} \tag{5.10}$$

The design factor f with the joint thickness s and the overlap length l_o:

$$f = \frac{\sqrt{s}}{l_o} \tag{5.11}$$

$$\tau_{Bm} = K \cdot M \cdot f = \tau_{Bmax} \cdot \sqrt{\frac{2Esd}{Gl_o^2}} \tag{5.12}$$

If $\tau_{Bm} > \tau_{mean}$, the bonding complies and will not fail in shear mode before the sensor fails in tensile mode.

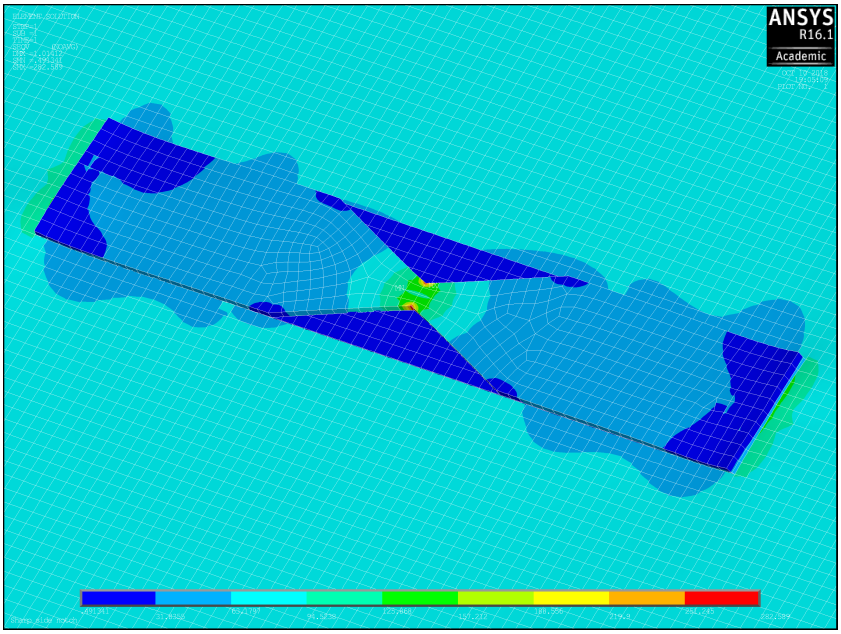

Figure 5.26: FEA of bonded sensor

5.4. Conclusion

First the requirements for the sensor design are set. The most important requirement for the fatigue sensor is to accelerate fatigue damage with respect to corresponding welded joints in order to get fatigue damage data from the vessels in a mean time frame of two years. From the morphological chart three general sensor concepts were derived: The centre hole concept, a bending concept, and a side notch concept. After performing some FEA on a conceptual level, the side notch concept is extracted from the analysis to proceed with. For the side notch concept similarity in fatigue resistance with a DS cruciform joint is preliminary determined with the NSIF method. The sensor will be laser cutted and bonded with a two component adhesive system. Calculations are performed to ensure that the bonding is strong enough to resist the loadings on board.

6

Total stress concept

"If we knew what it was we were doing, it would not be called research, would it?"

Albert Einstein

Before tests can be performed to test the hypothesis that the fatigue resistance of the sensor behaves according to the total stress concept, it is important to first understand the TS concept. In this chapter information will be provided to get understanding of the working of the sensor.

6.1. Total stress parameter

The total stress parameter S_T, see equation 6.1, is an equivalent structural response parameter. This parameter takes for weld toe notches the effective structural stress range $\Delta\sigma_s/(1-r_l)^{1-\gamma}$ and a notch crack growth integral I_N including size effects into account [4].

$$S_T = \frac{\Delta\sigma_s}{t_p^{(\prime)\frac{2-m}{2m}} \cdot I_N(r_s,n,m)^{\frac{1}{m}} \cdot (1-r_l)^{1-\gamma}} \tag{6.1}$$

With the crack growth integral I_N defined as follows:

$$I_N = \int_{\left(\frac{a_i}{t_p^{(\prime)}}\right)}^{\left(\frac{a_f}{t_p^{(\prime)}}\right)} \frac{1}{Y_n\left(\frac{a}{t_p^{(\prime)}}\right)^n \cdot Y_f\left(\frac{a}{t_p^{(\prime)}}\right)^m \cdot \left(\frac{a}{t_p^{(\prime)}}\right)^{\frac{m}{2}}} d\left(\frac{a}{t_p^{(\prime)}}\right) \tag{6.2}$$

With a_i and a_f as respectively the initial and final crack length. The initial crack length is, in the case of the sensor an fictivious defect since there is no crack manufactured. The assumed initial crack length for welded joints is the MLE value determined in [4]: $\frac{a_i}{t_p} = 5 \cdot 10^{-3}$. The final crack length for a through thickness crack in a plating is defined as the plate thickness. Y_n and Y_f are respectively the notch and far field factor and will be discussed in section 6.1.2. The parameter m is the fatigue resistance slope and n is the elasto-plasticity coefficient. In sections 6.1.1 until 6.1.3 the steps involved in finding the parameters used for solving the integral in equation 6.2 will be explained. Since the geometry of the sensor is not equal to the geometry of a DS cruciform joint the parameters have to be tuned to achieve fatigue resistance similarity. The effective structural stress range is clear and can be used for both geometries, but the crack growth integral and through thickness stress distribution are geometry dependent.

6.1.1. Weld toe notch stress distribution

For cracks initiated at the weld toe, the growth in general is in through thickness direction. This implies that a through thickness based criterion should be a good fatigue design parameter. An obvious through thickness

parameter is the through thickness stress distribution due to a relevant applied loading. The goal is to tune the stress distributions of the DS cruciform joint model in such a manner that it is equal to the stress distribution of the sensor. Knowing the stress distribution over the equivalent plate thickness of the sensor from the FEA, the stress distribution of a DS cruciform joint can be tuned in such a way that it becomes equal to these FEM results. The stress distribution in the cross section of the welded joint depends among other things on the weld load carrying coefficient C_{bw}. Locally the weld geometry induces a change in stiffness and a shift of the neutral axis which makes the weld load carrying. The question is to what extent the weld is load carrying. The parameter C_{bw} gives the factor of the far field stress carried by the weld. This load carrying effect of the weld induces a local bending moment. The shape of the bending moment over the plate thickness is a function of the type of joint, location of the notch and whether there is symmetry w.r.t half the plate thickness. In case of symmetry, which is the case for a DS cruciform joint, the considered bending stress σ_{bw} is only defined for half the plate thickness and is assumed to be the same for the other half. In equation 6.3 σ_{bw} is formulated for $(0 \leq \frac{r}{t_p} \leq \frac{1}{2})$.

$$\sigma_{bw}\left(\frac{r}{t_p}\right) = \sigma_s C_{bw} \cdot \left[4\left(\frac{r}{t_p}\right) - 1\right] \tag{6.3}$$

Before C_{bw} can be tuned, it must be noted that the equivalent thickness on the sensor to be compared with the plate thickness of the welded joint is not the plate thickness itself, but the smallest width in the middle of the sensor. This is because the crack will grow from the sides and the nominal stress is the highest at the smallest cross section of the sensor. Since the notch angle of the sensor is equivalent to the weld angle α of the welded joint, this seems to be obvious. It should be noted that the stress angle β for the sensor is different than on the welded joint. For the sensor this angle is equal to 0^o. For a definition of the different angles see figure 6.28. The effect of this difference in angle is small, provided that the stress distribution and stress intensities can be tuned in such a way that similarity is achieved.

The overall weld toe notch stress distribution for a pure membrane loading, formulated in equation 6.4, is a linear superposition of the linear structural field stress and the weld geometry stress consisting of the non-linear notch stress and weld load carrying stress.

$$\sigma_{nm}\left(\frac{r}{t_p}\right) = \sigma_s \cdot f\left(\frac{r}{t_p}\right) \tag{6.4}$$

Where $f\left(\frac{r}{t_p}\right)$ is a geometry dependent function over the plate thickness and σ_s is the far field stress. For a derivation, see appendix B [4].

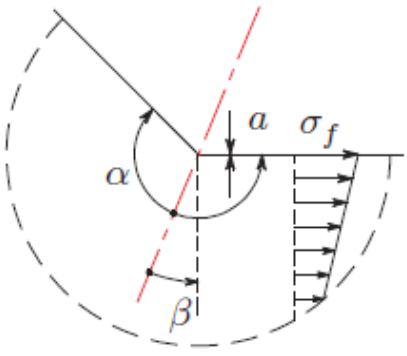

Figure 6.28: Definitions of different angles of notch [5]

In order to get to know the stress distribution over the equivalent plate thickness in the sensor, it will be modelled using *ANSYS* finite element software using solid elements of the type SOLID186. Furthermore a mode-I loading will be applied. From this FEA, the stress distribution will be extracted, see figure 6.29a and 6.29b.

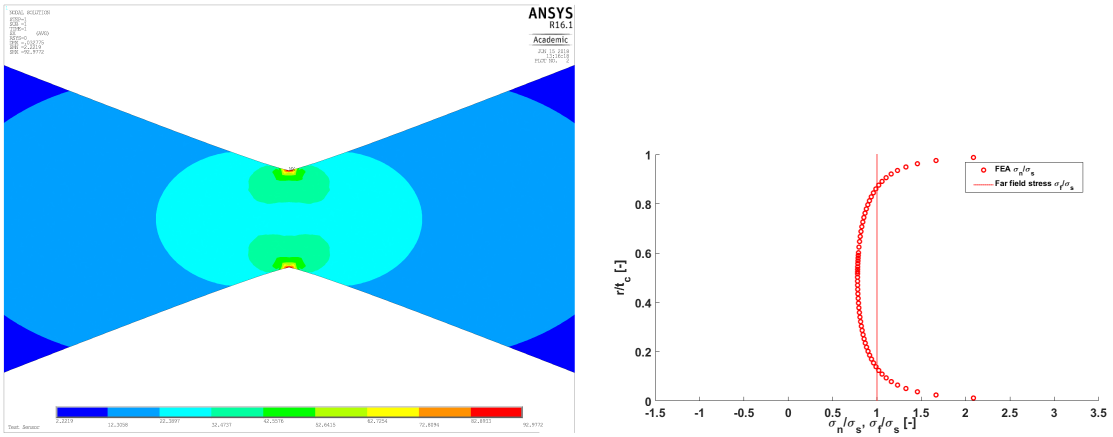

(a) FEM plot of the stresses due to a mode-I loading

(b) Through (equivalent) thickness stress distribution

Figure 6.29: Stress distribution obtained from FEA, both visual and numerical

Now the stress distribution for the DS cruciform joint can be calculated by a semi-analytical approach for different C_{bw} values, to find a solution where the stress distribution is similar. For C_{bw} = 0.09, which means 9% of the far field stress is carried by the weld, a good fit is obtained as shown in figure 6.30.

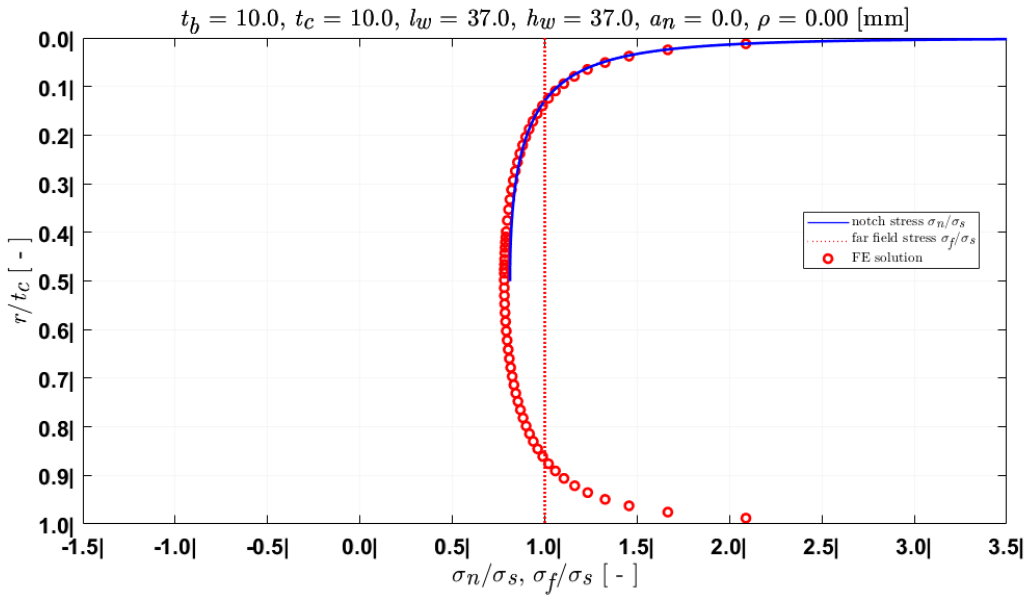

Figure 6.30: Through thickness stress distribution obtained from FEA results of the sensor and from the semi analytical approach for the welded joint with C_{bw}

=0.09

6.1.2. Weld toe notch stress intensity

The stress intensity factor (SIF) K_I is a cracked geometry parameter consisting of a crack size dependent notch- and far field factor, respectively Y_n and Y_f. These parameters relate, as shown in equation 6.5, to the parameter a as the crack length.

$$K_I = \sigma_s Y_n Y_f \sqrt{\pi a} \tag{6.5}$$

Using *ANSYS*, a cracked geometry is modelled in through width direction of the sensor, see figure 6.31a. This is the equivalent of the through thickness direction of the welded joint. The model is created with PLANE82 elements. Then the SIF K_I is numerically calculated from the cracked geometry for different crack lengths, using equation 6.5. In figure 6.31a, the FE model from which the SIF K_I is extraced is shown. This numerical calculation is performed for various crack lengths. The results are shown in figure 6.31b.

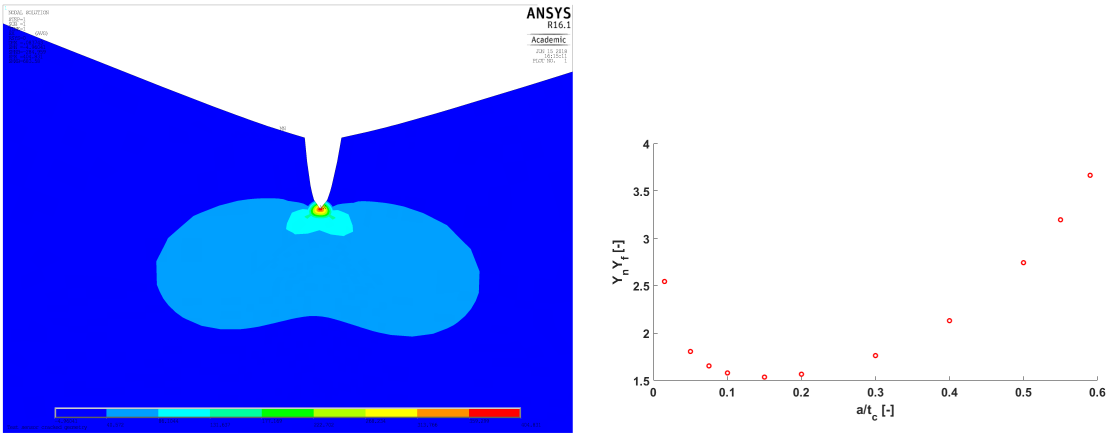

(a) FEM plot of the cracked geometry in the sensor

(b) $Y_n Y_f$ or in terms of the SIF: $\frac{K_I}{\sigma_s \cdot \sqrt{\pi a}}$ obtained from FEA

Figure 6.31: Stress distribution obtained from FEA, both visual and numerical

Next both factors Y_n and Y_f will be calculated and tuned in the DS cruciform joint model. A derivation obtained from [4] is presented in appendix C. Again, it depends on to what extent the weld is carrying the load, expressed in the factor C_{bw}. The best fit is achieved for $C_{bw} = 0.05$, see figure 6.32.

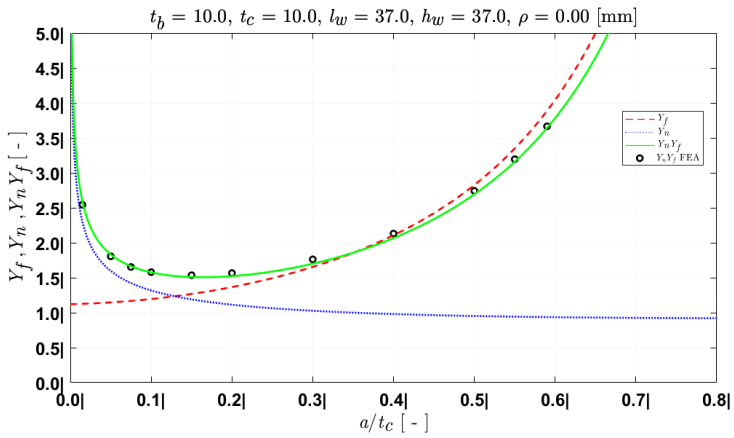

Figure 6.32: $Y_n Y_f$ values obtained from FEA results of the sensor and from the semi analytical approach for the welded joint for various crack lengths with $C_{bw} = 0.05$

6.1.3. Total stress parameter

The weld load carrying coefficient is tuned for both the through thickness stress distribution and for the SIF $Y_n Y_f$. As seen in the previous two sections, there is no unambiguous answer. Therefore it will be necessary to search for a value for C_{bw} satisfying both results. One criterion for this, is that greater value is attached to the goodness of fit close to the notch. Varying C_{bw} for both outputs shows that $Y_n Y_f$ is more sensitive around the notch to change of the coefficient, than the stress distribution. The best fit, taking into account the two outputs, is assumed to be $C_{bw} = 0.05$. Both distributions are presented in figure 6.33.

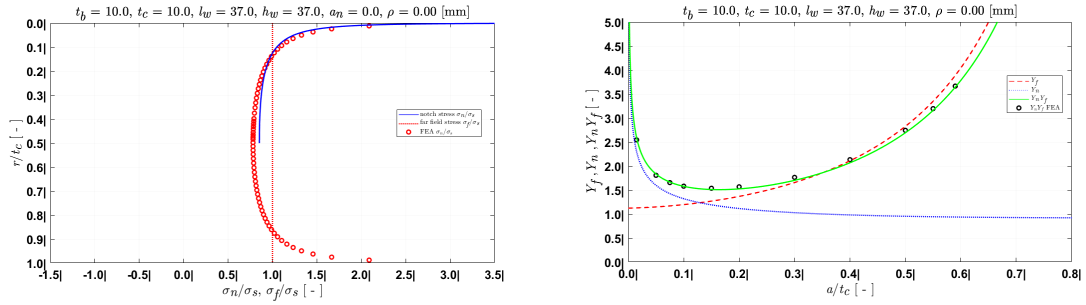

(a) Through (equivalent) thickness stress distribution

(b) Values for SIF $Y_n Y_f$

Figure 6.33: Final values for $C_{bw} = 0.05$

With the weld load carrying coefficient C_{bw} determined, the total stress paramater for any nominal stress range can be calculated. In this way the total stress parameter of the sensor is defined by an equivalent DS cruciform joint.

7

Laboratory testing

Experiments never lie, but you should ask the right question!

Jaap Schijve

In this section the philosophy behind the experiments will be explained. First the question why the experiments are performed is answered. Secondly a brief description of fatigue testing in general is given. Then the determination of the stress range that needs to be applied to reach the desired number of cycles until failure, is explained. Lastly the test setup and the results are discussed.

7.1. Goal of experiments

To come up with a design of experiments there should be a clear idea about the goal of the experiments. The goal is to test the hypothesis of similarity between the fatigue characteristics of the sensor and a DS cruciform joint. When this hypothesis is correct, the fatigue resistance of the sensor can be described by the fatigue resistance curves of the TS concept. The implication of this is that through the total stress parameter, the fatigue resistance can be translated to any aluminium welded joint. To investigate whether the data lies within the scatterband (I.e. within $\pm 2\sigma$ from the mean), extensive testing is not necessary. According to [22], testing 6-12 specimens is sufficient for these preliminary tests. Note that this is merely an indication for similarity in fatigue resistance. For conclusive evidence, more extensive testing is necessary. For this research there will be three specimens tested at three different stress levels. The main advantage of adopting the TS concept is the fact that when similarity with the DS cruciform joint is proven, there is similarity with all aluminium welded joint.

7.2. Fatigue testing in general

Fatigue test programs are usually defined in tables, indicating the number of specimens to be tested for each condition with the corresponding settings. To test the feasibility of the program it is a good practice to start with a single test for each condition. It is possible that these first test results will indicate that the test program must be reconsidered. Fatigue tests to determine an *SN* curve should start with a test at a high stress amplitude. If the tests are started with a low amplitude, the amplitude may be below the fatigue limit. The specimen will not fail (run-out) after a long testing time. The only information gained is that the stress amplitude was below the fatigue limit without knowing how much. If scatter at a high stress level appears to be low, which is usually the case, more specimens can be saved for later tests at low amplitudes. Such decisions require an immediate evaluation of the results of each test after it has been completed. Postponing the analysis until all tests have been completed is not a clever approach [28].

In general, large scatter in fatigue test series should be avoided as much as possible in order to accurately reveal experimental trends of the results. It starts with considerations about specimen production. All specimens for a test program must be made in exactly the same way [29].

7.3. Design of experiments

The hypothesis is that the fatigue resistance of the sensor sensor behaves according to the fatigue resistance of a DS cruciform joint. In the previous chapter is shown how the fatigue resistance model of a DS cruciform joint can be tuned to comply with the sensor. With the findings from chapter 6 the total stress parameter based on a tuned DS cruciform joint can be calculated. Recall the formulation for the total stress parameter, equation 6.1. This equation can be rewritten to equation 7.1 to calculate for a certain total stress value the corresponding nominal stress range.

$$\Delta\sigma_s = S_T \cdot \left(t_p^{(\prime)\,\frac{2-m}{2m}} \cdot I_N(r_s, n, m)^{\frac{1}{m}} \cdot (1-r_l)^{1-\gamma} \right) \tag{7.1}$$

To make an estimation for the to be applied nominal stress range to reach a certain number of cycles the single slope $S_T N$ curve is adopted. Note that the IIW definition is used, which means that also the $N > 5 \cdot 10^6$ cycles fatigue resistance data is used. Note that this specific curve is only used to make an estimation of the necessary stress range, in the analysis after the laboratory tests other definitions or curves can be used to test what gives the best fit.

In table 7.8 the maximum likelihood estimations (MLE's) for the single slope IIW definition mean curve, i.e. 50% reliability curve, parameters are shown. In figure 7.35 the corresponding $S_T N$ curve is shown including the upper and lower bound i.e. 5% and 95% reliability curves with 95% confidence.

Table 7.8: MLE's R50 $S_T N$ curve [4]

MLE	Value
C	12.50
m	3.87
n	0.90
σ (0.95 UB)	0.33

The $S_T N$ curve shows a Basquin type single slope relation, see equation 7.2.

$$log(N) = C - m \cdot log(S_T) \tag{7.2}$$

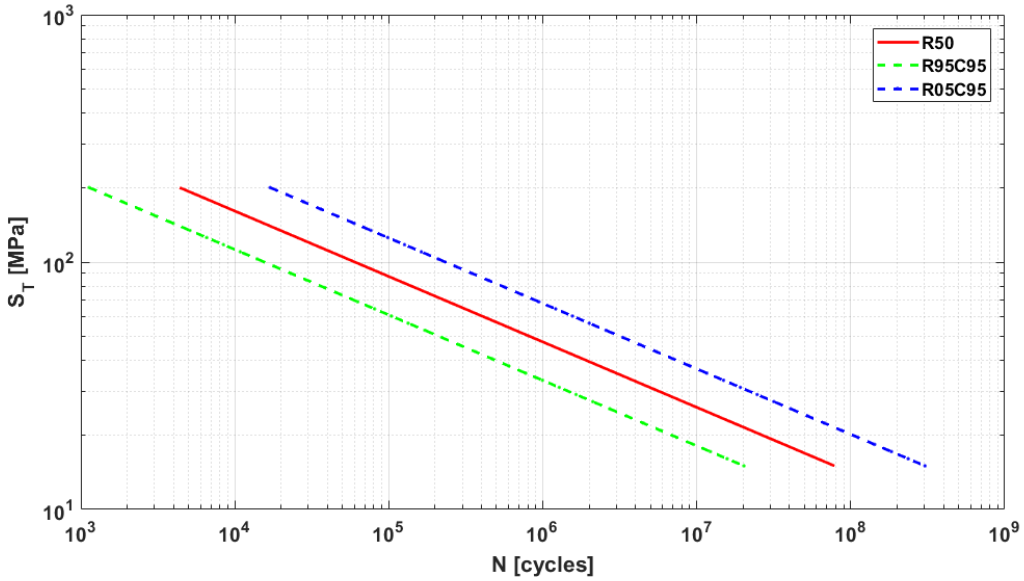

Figure 7.35: $S_T N$ curves for respectively 5%, 50% and 95% reliability with 95% confidence

When the desired number of cycles for the tests are chosen, the corresponding total stress value can be obtained as in figure 7.36. To have enough spread in the data there is chosen to aim for respectively $5 \cdot 10^4$, $2 \cdot 10^5$,

and 10^6 cycles. For the three levels the total stress value is derived from the mean $S_T N$ curve. With the weld load carrying coefficient C_{bw} determined, the next step is to establish the nominal stress range corresponding with the total stress level. Knowing the relevant S_T values and all the input necessary to evaluate the crack growth integral I_N, equation 6.1 can be rewritten into equation 7.1. The stress ranges will be rounded to steps of 5 MPa for convenience. In table 7.9, the scheme for the laboratory tests is presented. In the first column, the aimed number of cycles is presented, since fatigue is a stochastic process it will deviate from the expected number. Because the accuracy of the fatigue testing machine gets lower at low forces, the aim was to get as high as possible forces. To not introduce more uncertainties than strictly necessary, another intention was to keep the mechanical load ratio r_l i.e. $\frac{\sigma_{min}}{\sigma_{max}}$, equal for all tests. For these reasons a mechanical load ratio $r_l = 0.3$ was adopted. This value made the maximum stress for the O($5 \cdot 10^4$) cycles test, just below the yield stress of the material. The minimum and maximum nominal stress at the smallest cross section of the sensor is shown in the last two columns of table 7.9.

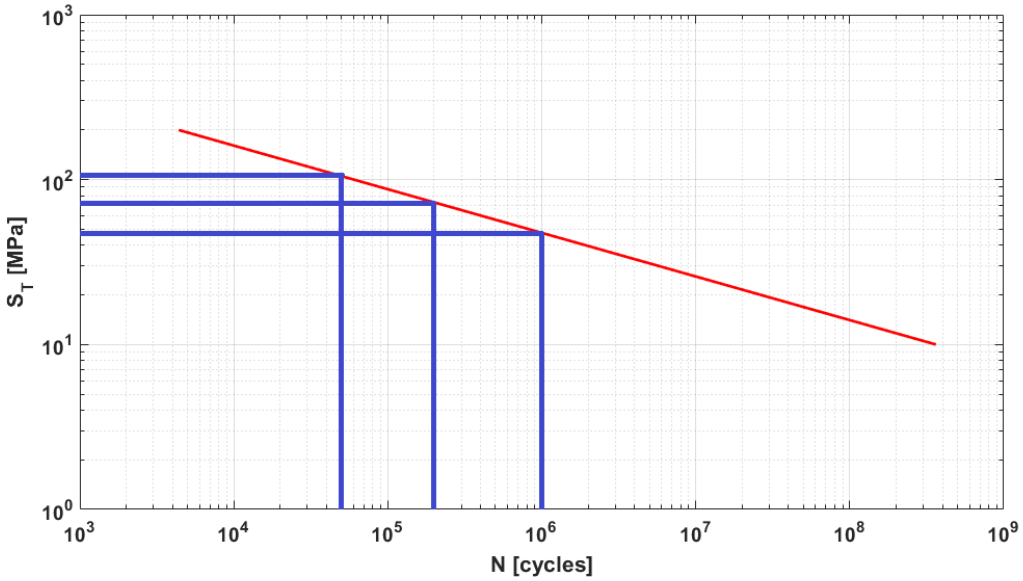

Figure 7.36: 50% $S_T N$ curve with different total stress levels indicated for lab tests

Table 7.9: Laboratory testing scheme

N_f [Cycles]	S_T [-]	r_l [-]	$\Delta\sigma$ [MPa]	$\sigma_{nom,min}$ [MPa]	$\sigma_{nom,max}$ [MPa]
O(5e04)	105	0.3	140	60	200
O(2e05)	75	0.3	100	43	143
O(1e06)	49	0.3	65	28	93

7.4. Results

In this section, the testing set up will be discussed, followed by a discussion of the modifications made to the scheme during the testing period and finally the results will be presented together with a review of the results.

7.4.1. Test Setup

All experiments will be performed on a *MTS* 250 kN test machine, with a load cell of 100 kN. See figure 7.37. After aligning and clamping the specimen, the software will be configured for the test. The necessary input is the mean force, the amplitude of the force and the frequency. The maximum applied frequency is 20 Hz.

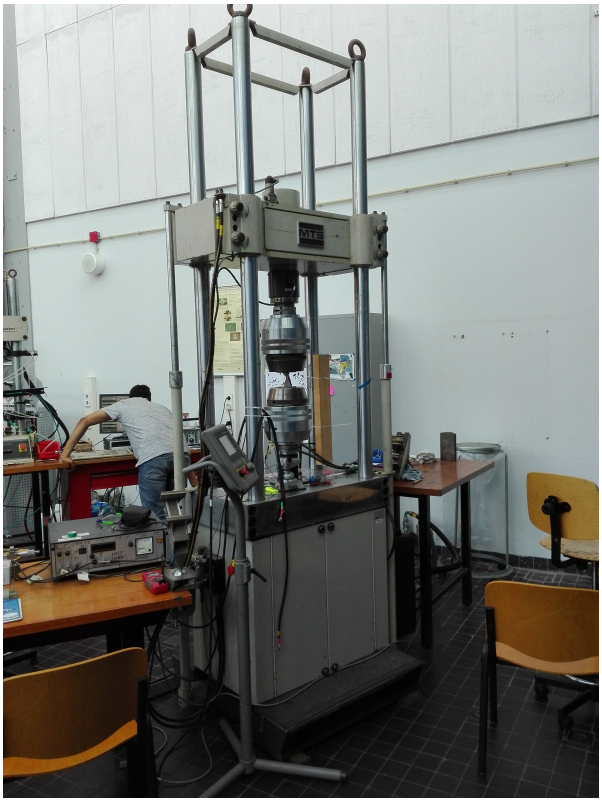

Figure 7.37: MTS 250 kN fatigue testing machine

7.4.2. Modifications of testing scheme

After doing six experiments, it was noted that the zero point was not calibrated to be zero. I.e. the measured loading when no loading is applied and no specimen is clamped in the machine. The control system of the machine displayed a force of 1.424 kN when no force was applied. This influences the mean force and with that the mechanical load ratio r_l. On the amplitude it has no influence. In table 7.10 the effects of this are summarised for the different tests. For the $\Delta\sigma = 65$ MPa test there even was compression involved. Since the difference in mean stress is known, this could be calculated afterwards for the tests already performed. For the remainder of the tests the zero calibration is done.

A second deviation made to the testing scheme is for the last test, since all the $O(10^6)$ cycles tests lasted much longer than the expectation based on the mean curve. The hypothesis was that this was due to the low nominal stress and therefore the maximum stress was raised by adopting a higher mechanical load ratio. For the last test of $N_f = O(10^6)$ a mechanical load ratio $r_l = 0.75$ was adopted with a stress range of $\Delta\sigma = 50$ MPa. This led to a maximum nominal stress of 200 MPa. Unfortunately this test had to be aborted prematurely because the time slot on the testing machine ended.

Table 7.10: Effects of not calibrated zero point

$\Delta\sigma$ [MPa]	$S_{T,req}$ [-]	$S_{T,real}$ [-]	$r_{l,req}$	$r_{l,real}$
140	105	99	0.3	0.148
100	75	69	0.3	0.068
65	49	42	0.3	-0.187

7.4.3. Results and discussion

The most expressive way to discuss the results, is to plot them in a graph with the three S_TN curves of respectively 5%, 50% and 95% reliability. This is presented in figure 7.38. For both $S_T = 99.31$ and $S_T = 74.65$ there are three specimens used.

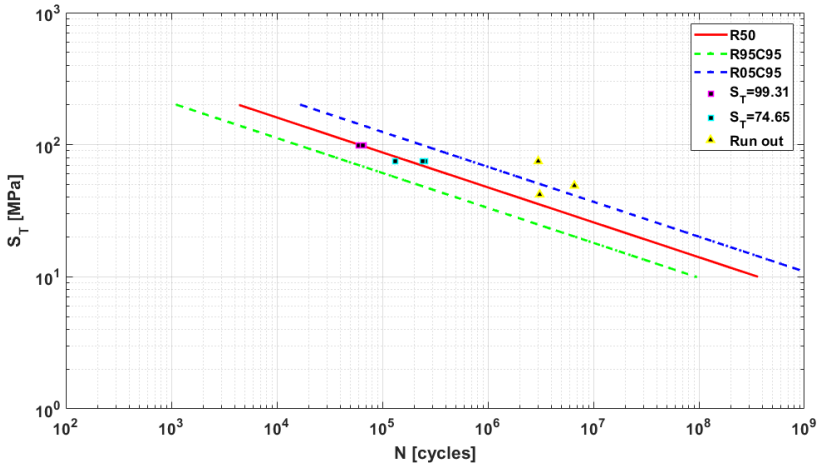

Figure 7.38: $S_T N$ curve with results and run-outs plotted

The 6 results in purple and blue are within the scatterband of the single slope curve and are by approximation following the mean curve. Striking is that all the $O(10^6)$ cycles tests are run outs as already mentioned in section 7.4.2. Also some bad luck is involved, since one of the two 'run outs' that are within the scatterbands is a test which has to be stopped because of an overload due to a power outage on the faculty. The second run out within the scatterbands had to be stopped, as was already mentioned, because the available time on the machine had run out. If the test data is plotted in the RFL model, see figure 7.39, from [4] together with all the test data from literature, it becomes clear that the run-outs could have been failed within the scatterband. The main draw back of these MCF-HCF tests is the time one test consumes.

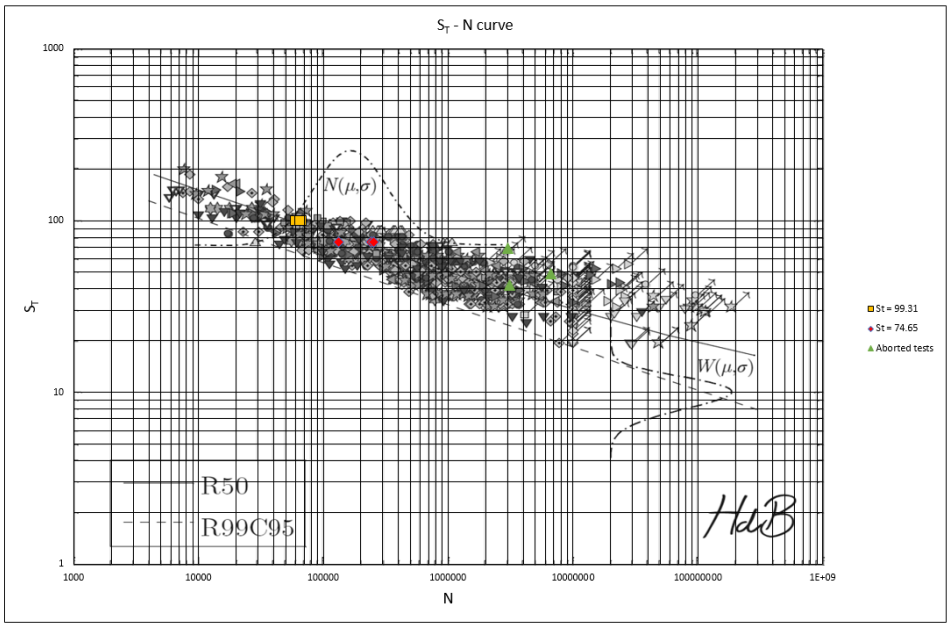

Figure 7.39: Test data plotted with RFL curves and fatigue resistance data from literature [4]

Recall equation 7.1, it becomes clear that the translation from S_T to $\Delta\sigma$ is a linear transformation depending on the geometry of, in this case, the sensor. There is looked into which variables can have an influence on the calculation of $\Delta\sigma$ and with that influence the test results. The sensitivity of a change of the weld load carrying coefficient C_{bw} is investigated and it turns out that the influence is rather low. A doubling and a halving of C_{bw} gives respectively an absolute change of $\Delta\sigma$ of 3.0% and 1.2%. In section 7.3 is stated that for the initial defect size the MLE value is used, this influences the crack growth integral and thus $\Delta\sigma$. It appears that the sensitivity of a_i/t_p on the structural stress range is very large. In figure 7.40 the shift of the mean curve as a

result of the variation in the relative initial crack size is shown. Note that a smaller initial crack size a_i yields to more fatigue resistance which is intuitive. Since there is no weld in the sensor one can state that ($a_i \rightarrow 0$), this especially has a big impact on the tests with the lower stress, because the scatter is large there anyway and the stresses are so low that the initiation period can take very long without an initial defect. Also because of the logarithmic scale a small shift of the curve can induce the testing time to double.

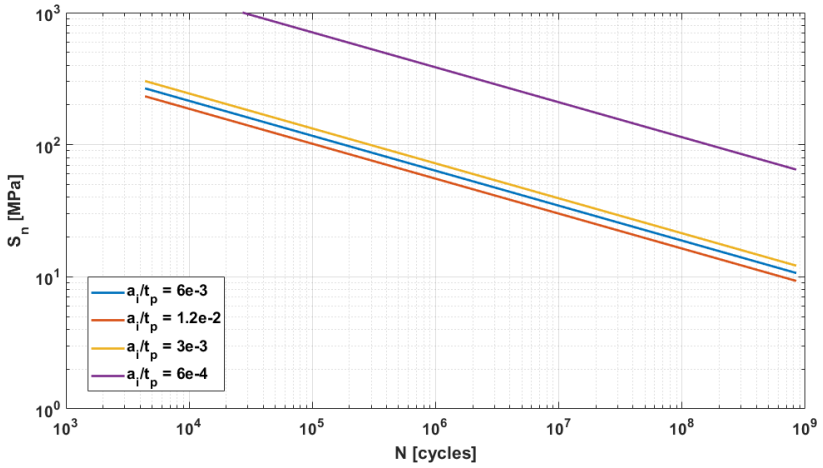

Figure 7.40: Shift of mean curve through varying $\frac{a_i}{t_p}$

7.5. Conclusion

The laboratory tests are performed to test the hypothesis that the fatigue damage sensor behaves according to the TS concept. To test this, the fatigue resistance model of a DS cruciform is tuned to predict the necessary nominal stress to reach a certain number of cycles. The LCF-MCF results are within the scatterband following the mean curve. The HCF tests are all run-outs, some due to bad luck and others because the time it takes to perform a HCF test run. With knowledge gathered it can be said that the fatigue resistance of the sensor behaves according to the TS concept. For more conclusive evidence, more tests have to be performed in the future.

8

Full scale testing sensor

"One single observation can invalidate a general statement derived from millennia of confirmatory sightings of millions of white swans. All you need is one single (and, I am told, quite ugly) black bird."

Nassim Nicholas Taleb

To get more confidence in the design, there is planned to test the sensor on full scale. To prove the concept, it important that there are strain measurements available. Therefore there has been searched for a vessel equipped with strain gauges. Damen is involved in the joint industry project (JIP) VALID II. Goal of the project is to further improve understanding of the fatigue lifetime, to increase the confidence level in predicting the fatigue lifetime and to forecast structural maintenance needs of Coast Guard Cutters [8]. The USCG cutter 'Bertholf' is one of the vessels which is being long-term monitored by MARIN. The opportunity was offered to install one sensor as a proof of concept on board of this vessel. In this chapter the trial and the dimensioning of the installed sensor will be discussed.

8.1. Design of experiment

To come up with the dimensions of a geometry based on the design explained in chapter 5, a number of steps must be taken. First the situation on board of the vessel will be discussed. Among other things, the locations for the measurements and the present loadings and responses. Then the dimensions will be defined for a predefined desired lifetime.

8.1.1. The ship

The considered vessel where the sensor will be applied is the USCGC 'Bertholf' (figure 3.3). For the main dimensions, see table 8.12.

Table 8.12: Main particulars USCGC 'Bertholf'

Parameter	**Value**
Length overall L_{oa} [m]	127.59
Beam waterline B_{wl} [m]	14.9
Design draft T_d [m]	4.39
Displacement Δ [ton]	4500

8.1.2. Possible sensor locations

MARIN has installed unidirectional strain gauges at three locations, these are the same locations as on board of the USCGC 'Stratton' in an earlier research of MARIN. A choice has to be made where the fatigue sensor will be placed, therefore the three possible locations will be briefly discussed hereafter.

Location 1
Strain gauge 1 is located at frame 47 on port side at the gas turbine intake, figure 8.42. There is enough space for the application of a fatigue sensor. A disadvantage of this location is the fact that the plate is locally not stiffened. The consequence of this, is that the sensor could affect the stress in the detail and possibly cause out of plane deformations. The strain gauges will be placed under an angle of 45^o, since according to MARIN the stresses are the highest under that angle for this location.

Figure 8.42: location strain gauge 1 [23]

Location 2
The second location, see figure 8.43, is on a bracket at port side of frame 44. Since there is not enough space to apply the fatigue sensor, this is not a valid option.

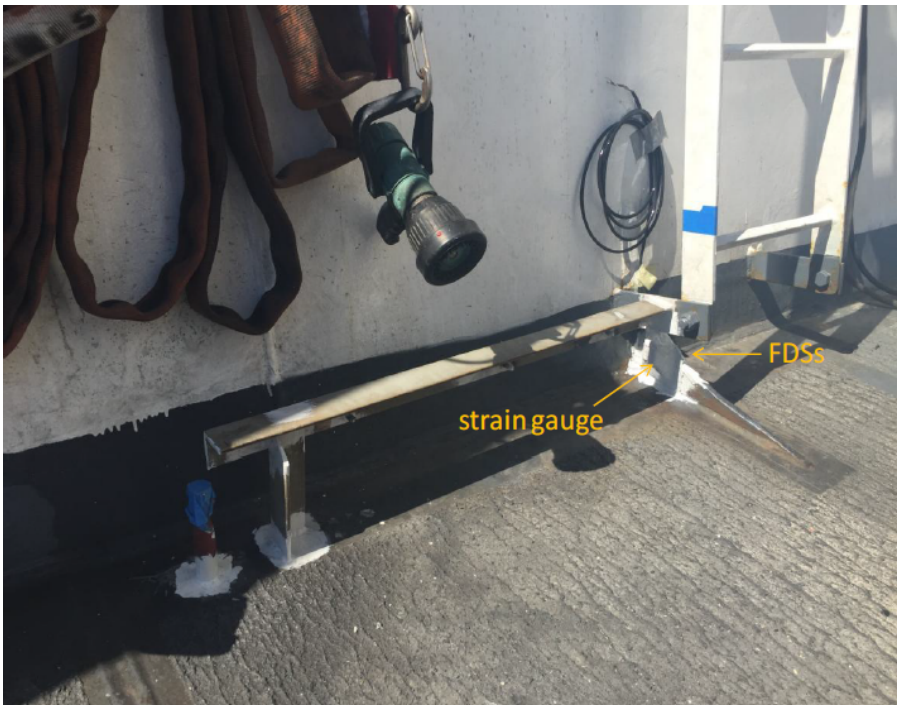

Figure 8.43: location strain gauge 2 [23]

Location 3
Location 3 is on the flange of a stiffener forward of frame 28. According to MARIN, the stress at this location is much lower and the damage is artificially raised by the use of the SN-curve of a butt joint. Since there is aimed for a high stressed location to receive as early as possible feedback on the fatigue damage it a less preferred location.

Figure 8.44: location strain gauge 3 [23]

Preferred sensor location

Taking all of the above into account, sensor location 1 is the preferred location since there is enough space and the highest stresses are reached. Since the stresses are the highest under an angle of 45^o, the sensor and the strain gauges will be placed in the same orientation. In appendix A the sensor installation procedure provided to MARIN is presented.

8.1.3. Analysis sensor location

From previous tests on the 'Bertholf' there is a lot of data gathered, which will be used as input for the sensor dimensioning. There is a design and measured operational profile, design and measured wave data and the calculated stress RAO's. The occurring stresses must be known to determine the required stress concentration of the sensor.

Operational profile

Prior to the Valid project an estimation was made for the operational profile by the USCG. It turned out that the measured data deviated a lot from the predicted operational profile. The difference had a big impact on the damage predictions. The measured operational profile is shown in table 8.13. This operational profile gives fractions of the time sailing a certain speed. The number of operating hours per year is $170 \cdot 24 = 4080$ hours [9].

Table 8.13: Measured operational profile 'Bertholf'

Speed [kn]	Fraction of sailing time [%]	Hours per year [hr]
0	9.1	370
5	39.2	1595
15	39.4	1602
18	7.6	309
21	4.6	189
28	0.4	15

Wave data

Just as in the operational profile, there is a large discrepancy between the predicted and the measured wave data. This can be because the weather was relatively mild during the testing period. But more obvious is that the master of the vessel changes the route in heavy weather and anticipates severe seas. In figure 8.45 the big difference is shown between; on the left hand side the global wave statistics of the North Pacific used for the preliminary predictions in VALID, and on the right hand side the on board measured wave data. In figure 8.46 the measured wave scatter diagram is shown.

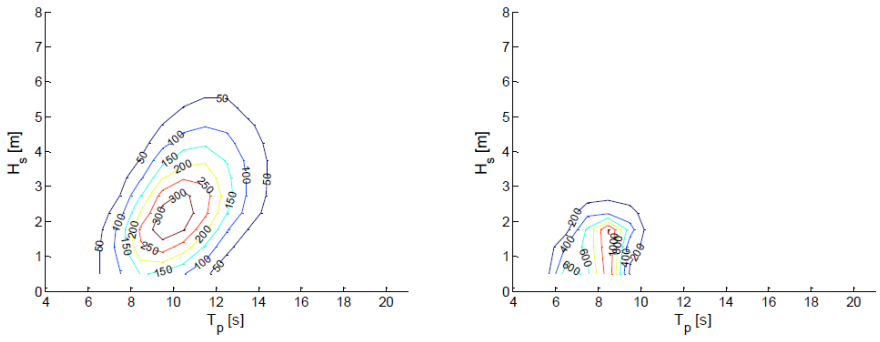

Figure 8.45: Contour of global wave statistics North Pacific scatter diagram (left) and the scatter diagram (right) derived from the measurements [9]

	T_p [s]																
H_s [m]	<5	5.5	6.5	7.5	8.5	9.5	10.5	11.5	12.5	13.5	14.5	15.5	16.5	17.5	18.5	19.5	>20
<1		47	568	459	894	182	157	47	38	19	2	9	14				
1 - 1.5		70	545	574	1051	373	238	192	150	81	137	32	12	10	1		
1.5 - 2		4	111	529	1060	451	112	41	38	55	95	118					
2 - 2.5			41	291	273	261	25	8	14	11	12	26					
2.5 - 3				71	101	49	45	2	3	1							
3 - 3.5					26	24	34	5	10		2						
3.5 - 4					2	16	5	5	12	6	2						
4 - 4.5						6	18	10	8	5	13						
4.5 - 5						10	11			5	1						
5 - 5.5											7						
5.5 - 6											1	8					
6 - 6.5												5	8				
>7																	

Figure 8.46: Measured wave scatter diagram [9]

Stress RAO's

Using Bureau Veritas' hydro-structure software *Homer*, MARIN has derived the Stress RAO's for the 'Bertholf' for different speeds and headings. In figure 8.47 the stress RAO's are shown for different speeds in head waves.

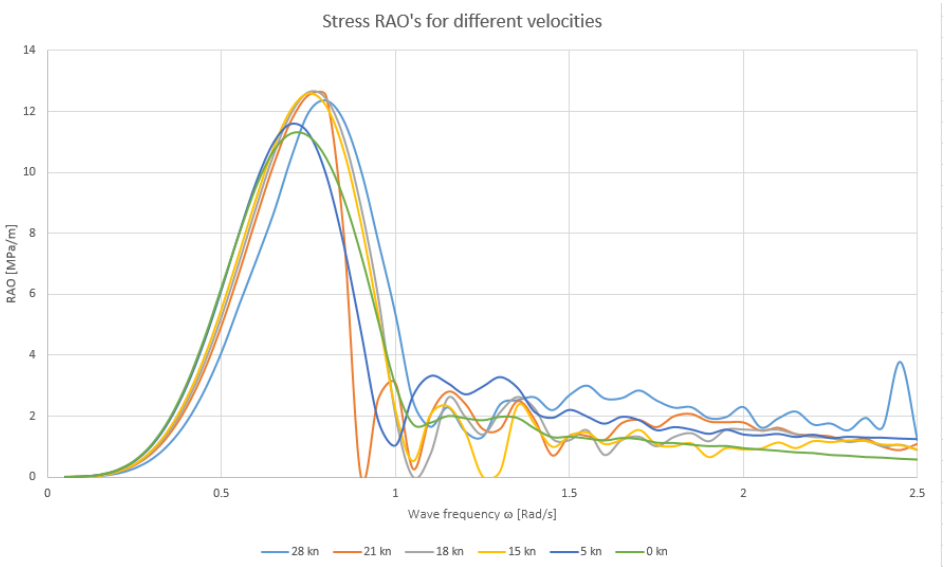

Figure 8.47: Stress RAO's in head seas for various speeds at location 1

What is striking is the height of the maxima in the plot of the stress RAO's of location 1. The maximum value

lies around $12 MPa/m$. If you combine this with the WSD in figure 8.46 where you can see that the maximum wave height is 6m, it is obvious that the occurring stresses are relatively low. Especially because waves of $H_S > 5$ m are very rare as can be seen in figure 8.46.

8.1.4. Sensor design

Since the nominal stresses on board are rather low, the aim is to use a sensor design with a high stress raising factor K_s. Only one sensor could be applied by the engineers of MARIN and the choice is made for a sensor with a width of 28 mm and a stress raising factor of $K_s = 5.6$. In figure 8.48 the dimensions of the installed sensor are shown and a picture of the sensor installed on board can be seen in figure 8.49.

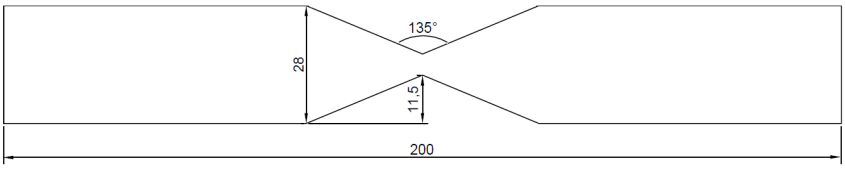

Figure 8.48: Drawing of installed sensor

Figure 8.49: Installed sensor together with strain gauges on board of USCGC 'Bertholf'

Design of bonding

The method to design the adhesive joint is presented in chapter 5. For the sensor applied on the cutter, the mean shear stress on the bonding at yielding of the sensor is calculated in equation 8.1.

$$\tau_{mean} = \frac{\sigma_y \cdot t \cdot W_{small}}{A_{sensor}} = \frac{235 \cdot 2 \cdot 5}{4961.4} = 0.47 MPa \tag{8.1}$$

The allowed shear stress is:

$$\tau_{Bm} = K \cdot M \cdot f = \tau_{Bmax} \cdot \sqrt{\frac{2Esd}{Gl_o^2}} = 25 \cdot \sqrt{\frac{2 \cdot 200E03 \cdot 2 \cdot 0.5}{692 \cdot 200^2}} = 3.0 MPa \tag{8.2}$$

Since $\tau_{Bm} > \tau_{mean}$, the bonding complies and will not fail in shear mode before the sensor fails in tensile mode.

8.1.5. Fatigue lifetime prediction

A first estimate is made using the measured fatigue damage by MARIN over a period of 2.5 year. This accumulated damage is extrapolated to get an estimate of the total life time. For location 1 the accumulated damage over the considered period is equal to $1.8 \cdot 10^{-4}$. Extrapolating the time until the damage reaches unity, gives

a life time of ±14.000 year. This is off course unrealistic and emphasises that the stress and strains are very low. According to the preliminary results of the TS concept based on steel fatigue resistance data, the fatigue resistance slope m is virtually the same as in aluminium welded structures. Therefore a quick estimation of the lifetime of the sensor by extrapolating the accumulated damage can be made:

$$\text{Life time sensor} = \frac{14000}{(5.6 \cdot 0.85)^{3.78}} = 38 \text{ years and 6 months} \tag{8.3}$$

Using Damen's in house MATLAB tool Alufastship, there is also a fatigue lifetime prediction made. This is done using the above mentioned data as input. Another input in the tool is the SCF and the corresponding GL FAT class. Since the hypothesis is that the sensor should have similarity with a cruciform joint, the used FAT class is FAT-71 for steel cruciform joints, see figure 8.50. If the predicted environmental data and the characteristics of the vessel (operational profile and RAO's) are entered in *Alufastship*, this will give a design life time of 11.9 years for the sensor with this stress raising factor. Note that this is based on a design curve i.e. it has 97.5% probability of surviving that calculated lifetime instead of real damage which will more likely correspond with a mean curve. It is thus very likely that the sensor will not fail within the period of this research. However it is a good proof of the feasibility rest of the concept, for example to find issues regarding the installation of the sensor and the strength of the bonding.

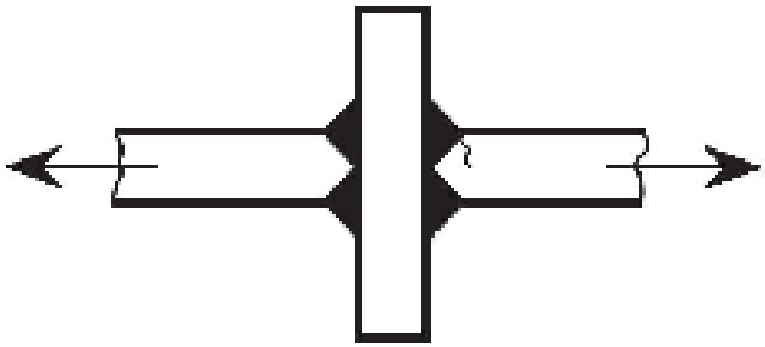

Figure 8.50: Schematic view of weld detail corresponding to FAT-71 [10]

8.2. Results

After six months MARIN returned to the vessel to gather strain gauge data and to inspect the sensor. As expected the sensor was still intact. One of the main reasons to perform the test on board of the 'Bertholf' was to test the bonding in an harsh environment like a ship's hull and to validate and get feedback on the procedures. After six months the bonding was still intact. The installation procedures provided to the equipment installation crew of MARIN are shown in appendix A. The feedback from MARIN was that the installation and inspection procedures were well structured and similar to their own procedures regarding the installation of strain gauges. Figure 8.51 shows a picture of the sensor taken six months after installation. What should be noted from figure 8.51 is the thickness of the layer of paint. This was not well prescribed in the procedure and when another sensor will be applied on a steel hull there must be clear instructions given about the thickness of the layer of paint because now it is not sure if a beginning or fully developed crack will be noticed by the crew. Since the sensor is developed to be produced in aluminium to be applied on the inside of an aluminium hull the layer of paint was not described in the manual.

Figure 8.51: Picture of sensor taken six months after installation

8.3. Conclusion

Since the opportunity was given by MARIN to incorporate the fatigue damage sensor in their testing campaign on board of the USCGC 'Bertholf', first the possible sensor locations are investigated with the information provided by MARIN. The preferred location turned out to be at frame 47 on port side at the gas turbine intake. At this location the highest stresses were measured. However the stresses are still very low and calculations concluded that it is highly likely that the sensor will not crack during this research. Therefore it is merely an experiment to test the installation and inspection procedures and to test the structural integrity of the adhesive layer. After six months the sensor and the adhesive layer were still intact and lessons are learned regarding the procedures.

9

Using sensor data to predict expected lifetime of welded joints

"If you try and take a cat apart to see how it works, the first thing you have on your hands is a non-working cat."

Douglas Adams

The ultimate goal of this thesis is to make a judgement about the lifetime of a ship or a structural detail, based on the failure of one or multiple sensors. In this chapter insight in the statistics behind the fatigue damage mechanisms will be given and the procedure to make a prediction of the expected lifetime of a structural detail will be given. This will be done by first explaining the method on a conceptual level and then explain it with the help of a realistic example. Since the laboratory tests showed for the fatigue resistance of the sensor a good fit with the RFL model, this model will be used in the probabilistic calculations.

9.1. Problem description

The output of the sensor is a through thickness crack, this has to be noticed by the crew and reported to their representative of Damen Shipyards. In appendix D the inspection procedure provided to the ship's crew is shown. Hereafter Damen has to analyse the lifetime of the sensor and make a reliable prediction of the remaining fatigue lifetime of the structure.

Fatigue resistance is based on random processes and thus depending on stochastic variables. This means that both the lifetime of the sensor and the lifetime of the considered structural detail are stochastic variables. There is a hypothetical chance that, for example, there is a combination of a very good sensor and an inferior welded joint such that the structural detail fails before the sensor cracks. Or the possibility of having an inferior sensor with an above average welded joint. Or everything in between these two extreme cases. This is made clear by figure 9.53, where the probability density functions (PDF's) of the fatigue resistance of a structural detail and of a sensor with a stress raising factor $k_s = 2.5$ on a arbitrary stress level are shown. In the figure it becomes clear that there has to be dealt with two stochastic variables and that the translation from a failed sensor to a prediction of the remaining fatigue lifetime of the welded joint cannot be unambiguously made. The difference in the random lifetime distribution between the sensor and the underlying structure shown in figure 9.53 is mainly due to the fact that the stress is a factor higher in the sensor than in the structure. The change in stress induces a difference in the governing fatigue damage mechanism, where for the lower stress crack initiation is governing and for the higher stress crack growth becomes more important and with that the random distribution changes.

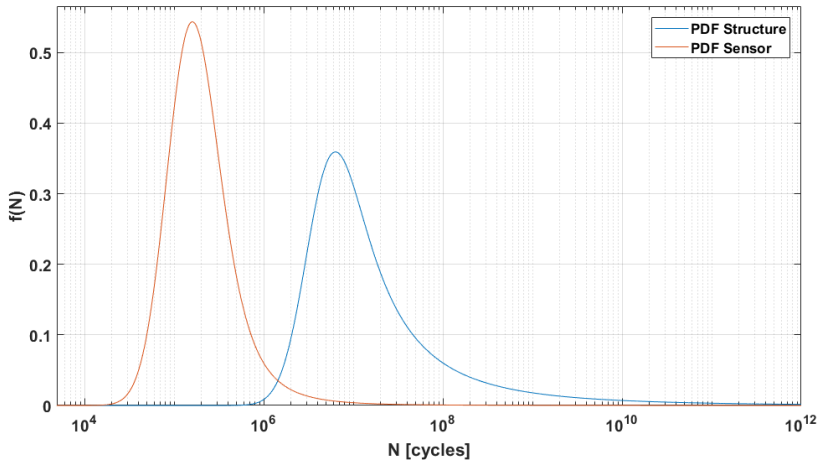

Figure 9.53: Probability density function of a structural detail and a sensor with $k_s = 2.5$ compared to the structural detail at an arbitrary stress level. Extracted from the RFL model based on the data of [4]

In section 3.3, in the research questions was stated that the aim is to develop a sensor that has a mechanical output. This means that after the validation and testing period, the sensor should be able to work without strain gauges. As a consequence, the stresses to which the structure is subjected during its lifetime are unknown.

9.2. Predicting the remaining lifetime of the structure

When a sensor cracks it is unknown what stresses it has encountered. And it is also unknown whether the sensor has failed at the expected value. There are statistically extreme situations possible. It is for example possible that the sensor fails far earlier than its expectation and the welded detail later than its expected lifetime or vice versa. The latter means that the factor on lifetime between the sensor and the structural detail (LTF) cannot be a constant factor.

The fatigue resistance of sensor and the welded joints on board of the ships are assumed to behave according to the TS concept. To be able to make a statement about the lifetime of the structure based on the lifetime of the sensor a dependency between the two must exist. This dependency has to be in the applied stress since the stress in the sensor is a function of the stress in the underlying structure and thus of the corresponding welded joint. When a dependency between the two stochastic parameters is present, a correlation in the joint probability distribution of the two has to be found. To understand the important principles involved, in the following section a simplified model will be build up to eventually come up with the final model.

9.2.1. Joint probability distributions

To be able to make a statement about the lifetime of the structure based on a failed sensor, the relation between the two lifetimes has to be known. The relation between the lifetime of the sensor and the lifetime of the structure is rather probabilistic than deterministic. This is because fatigue is a highly random phenomenon. This section will, using the numbered figures in 9.57 and 9.58, describe the method regarding the calculation of the probabilistics of the fatigue lifetime of the structure based on one or multiple sensors. First a simplified model will be described in order to expand it and come up with the final model.

In the simplified model the fatigue loading will be approximated with a Weibull stress spectrum with fixed Weibull parameters. If subsequently numerous random SN curves for both the sensor and the structure are drawn from the known random distributions, for every combination of random SN curves a damage can be calculated and this can then be translated to a lifetime. Next a Monte Carlo simulation will be performed to calculate the joint probability distribution of the lifetime of the sensor and structural detail. More about this later in this section. For a constant stress spectrum and random fatigue resistance this looks like in figure 9.54a. The shape of this distribution already shows that there is no correlation between the lifetime of the sensor and of the structure. This can be explained by the fact that the only dependency between the lifetime of the sensor and the structural detail is in the applied stress. In this example the fatigue loading is a constant spectrum and the fatigue resistance of the sensor and the structure are not depending on each other. When this procedure is repeated for a stress spectrum with a maximum stress S_0 which is six times higher the effect

of the stress spectrum on the lifetime becomes clear. This can be seen in figure 9.54b.

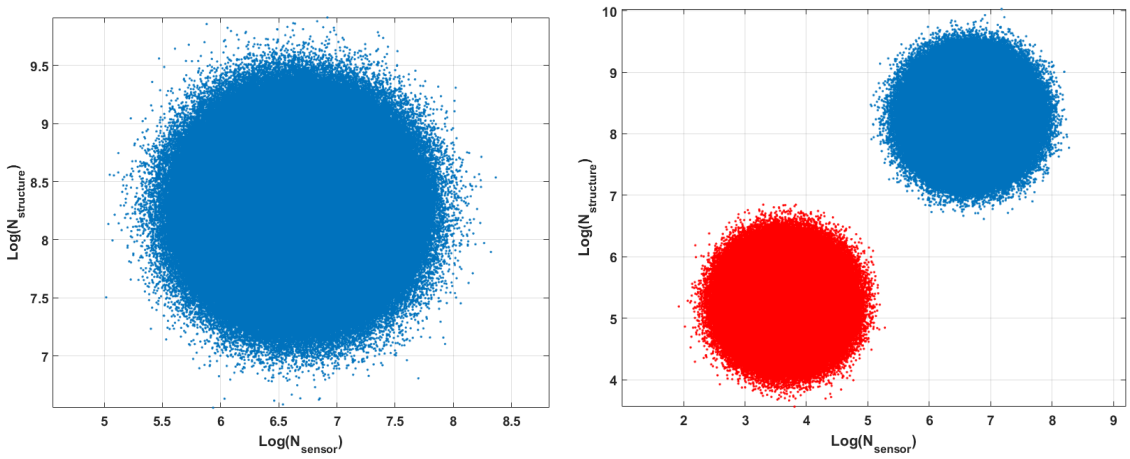

(a) Distribution based on a constant Weibull spectrum $S_0 = S$

(b) Distribution based on Weibull spectra with $S_0 = S$ (blue) and $S_0 = 6S$ (red)

Figure 9.54: Joint probability distribution of logarithmic lifetime

When instead of a constant stress spectrum with respectively $S_0 = S$ and $S_0 = 6S$ a random stress spectrum is used with S_0 uniform distributed between S and $6 \cdot S$ it can be seen that a correlation emerges between the logarithmic lifetime of the sensor and of the structure, see figure 9.55a. Note that the two ends are equal to the red and the blue in figure 9.54b. When this stress range is more expanded, for example $S_0 = U(0.5S, 12S)$ the relation becomes as in figure 9.55b.

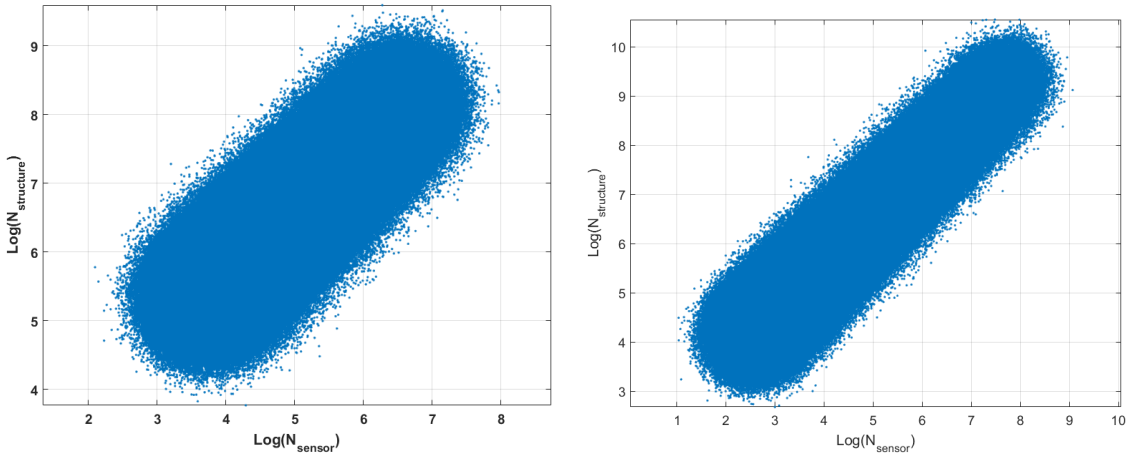

(a) Distribution based on Weibull spectrum with $S_0 = U(S, 6S)$

(b) Distribution based on Weibull spectrum with $S_0 = U(0.5S, 12S)$

Figure 9.55: Joint probability distribution of logarithmic lifetime

Note that spread on the diagonal does not change when the range of S_0 is extended. This becomes more clear when there will be zoomed in on the range $5-6$ on the x-axis. Here can be seen that the extreme values in the uniform distribution do not matter for the part between the ends of the logarithmic lifetime relation. In figures 9.56a and 9.56b it can be seen that the graph with on the x-axis the logarithmic number of cycles ranging from five to six, is the same for different uniform distributions of S_0. This indicates that when the extreme values of a and b in $S_0 = U(a, b)$ are far from any relevant values the relevant part of the graph will remain constant.

Knowing this, the right approach seems to be to first make a prediction of the expected stress spectrum based on the judgement of experts. Since this is only an approximation it is then important to distribute the stress spectra in such a way that the extreme spectra are highly unlikely. As a consequence of this, the remaining middle part of the joint probability distribution becomes invariant of the extreme values of the random distribution of stress spectra.

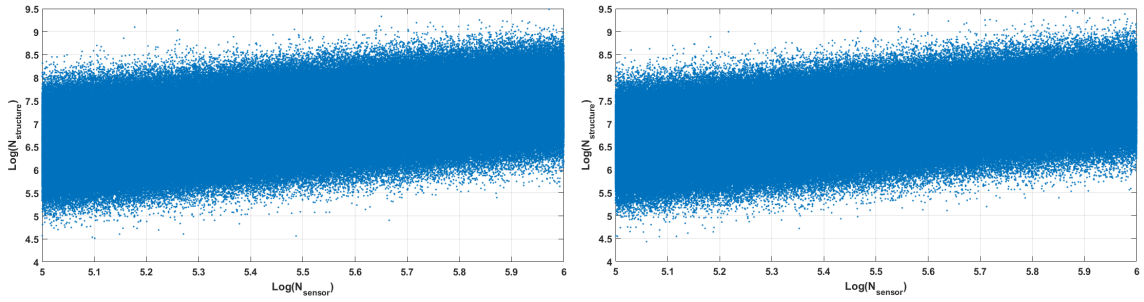

(a) Distribution based on Weibull spectrum with $S_0 = U(S, 6S)$

(b) Distribution based on Weibull spectrum with $S_0 = U(0.5S, 12S)$

Figure 9.56: Joint probability distribution of logarithmic lifetime zoomed in on middle part

With the basis of the model clarified, here the procedure to relate the observation of a crack in the sensor to an expected lifetime of the structure will be discussed in more detail. To keep the overview, the procedure will be explained using the numbered figures **1** to **4** in 9.57 and 9.58.

figure 1
The long-term stress spectrum, i.e. the fatigue loading, can be approximated by a Weibull distribution [13]. This is shown in figure **1** in 9.57. There are two parameters important in this long-term stress distribution: The Weibull distribution shape parameter k and the stress range at a probability of exceedance of 10^{-8}, S_0 (i.e. the stress range that appears once in a lifetime). The once in twenty years stress range S_0 is uniform distributed between a and b. Where a and b are highly unlikely extremes, respectively far smaller and far greater then the expected value. The parameter k describes the convexity of the curve and is uniform distributed between c and d. The sensor and the structure are subjected to the same stress spectrum, however the nominal stress in the sensor is a factor k_S higher for the same number of cycles.

figure 2
Like the fatigue loading, the fatigue resistance is also a stochastic parameter. This means: When there is an arbitrary sensor and an arbitrary structural detail, the fatigue resistance of the two are respectively random draws from the probability distribution. The random draws are independent of each other and there is a chance, however small, that the sensor has an extreme high fatigue resistance and the underlying structure an extreme poor fatigue resistance or vice versa and anything in-between. Figure **2a** shows this behaviour for an arbitrary sensor and structural detail with arbitrary probability distributions over the number of cycles. The random draw from the probability distribution shown in figure **2a**, corresponds with an SN curve. Figure **2b** shows the fatigue resistance curves for an arbitrary combination of a sensor (green line) and a structural detail (red line). In this case, the sensor has an fatigue resistance below-average and the underlying structural detail has an above-average fatigue resistance. In reality it can be any combination from the probability distribution.

figure 3
Now there are random draws for the Weibull distribution shape parameters k and S_0 with which an arbitrary stress spectrum can be constructed for the structure. The sensor encounters the same stress, but then a factor higher. The fatigue resistance of the sensor and structure are also two independent random draws from a known distribution. Lastly the operability coefficient OC i.e. the ratio of sailing hours per year and total hours per year will randomly be drawn from a uniform distribution.

The fatigue damage as a result of a stress spectrum can be calculated by applying Miner's rule for the arbitrary structural detail and sensor. An accumulated damage equal to one indicates a failure, the total

lifetime calculation in number of cycles and in number of year is shown in equation 9.1. Note here that the accumulated damage is a function of the geometry of the sensor, the fatigue resistance, and the encountered stress.

$$N_{Lifetime,cycles} = \frac{1}{D_{accumulated}} \cdot \sum(N_{i,\ spectrum}) \quad N_{Lifetime,year} = \frac{20yr}{OC \cdot D_{accumulated}} \tag{9.1}$$

With for $D_{accumulated}$ the accumulated damage as a result of the long-term stress distribution and $\sum(N_{i,\ spectrum})$ the total number of cycles in the long-term stress distribution.

This gives a logarithmic lifetime in number of cycles for both the structural detail and the sensor. The relation between the two can be presented as in figure **3**.

figure 4

Since both the fatigue loading and the fatigue resistance are random parameters, the result in figure **3** is a random draw from the joint probability distribution. However the joint probability distribution of the sensor lifetime and structural lifetime is not known. Especially when the fatigue resistance and long-term stress distributions follow arbitrary probability distributions it cannot straightforward be calculated analytically. Performing the method from figure **1** till **3**, provides only a single point of the joint probability between the lifetimes.

Running the above described model repeatedly is sampling from an infinitely large population, namely all possible outcomes of the model [2]. When this sample is large enough, numerically the joint probability distribution between the lifetime of both the sensor and the structure is approximated in figure **4a**. Finally a probability of the structure surviving a certain lifetime of N_Y cycles based on the observation of a failed sensor after N_X cycles is desired. Since the calculated accumulated fatigue damage and thus the lifetime of the sensor is already a function of, among others, the encountered stress spectrum the stress has not to be measured directly. In other words, the observed realization i.e. a crack in the sensor after a certain time is the consequence of a certain stress history and can be called an indirect measurement of the encountered stress. In figure **4b** the probability calculation is schematically presented. The steps involved in calculating the probability of the structure exceeding a certain lifetime based on the observed lifetime of the sensor will be discussed here. First the observed lifetime of the sensor is not the exact lifetime per se. What is known is that when a lifetime is observed, the exact lifetime of the sensor is in the interval between the time of the previous inspection and the time of the observation of a crack in the sensor. In words the interesting conditional probability is as follows: The probability of the structure getting older than N_Y years given that the a crack in the sensor occurred between now (N_X) and the previous inspection of the sensor ($N_X - d$). To calculate this probability, Bayes' theorem is adopted, see equation 9.2. Bayes' theorem describes the probability of an event, based on prior knowledge of conditions that might be related to the event [3].

$$P(A|B) = \frac{P(B|A) \cdot P(A)}{P(B)} \tag{9.2}$$

$$A : (N_{structure} > N_Y) \quad B : (N_X - d \leq N_{sensor} \leq N_X)$$

In figure **4b**, a schematic representation of the variables A and B is shown. The number of realizations above N_Y is the variable A. The variable B corresponds to the red and the blue realizations together. This means that the $P(A)$ is the sum of the realizations that comply with A divided by the total number of realizations. The probability of B is the number of realizations meeting the statement in B divided by the total number of realizations. $P(B|A)$ is a conditional statement which is equal to the realizations in red and blue divided by the number of realizations in red. And finally the probability which is the required output: $P(A|B)$, this is the number of realizations in blue divided by the number of realizations in red and blue together.

When equation 9.2 is looped over all possible combinations of N_X and N_Y a probability chart is created like in figure **4c**. For any observed lifetime of the sensor, the probability of the structure exceeding a certain lifetime can be read on this chart.

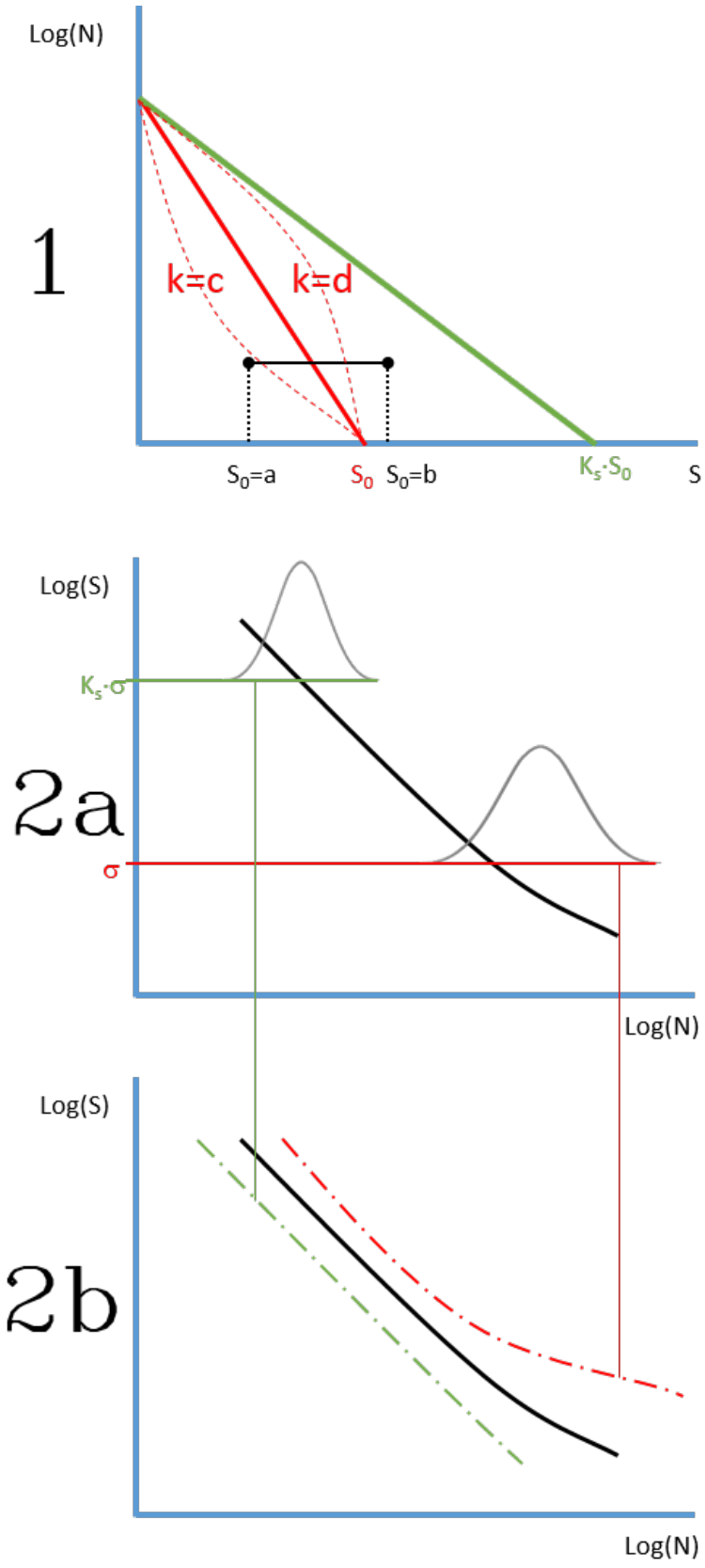

Figure 9.57: Schematic steps involved in probabilistic calculation figures **1-2b**

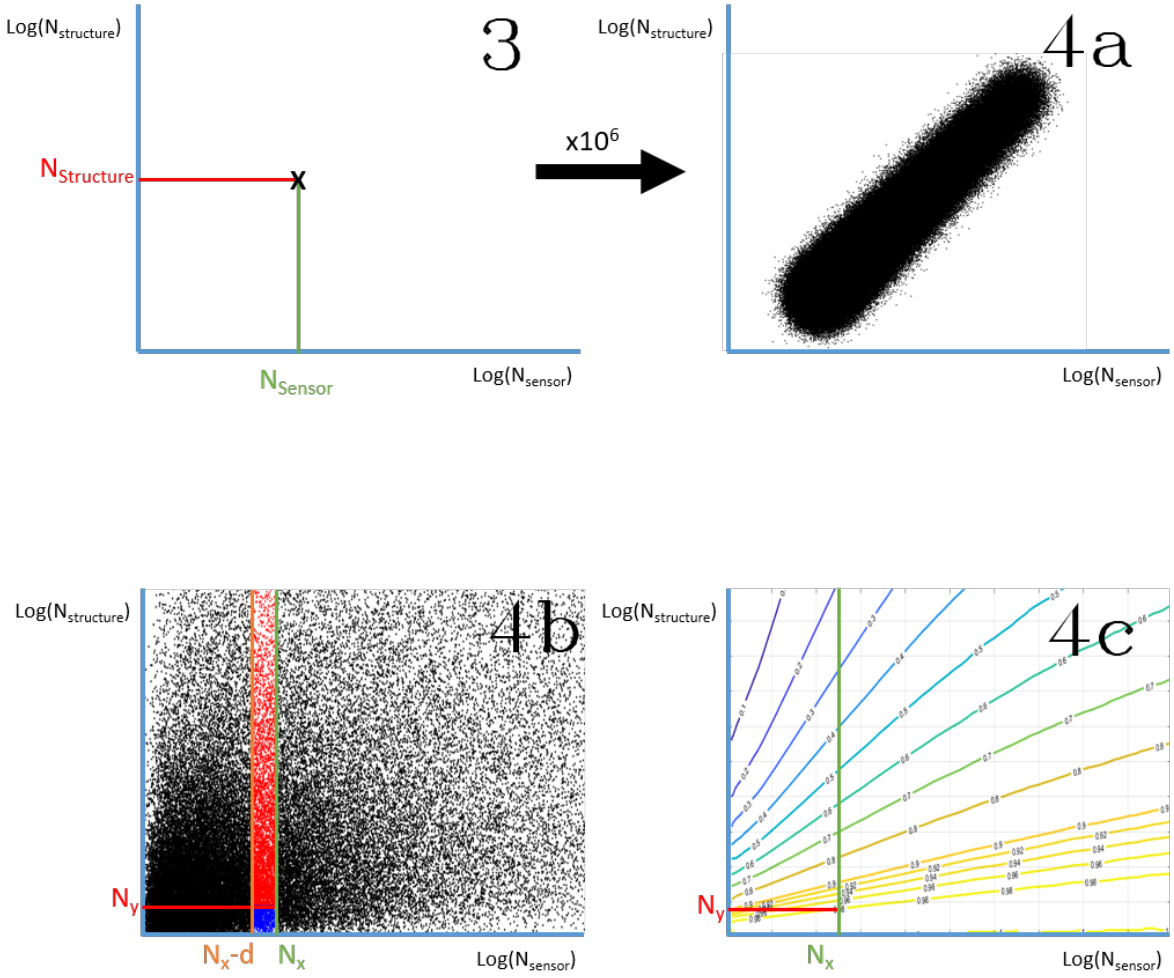

Figure 9.58: Schematic steps involved in probabilistic calculation figures **3-4c**

9.2.2. Realistic example

In this section the schematic overview of the procedure in the previous section will be applied on a realistic example. In this example the probability that the expected lifetime of a welded joint exceeds twenty years will be related to the lifetime of a sensor. The welded joint in this example is a DS cruciform joint, note that this can be calculated for any welded joint. The dimensions of the structural detail can be seen in table 9.15.

To have an indication about the design loads, there will be looked for a constant stress spectrum where $P(LT_{structure} > 20yr) = 0.975$. The 97.5% probability is chosen since the current standard within Damen high speed craft is to have a fatigue design with a 97.5% chance of surviving twenty years. A stress spectrum with the following Weibull parameters is meeting this criterium: $S_0 = 100$ MPa and $k = 1$. Figure 9.59 shows the design stress spectrum. Suppose the sensor has a desired lifetime of two years, then k_s will be tuned such that probability of the sensor surviving two years is 50%. For this example, this means $k_s = 4.5$. Practically this means for the geometry $W_{widest} = W_{smallest} \cdot \frac{4.5}{0.85}$. The factor for the geometry becomes $\frac{k_s}{0.85}$ due to the bonding layer, described in chapter 5. This means for a sensor of length 200 mm and width 50 mm, that the smallest width at $L = 100$ is equal to 9.45 mm.

Table 9.15: Dimensions DS cruciform joint example

Parameter	Value
t_b [mm]	8.0
t_c [mm]	8.0
l_w [mm]	8.0
h_w [mm]	8.0

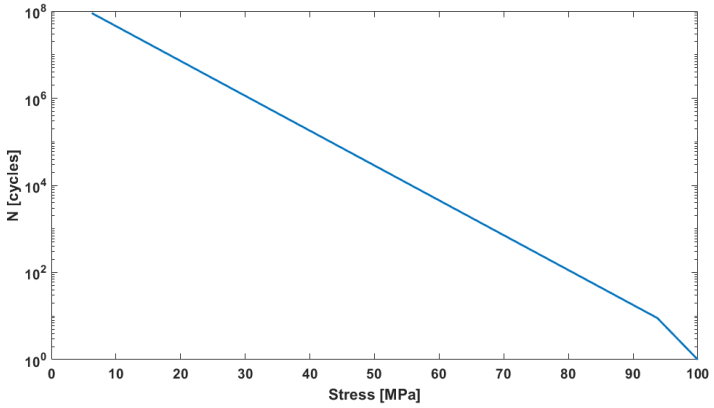

Figure 9.59: Stress spectrum which gives a 97.5% chance of the welded joint surviving twenty years

The next step in this process is to calculate random long-term stress spectra around the expected spectrum. The stress spectra will be uniform distributed by taking random draws of $S_0 = U(25,400)$ MPa. Figure 9.60 shows the random drawn stress spectra. The knuckles around one cycle is because of the definition used that the lowest stress corresponds to one cycle. Note that the stress in the sensor follows the same spectrum with stress multiplied by factor k_s.

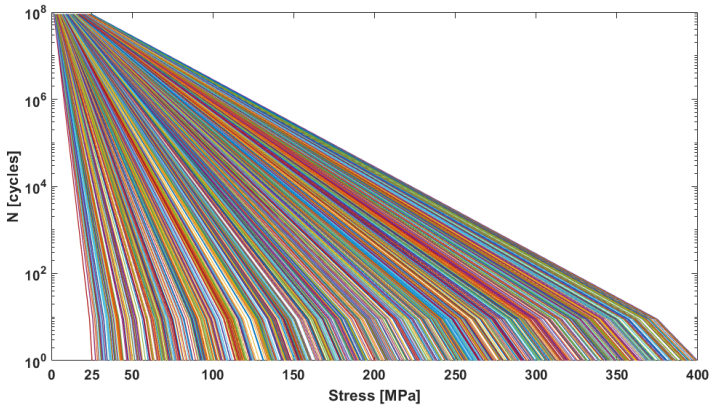

Figure 9.60: Random long-term stress spectra

For every random chosen stress spectrum a corresponding combination of random drawn SN curves for both the sensor and the welded joint will be created. Figure 9.62 shows these random drawn curves. Note that the points in the curves are calculated for a discrete number of stress levels corresponding with the loading. Unlike the stress spectra the SN curves of the sensor and the welded joint are independent of each other. This is done for the sensor and for the welded joint.

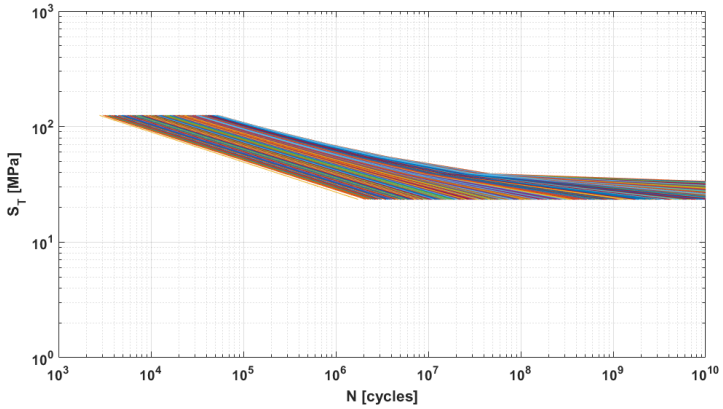

Figure 9.61: Random drawn $S_T N$ curves (RFL approach)

Next the logarithmic lifetimes for each combination of sensor, structure, stress spectrum and operational profile will be calculated. The operational profile is uniform distributed between 0.25 and 4. Here can graphically be noted that a correlation exist between the lifetime of the sensor and the lifetime of the structure. Since fatigue damage already implicit contains information about the encountered stress cycles, operational profile etc. it is not necessary to measure the strains.

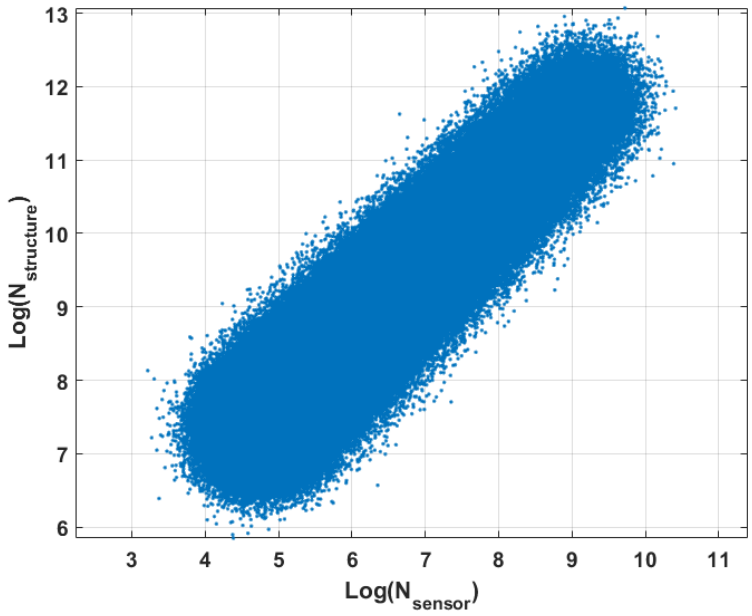

Figure 9.62: Joint probability distribution of the logarithmic number of cycles sensor plotted against welded joint for $1 \cdot 10^6$ random realizations (RFL approach)

The combination of both lifetimes gives a numerical relationship between the two lifetimes. In other words, when the sensor fails, a probability of a certain minimal lifetime of the considered structural detail can be calculated. Equation 9.2 shows the method of calculating the probability of a minimal lifetime of a certain structural detail based on the observed lifetime of the sensor. Suppose the sensor cracks after 1.5 years and the previous inspection was three months before. In the begin of this section was stated that the question of this example is: What is the probability of the welded joint surviving twenty years, given the total lifetime of the sensor? To calculate this, equation 9.2 can be used with in equation 9.3 the statements for A and B showed.

$$A : (N_{structure} > 20) \quad B : (1.5 - \frac{3}{12} \leq N_{sensor} \leq 1.5) \tag{9.3}$$

After performing the Monte Carlo simulation with 10^7 simulations, the probability chart can be calculated as described in the previous section. Figure 9.63 shows the probability chart. The chart can be read by finding the intersection between $X = 1.5$ and $Y = 20$. For a more precise result the probability can also be numerically calculated, see equation 9.4.

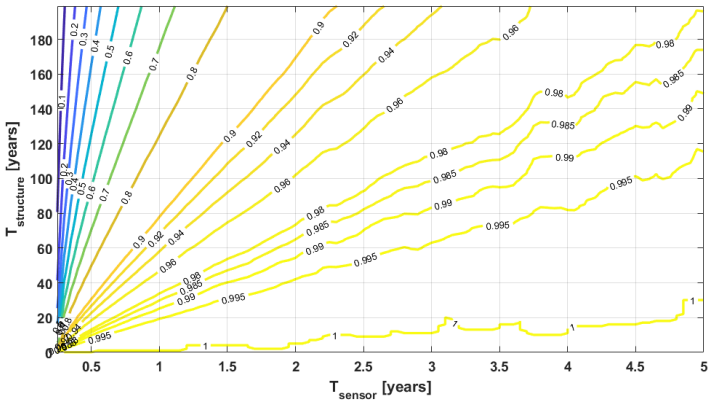

Figure 9.63: Probability chart, gives the probability $P(A|B)$ for any combination of $A : (N_{structure} > N_Y)$ and $B : (N_X - d \leq N_{sensor} \leq N_X)$

$$P(N_{structure} > 20 \mid 1.5 - \frac{3}{12} \leq N_{sensor} \leq 1.5) = 99.9\% \tag{9.4}$$

9.2.3. Sensitivity analysis

When using a probabilistic model it is a good use to perform a sensitivity analysis of the input of the model. This is done by subsequently varying one parameter at a time. Important input parameters are the stress raising factor K_s, the sailing time per year, and the Weibull stress spectrum parameters. Section 9.2 already showed that when the outer limits of S_0 are chosen far from the relevant values, this parameter is invariant for the lifetime in the relevant region. The same yields for the operability coefficient and the shape parameter k. The greatest influence of the outcome is caused by the stress raising factor of the sensor k_s. This is because the dependency between the sensor and the corresponding structural detail is the relation between the encountered stress. The same yields for the dimensions of the corresponding detail. Figure 9.64 shows for $k_s = 1.75$ the probability chart. Compared to the chart for $k_s = 4.75$ in figure 9.63 the probability plot, it can be seen that the stress raising factor k_s controls the angle of the probability contours. It is thus very important to to know the exact stress raising factor

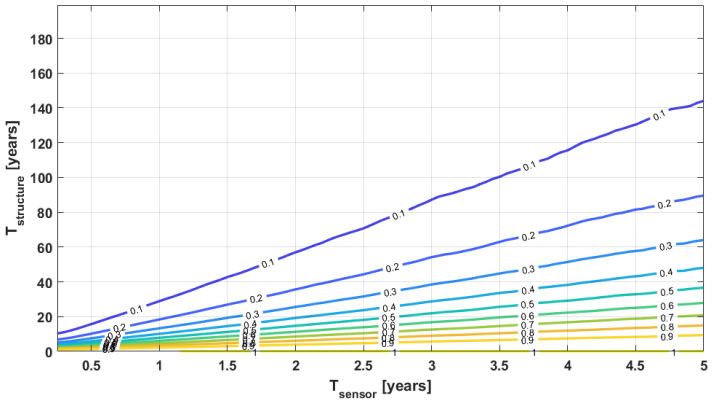

Figure 9.64: Probability chart, gives the probability $P(A|B)$ for any combination of $A : (N_{structure} > N_Y)$ and $B : (N_X - d \leq N_{sensor} \leq N_X)$

To increase confidence in the outcome the choice can be made to use multiple sensors, the hypothesis is that it will decrease the spread on the relation between the logarithmic lifetime of the sensor and of the corresponding welded joint. Multiple identical sensor will be applied in the same location. The same calculation

as described above in this chapter can be applied, with the difference that for the lifetime of the sensor the mean lifetime of the multiple sensors will be used.

In the Monte Carlo simulation this can also be taken into account. In figure 9.65 The logarithmic lifetime relation is show with in black the joint probability distribution for a single sensor and in blue the joint probability distribution for the two sensor case.

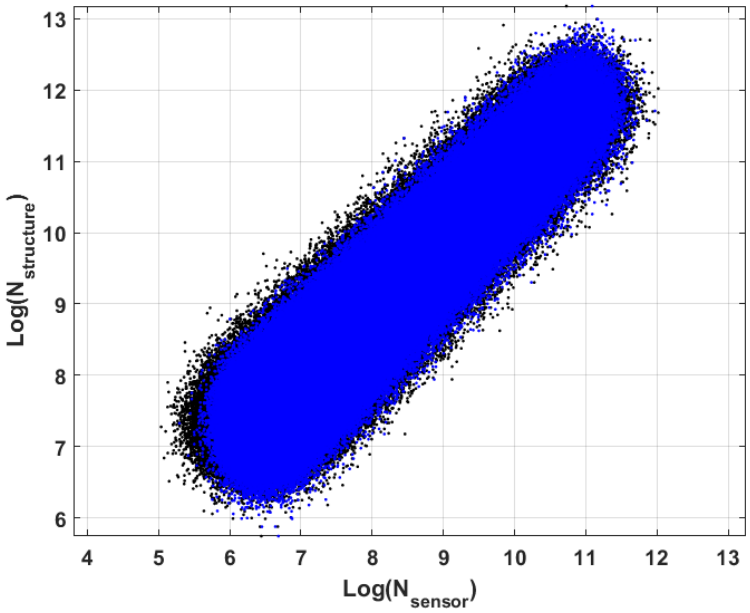

Figure 9.65: Joint probability distribution logarithmic lifetime sensor-structure with one sensor (black) and two cracked sensors (blue)

9.3. Conclusion

Because the fatigue lifetime of both the sensor and of welded joints are random variables one cannot relate them unambiguously. By performing Monte Carlo simulations joint probability distributions are created of the lifetime of the sensor and of a corresponding structural detail. Bayes' theorem is finally used to calculate the probability of a certain welded joint surviving an arbitrary lifetime based on the observation of one or multiple cracked sensors.

10

Effects of implementing the TS concept

"Extraordinary claims require extraordinary evidence."

Carl Sagan

Before implementing a new method it should be known what is the current practice regarding fatigue prediction at Damen Shipyards. Currently the in house tool Alufastship is used, the ideas behind this program will be briefly discussed in this chapter and a schematic overview is shown in figure 10.67. In fatigue analysis there is a loading part and a fatigue resistance part which both play a role in the fatigue prediction calculations. The prediction method is made for the combination of the two. This means that the loading part also has to be revised when implementing new fatigue resistance curves. The implementation of the TS concept will have a great impact on the the fatigue resistance part and thus on the weight of new build ships. The increase of the fatigue resistance in comparison with the currently used method is presented in this chapter.

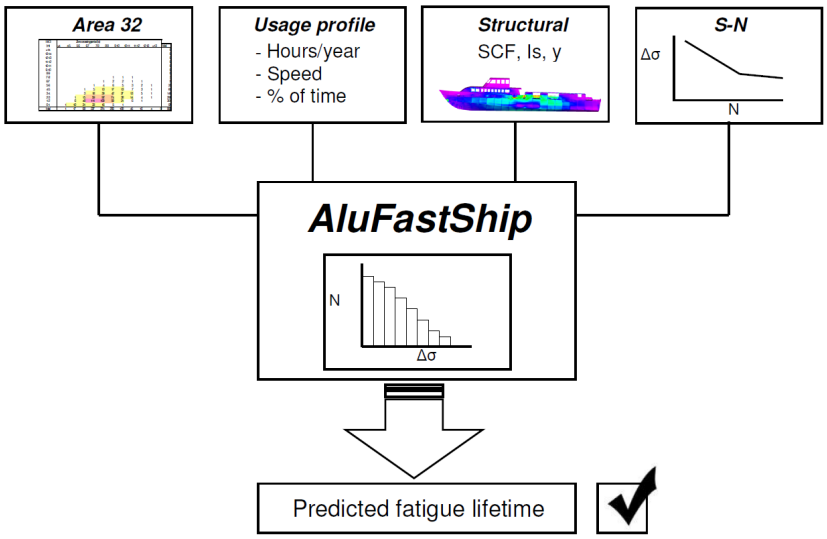

Figure 10.67: Schematic overview of current fatigue prediction procedure in Alufastship [30]

10.1. Current practice

The two main parameters on the loading side of the calculation are the stress levels and the number of cycles per stress level. The input necessary for this is a wave scatter diagram (WSD) of a dedicated area, or one of the by class recommended WSD's. Secondly the operational profile should be entered together with an

estimation of the total sailing time per year. From the wave periods in the WSD the encounter frequency is determined for the different ship speeds.
Using PIAS, SEAWAY or any other hydromechanical program the bending moments per meter wave height can be calculated, the so called response amplitude operators (RAO's). The stress cycles the ship is subjected to have to be calculated. The current cycle counting method in Alufastship translates the ocean wave spectrum, existing of irregular waves, to regular waves. This is done by assuming the wave height of a certain sea state equal to the significant wave height and the corresponding zero crossing wave period. However when this counting method is compared to a spectral approach a difference in results is found. In Alufastship this problem is solved by taking into account the energy in the waves for the different approaches. Since the wave energy is proportional to the wave height squared, the root mean square (RMS) of the significant wave height can be seen as a measure for the energy content in the waves [12]. For regular waves like a sine, the RMS of the significant wave height $H_{1/3}$ is equal to $RMS_{regular} = \frac{1}{2}\sqrt{2} \cdot H_{1/3} \approx 0.35 \cdot H_{1/3}$. The RMS of an irregular wave is typically $RMS_{irregular} = \frac{1}{4}H_{1/3} = 0.25 \cdot H_{1/3}$. The difference in the RMS of both approaches means that the wave energy is overestimated with 40% compared with the spectral approach. To correct for this there is decided to introduce a factor C, see equation 10.1, to scale the significant wave height. In figure 10.68 the difference between the two approaches is visualized.

$$C = \frac{RMS_{irregular}}{RMS_{regular}} \approx \frac{0.25}{0.35} \approx 0.714 \tag{10.1}$$

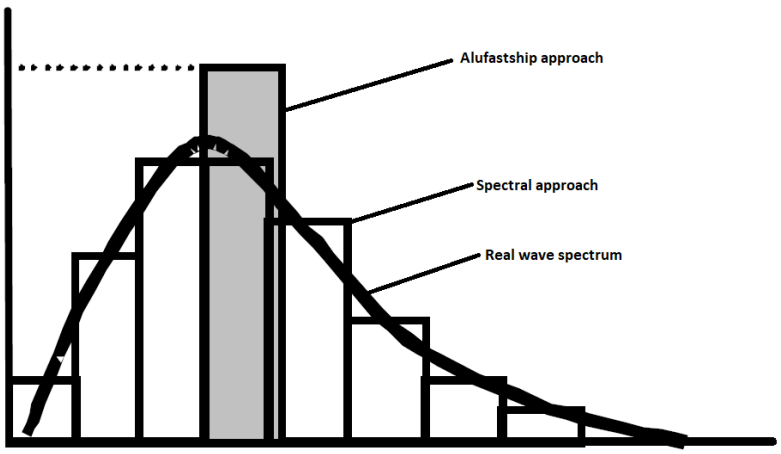

Figure 10.68: Difference in wave spectrum approach between *Alufastship* and the spectral approach

Now the stresses can be calculated by calculating the stress $\sigma = H_{1/3} \cdot C \cdot RAO_{\omega}$ for every entry in the WSD. Optionally the maximum wave height can be truncated, to account only for the lower wave heights to make it more representative. Using the probabilities on every sea state and the total sailing time the stress spectrum can be calculated. If the stress spectrum is known the loading side is complete and this can be combined with the relevant SN curves on the resistance side to either calculate the fatigue damage for a cross section with a particular section modulus or calculate the required section modulus for a certain life time, for example 20 years. Currently the SN-curves of Germanischer Lloyd (GL) are used [10]. For every welded joint there is another design curve.

10.2. Fatigue resistance using TS curves

In the TS concept, one single fatigue resistance curve is adopted for all welded joint details. Therefore a lot more test data is used in comparison to conventional fatigue resistance curves, which increases the confidence and shifts the curve upwards leading to a higher fatigue resistance.
One of the main requirements for this implementation is that the application must remain easy to use. If it's too complex or time consuming it won't be used by the engineers.

There are various approaches to deal with test data the test data used in [4]. There is a single slope formulation where the test specimens are used until the region where a change of slope is noticed. This point is assumed to be at $N \approx 5 \cdot 10^6$ cycles, so all test data beyond this point is excluded from the curve fitting procedure. With this approach a single slope $S_T - N$ curve is obtained following the well known equation:

$$log(N) = C - m \cdot log(S) \tag{10.2}$$

Secondly a $S_T N$ curve is made following a dual slope formulation. This is a continuous dual slope formulation instead of a piece wise linear one like the one adopted by GL for example. The advantage of adopting a dual slope curve is the better description of the fatigue resistance in the MCF-HCF regime due to the change of governing damage mechanism. The dual slope formulation follows the relationship in equation 10.3. Due to the amount of run outs and the low number of data in general in the HCF regime the second slope is very uncertain. In the profile likelihood graph of the second slope m_2 in figure 10.69 this uncertainty is visualized by the profile likelihood graph of the parameter m_2.

$$log(N) = C - m_1 \cdot log(S) - \left(\left(\frac{m_1}{m_2}\right) - 1\right) \cdot log[1 + exp\{log(S) - log(S_c)\}^{-m_2}] \tag{10.3}$$

With S_c as the stress coalescence point

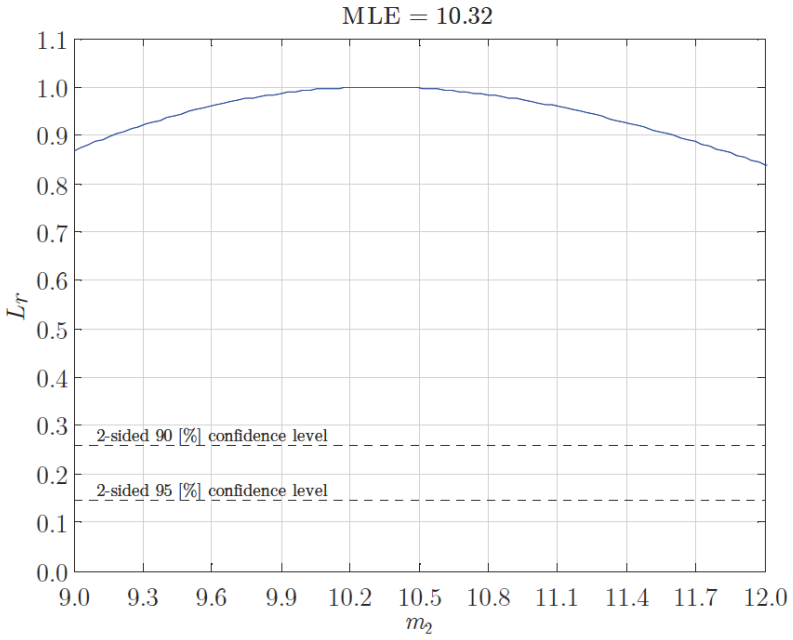

Figure 10.69: Profile likelihood graph slope m_2 of dual slope approach [4]

One step further when the HCF slope goes to infinity the continuous dual slope model changes in the random fatigue limit. The fatigue limit is a stochastic variable $S_\infty(\mu,\sigma)$. This means that one cannot simply calculate the fatigue limit and draw the curve. The $S_T N$ curve is known and depending on a joint probability density function of two random variables with a different distribution. The stress is due to the fatigue limit Weibull distributed and the life time is normally distributed.

Considering the fact that Alufastship is a design tool, the focus is on the design curves i.e the R95C95 curves of the different approaches. The single slope would be an interesting option to use because of its simplicity. The drawback of this option is that the validity is limited because not all the fatigue resistance data is used. only 772 of the 911 data points are used i.e. all data with $N < 5 \cdot 10^6$. However when the IIW definition is adopted the transition point between MCF and HCF changes and all data is used.

The dual slope approach adopted in [4] is a precarious option due to the uncertainty in the MCF-HCF region. An option to do use a dual slope approach is to perform a new regression with the fatigue resistance data and adopt a piece wise linear dual slope curve rather than the continuous one used in [4]. In the piece wise

linear dual slope formulation both curves would have a dedicated variance to account for the uncertainty in the MCF-HCF region.

The most favourable alternative would be to use the RFL approach. Looking at the complex formulation this may seem contradictory. When looking at the R95C95 design curve, one can see that it can be approximated by a single slope without having much error. See figure 10.70 for The R95C95 RFL curve and the linearized design curve in one graph. Note that for curves with lower reliabilities the fatigue limit becomes more dominant and it cannot be assumed by a linear curve anymore but since for design purposes only the R95C95 curve is important the linearized curve will suffice.

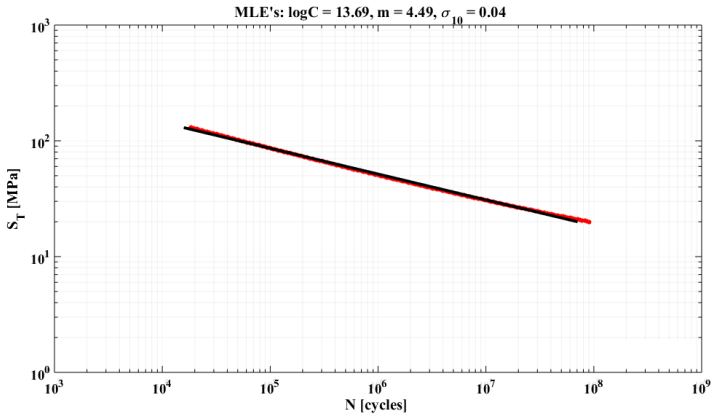

Figure 10.70: Linearized R95C95 RFL curve

10.2.1. Assumptions regarding fatigue resistance

In the previous section the linearized RFL curve is introduced. Note that this curve is a $S_T N$ curve. To calculate the fatigue resistance of a specific welded joint the total stress curve has to be converted to a nominal stress curve. There is a lot more input necessary to calculate the total stress than there is input necessary using a certain GL FAT class. For simplicity one can reason that more necessary input makes the method more complex and less generic to use. To avoid that, assumptions are made regarding standard dimensions of welded joints. In table 10.17 typical dimensions for standard welded joints are shown.

Table 10.17: Typical dimensions standard Damen details

Parameter	**Value**
t_b [mm]	8.0
t_c [mm]	8.0
l_w (butt joint) [mm]	10.0
l_w (other) [mm]	8.0
h_w (butt joint) [mm]	1.5
h_w (other) [mm]	8.0

A MATLAB script is made to be able to extract dedicated *SN* curves from the program to use in *Alufastship*. It is also possible to make a comparison with a certain FAT class from GL. In appendix E some screenshots are shown of this program.

10.2.2. Consequences of the implementation of the TS concept

During the start of this research the hypothesis was that when the TS concept would be adopted, the fatigue resistance would increase with respect to the fatigue resistance of the GL *SN* curves. There is looked for ways to quantify this.

The most intuitive way to quantify the difference between the curves is to plot them together in one graph. However the dependent variable in the TS concept is the total stress parameter S_T and in the GL curves the nominal stress S_N. Therefore the *SN* curves from GL are translated to $S_T N$ curves by calculating the total stress parameter for every detail. In figure 10.71 the converted GL curves together with the R95C95 RFL curve are plotted. Note that the GL curves are almost in line with each other on S_T scale while on nominal stress

scale the different FAT classes are separated from each other. This graph indicates already that the fatigue resistance is higher for the RFL curve but it cannot be stated for sure since judging only this curve one cannot assess the contribution of the damage below the cutoff of the GL curves.

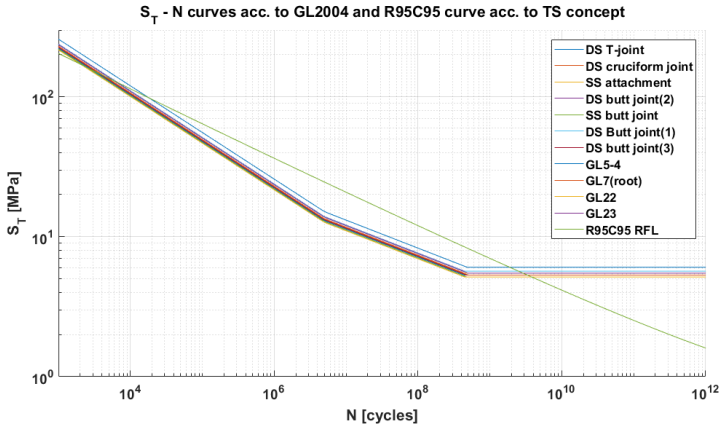

Figure 10.71: Comparison between $S_T N$ curves of GL and the RFL curve obtained from the TS concept

To find out the real effect on the fatigue resistance of welded joints a comparison is made on basis of accumulated fatigue damage. For this, the standard Weibull spectrum with 85 MPa as the once in a lifetime stress range is used and shape factor $k = 1$. In figure 10.72 the damage calculated for an arbitrary aluminium welded joint is shown for both the GL and the TS approach. Here can be seen that the factor on lifetime effectively equal is to $D_{GL}/D_{TS} \approx 10$. Note that for the left two curves the x-axis indicates damage and for the three curves on the right it indicates a number of cycles.

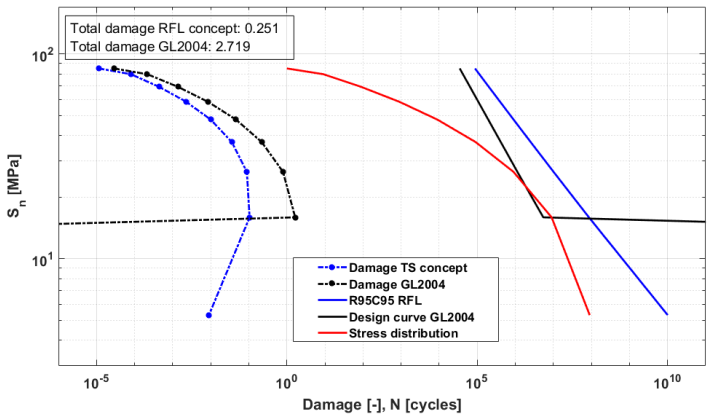

Figure 10.72: Fatigue damage calculation for GL2004 and TS concept us a standard Weibull stress spectrum with $\sigma_0 = 85$ MPa

10.3. Conclusion

After first investigating the current practices regarding fatigue lifetime predictions at Damen Shipyards, the effect of implementing the TS concept is assessed. With basic analysis it has been found that the effect on fatigue resistance for aluminium welded joints on board of HSC can be huge. This implies that the lifetime of the HSC is longer than expected and thus that material can be saved for new built HSC. It has been found that a factor ten on lifetime can be achieved when the fatigue resistance curves from the TS concept will be implemented.

11

Conclusions and Recommendations

11.1. Conclusions

A pragmatic application of the TS concept, developed during the VOMAS JIP, is presented in this thesis. At the start of this project there were a few objectives to meet, here the results and conclusions will be discussed.

To develop a low cost and simple to produce and install sensor, able to accelerate fatigue damage on board of HSC to give early fatigue damage information.
A low-cost and easy to install sensor to predict the remaining fatigue lifetime of aluminium HSC is developed. Since the TS concept is adopted as a fatigue resistance approach, it means that when similarity is proven with one welded joint type from the TS concept, the predictions can be translated to any welded joint detail. The sensor is designed in a way that the notch angle is similar to the weld angle of a DS cruciform joint. Figure 11.74 shows the final design of the fatigue damage sensor and an schematic explanation of the ideas behind the design.

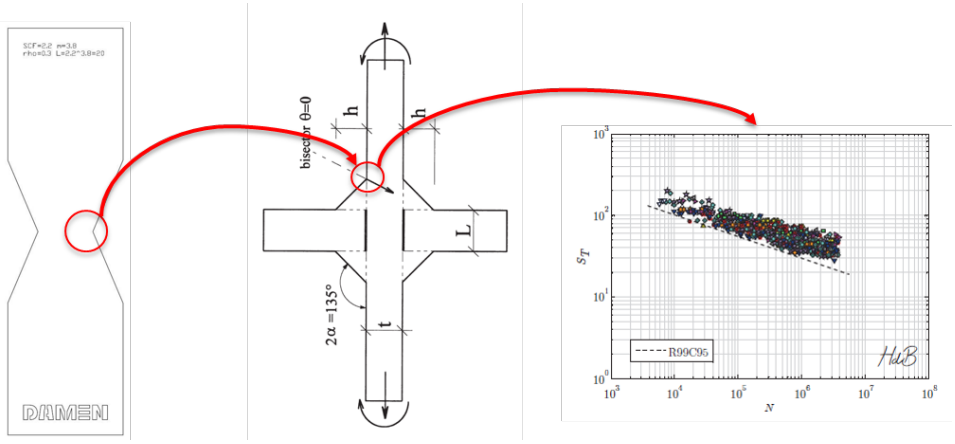

Figure 11.74: Final design fatigue damage sensor

The width reduction ensures the acceleration of the fatigue damage by raising the nominal stress locally with respect to the underlying structure. The sensor will be bonded to the hull, preferably at a high stressed location to get feedback as early as possible. Caution must be exercised to prevent the nominal stress in the sensor to exceed the yield stress of the material.

The verification and validation of the method by doing laboratory tests for similarity in the fatigue mechanisms using the total stress concept.
Through fatigue experiments similarity in fatigue resistance characteristics between the developed fatigue damage sensor and a double sided cruciform joint from the TS concept is found. Because of this, the stochas-

tic parameters defined in the TS concept can be used to calculate the fatigue resistance of the sensor. At low stresses the tests are stopped before the failure. This is because these tests are very time consuming and the fatigue testing facility was available for only a limited time frame. At low stresses typically a large scatter is found, the interrupted tests were still within the scatter bands of the RFL model.

Simultaneously to the laboratory experiments, the conceptual design of the fatigue damage sensor is tested on board of the USCGC 'Bertholf' as part of a long-term fatigue life assessment project of MARIN. The goal of these full scale trials of the sensor is mainly the testing of the provided installation and inspection procedures and to verify the applied bonding method in a harsh environment i.e. the ship's hull. After six months MARIN returned to the vessel, the sensor and adhesive layer were still intact and lessons are learned regarding the installation and inspection procedures.

To describe how to make a reliable prediction of the remaining lifetime of the vessel, based on one or multiple failed sensors.
To make a statement about the probability of the structural detail exceeding a certain lifetime, joint probability distributions between the lifetime of the sensor and of the structure had to be made. To calculate numerous combinations of the lifetime of the sensor and the structural lifetime Monte Carlo simulations were performed. Hereby random combinations of SN curves were drawn to calculate the corresponding lifetime with an encountered fatigue loading based on a probabilistic operational profile and long-term stress spectrum.

To investigate the implementation of the total stress concept in the Damen fatigue prediction methods
Currently the fatigue resistance curves from GL [10] are used in the fatigue assessment of HSC at Damen Shipyards. A comparative study is performed to indicate the effects on the fatigue resistance of welded joints when the TS concept would be adopted. The result of this study is that lifetime extensions of a factor ten, or corresponding reductions of the section modulus, are possible.

11.2. Recommendations

Extensive fatigue testing sensor
For this thesis a total of nine experiments are performed to indicate the similarity between the fatigue damage sensor and a DS cruciform joint. When this sensor design will be actually applied it may be worthwhile to do more extensive testing to be able to produce an SN curve from the measured data. Since the sensors can be made with very low building tolerances and there are no welds that provide a high scatter it can be assumed that the standard deviation on lifetime is lower than the one in the TS concept. With a lower standard deviation on the lifetime of the sensor, the predictions on the lifetime of the underlying structure can me made more reliable.

Testing of sensor adhesive combination
Tests should also be performed with the sensor bonded to a plate. These tests can be static to investigate with the help of strain gauges what load exactly is transferred from the plating into the sensor. If deemed necessary, fatigue tests with the sensor bonded on a base plate can be performed to investigate the influence of the adhesive layer on the fatigue damage in the sensor and next to that to test the fatigue resistance of the adhesive layer.

Remote fatigue loading monitoring
In this research is shown that when the TS concept will be implemented in the fatigue prediction methods used at Damen Shipyards, the fatigue resistance will be much higher. Another way to extend the predicted lifetime or with other words reduce the structural weight, keeping the same lifetime, is to make more reliable predictions of the fatigue loading. The fatigue loading and operational profile are random variables. With new techniques, it becomes easier to monitor vessels during their lifetime. This data can be used to make more reliable prediction for new build vessels.

Bibliography

[1] B. Boon and S. Hylarides. *College dictaat MT832 Construeren en sterkte 3*. TU Delft, 2003.

[2] M. D. Byrne. How many times should a stochastic model be run? an approach based on confidence intervals, 1963.

[3] F. M. Dekking, C. Kraaikamp, H. P. Lopuhaä, and L. E. Meester. *A Modern Introduction to Probability and Statistics*. Springer-Verlag London, 2005.

[4] J. H. den Besten. *Fatigue resistance of welded joints in aluminium high-speed craft: A TOTAL STRESS CONCEPT*. PhD thesis, Delft University of Technology, 2015.

[5] J. H. den Besten. Fatigue and fracture in marine structures. lecture series at delft university of technology., 2016-2017.

[6] J. H. den Besten and R. H. M. Huijsmans. Fatigue of high-speed aluminium ships: A master curve formulation, 2011.

[7] I. Drummen. Description valid project, 1999. URL `http://www.marin.nl/web/JIPs-Networks/Archive-JIPs-public/Valid.htm`.

[8] I. Drummen. Description valid ii project, 2015. URL `http://www.marin.nl/web/JIPs-Networks/JIPs-public/VALID-II.htm`.

[9] I. Drummen, R. Hageman, and M. Schiere. Valid jip - analysis report, 2013.

[10] *GL 2004: Pt.1 Sec.20 Fatigue Strength*. Germanischer Lloyd, 2004.

[11] A. F. Hobbacher. *Recommendations for fatigue design of welded joints and components*. Springer, 2016.

[12] L. H. Holthuijsen. *Waves in oceanic and coastal waters*. Cambridge university press, 2007.

[13] O.F. Hughes and J.K. Paik. *Ship structural analysis and design*. The society of naval architects and marine engineers, 2010.

[14] *Technical data sheet Araldite 2021-1*. Huntsman advanced materials, .

[15] *User's guide adhesives technology*. Huntsman advanced materials, .

[16] S. R. Ignatovich, A. Menou, M. V. Karuskevich, and P. O. Maruschak. Fatigue damage and sensor development for aircraft structural health monitoring. *Theoretical and Applied Fracture Mechanics*, 65:23–27, 2013.

[17] M. F. Kanninen and C. H. Popelar. *Advanced fracture mechanics*. Oxford University Press, 1985.

[18] H. Kleinert, F. Dotschko, and B. Purche. Calculating the strength of metal to metal bonded lap joints through the experimental determination of adhesive factors. *Welding international*, 4:2, 1990.

[19] C. Lalanne. *Mechanical vibration and shock analysis - Fatigue Damage*. John Wiley & Sons Inc., 2002.

[20] T. Lassen and N. Récho. *Fatigue Life Analyses of Welded Structures*. ISTE Ltd, 2006.

[21] P. Lazzarin and P. Livieri. Notch stress intensity factors and fatigue strength of aluminium and steel welded joints. *International journal of fatigue*, pages 225–232, 2000.

[22] Y. Lee, J. Pan, and R. Hathaway. *Fatigue Testing and Analysis - Theory and Practice*. Elsevier, 2005.

[23] MARIN. Presentation: Stratton installation and results, 2017.

[24] P. W. Marshall and R. D. Larrabee. The cognac fatigue experiment. *Offshore Technology Conference*, 15: 83–93, 1983.

[25] N/A. Damen company information.

[26] D. Radaj, C. M. Sonsino, and W. Fricke. *Fatigue assessment of welded joints by local approaches*. Woodhead Publishing Ltd, 2006.

[27] M. P. Savruk and A. Kazberuk. *Stress concentration at notches*. Springer, 2017.

[28] J. Schijve. *Fatigue of Structures and Materials*. Springer, 2009.

[29] W. Schütz. Fatigue strength of single shear riveted joints of aluminum alloys, 1963.

[30] G. Segers. Validation "alufastship" mathcad application, 2004.

[31] H. Tada, P. C. Paris, and G. R. Irwin. *The stress analysis of cracks handbook*. ASME press, 2000.

[32] Y. Takaoka, K. Nihei, P. Vargas, P. Aalberts, and M. L. Kaminski. In *Application of Fatigue Damage Sensors in the Monitas System*. Offshore Technology Conference, 2010.

[33] M. L. Williams. Stress singularities resulting from various boundary conditions in angular corners of plates in extension. 1952.

A

Sensor installation procedure

1. Check whether adhesive has not expired and whether it has been stored under the right conditions. In case you have any doubts about the quality of the adhesive, do not proceed.

2. Check whether environmental conditions are suited for bonding (valid for all Damen standard adhesives):

    - Temperature window: 5°C to 35°C
    - b. Humidity: 40% to 85% (according to paint spec from International Paint (`http://www.yachtpaint.com/sgp/diy/ask-the-experts/whether-to-paint-depends-on-the-weather.aspx`; adhesion of paint and adhesives rely on similar chemical processes)
    - Minimum 3 degrees above dew point

3. Wear gloves and safety glasses while working with adhesives and solvents

4. Degrease both the sensor and the part of the ship's hull where it has to be applied with Isopropanol or acetone. Use paper towels and degrease by sweeping in one direction (avoid making circular motions as this will only spread the dirt around). Keep on degreasing until paper towel remains white.

5. Remove paint surface around the preferred location of the sensor, see figure A.76. Abrade surfaces thoroughly to remove the brittle oxide layer (P180), see figure A.77.

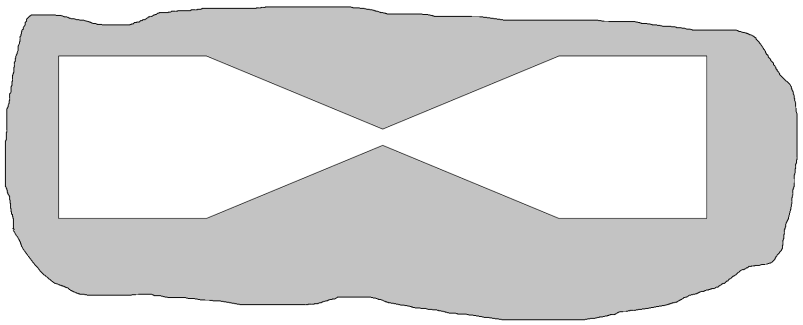

Figure A.76: Remove paint around sensor

Figure A.77: Abraded surface should look dull

6. Remove the dust from the abrading process using a vacuum cleaner. In case there is a long waiting time before the bonding process taking place cover the substrates to avoid contamination by dust or other particles.

7. Degrease a second time prior to bonding according to the same procedure as in step 4. Wait 15 min to allow solvent to evaporate.

8. Apply adhesive:

    - Apply per sensor 4 small pieces of double sided tape (5mm thick) to fix the adhesive thickness and keep it in place while curing. See figure A.78.
    - Dispose the first bit of adhesive coming out of the mixer until a mixture with a uniform color comes out (pale yellow).

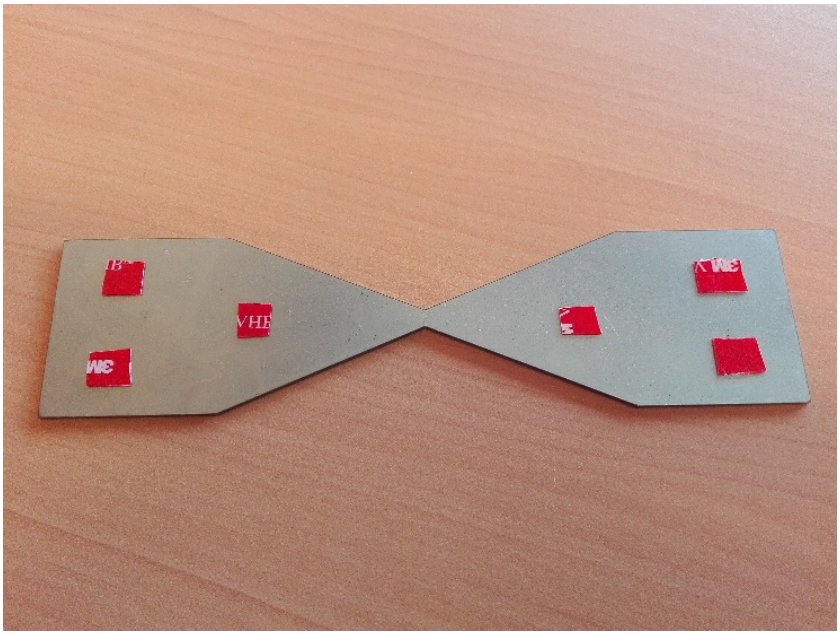

Figure A.78: Double sided tape on sensor

- Apply approximately 1mm thick adhesive on sensor. From 1 tube, approximately 5 sets of sensor can be bonded, so use about 1/5 of a tube for a set of two sensors.
- The maximal processing time at 20°C is around 5 mins. For every 10°C in temperature rise the open time of the adhesive is halved.
- Locate the sensor in the direction parallel to the longitudinal strain gauge. Press the sensor on the ship's hull until it reaches the double sided tape and fixate it during curing.
- Finish bondline using a finger, putty knife or piece of PVC pipe, see figure A.79. Remove adhesive squeeze-out before it is cured. All tools should be cleaned with solvent before adhesives residues have had time to cure.
- Depending on the temperature, cure the adhesive according to figure A.80.

Temperature	°C	10	15	23	40
Cure time to reach	hours	-	-	-	-
LSS > 1MPa	minutes	20	13	9	2
Cure time to reach	hours	-	-	-	-
LSS > 10MPa	minutes	30	19	13	6

Figure A.79: Curing time for different temperatures

Figure A.80: Finishing of bondline

9. When you are finished working, make sure to wash your hands properly before eating and or smoking.
10. Seal the edges using sealant and conserve the bare material with paint
11. Write the installation date on the sensor with a permanent marker

B

Derivation of σ_{nm}

In this appendix the formulation of the notch stress assuming a pure membrane loading and a first order weld carrying stress will be derived according to [4]. The welded joint is assumed to be symetric which is the case by for example a DS cruciform joint.

First the total formulation of the notch stress will be given in equation B.1. Then the derivation of the seperate parts will be given.

$$\sigma_{nm}\left(\frac{r}{t_p}\right) = \sigma_s \cdot \left[\left(\frac{r}{t_p}\right)^{\lambda_s - 1} \mu_s \lambda_s (\lambda_s + 1)[cos((\lambda_s + 1)\beta) - \chi_s cos((\lambda_s - 1)\beta)] + \left(\frac{r}{t_p}\right)^{\lambda_a - 1} \mu_a \lambda_a (\lambda_a + 1)[sin((\lambda_a + 1)\beta) - \chi_a sin((\lambda_a - 1)\beta)] + C_{bw}\left(4\left(\frac{r}{t_p}\right) - 1\right)\right. \tag{B.1}$$

Only $0 \leq \left(\frac{r}{t_p}\right) \leq \frac{1}{2}$ is considered for the calculation of the stress amplitudes μ_s and μ_a. Since the welded joint is assumed to be symmetric this suffices. To get these parameters, three equations have to be solves. From equation B.2 till B.4 respectively force equilibrium, moment equilibrium and a symmetry constraint.

$$\int_0^{\frac{1}{2}} \left(\sigma_{nm}\left(\frac{r}{t_p}\right)\right) \quad d\left(\frac{r}{t_p}\right) = \int_0^{\frac{1}{2}} \sigma_s \quad d\left(\frac{r}{t_p}\right) \tag{B.2}$$

$$\int_0^{\frac{1}{2}} \left(\sigma_{nm}\left(\frac{r}{t_p}\right)\right) \cdot \left(\frac{r}{t_p}\right) \quad d\left(\frac{r}{t_p}\right) = \int_0^{\frac{1}{2}} \sigma_s \cdot \left(\frac{r}{t_p}\right) \quad d\left(\frac{r}{t_p}\right) \tag{B.3}$$

$$\frac{d\sigma_{nm}\left(\frac{r}{t_p}\right)}{d\left(\frac{r}{t_p}\right)} = 0 \quad \text{for} \quad \left(\frac{r}{t_p}\right) = \frac{1}{2} \tag{B.4}$$

Rewriting this integral in matrix form to get a system of equations to solve gives:

$$\begin{bmatrix} C_{11} & C_{12} \\ C_{21} & C_{22} \\ C_{31} & C_{32} \end{bmatrix} \cdot \begin{vmatrix} \mu_s \\ \mu_a \end{vmatrix} = \begin{vmatrix} F_1 \\ F_2 \\ F_3 \end{vmatrix} \tag{B.5}$$

With the C and F entries as follows:

$$C_{11} = \left(\frac{1}{2}\right)^{\lambda_s} (\lambda_s + 1) \cdot [cos((\lambda_s + 1)\beta) - \chi_s \cdot cos((\lambda_s - 1)\beta)] \tag{B.6}$$

$$C_{12} = \left(\frac{1}{2}\right)^{\lambda_a} (\lambda_a + 1) \cdot [sin((\lambda_a + 1)\beta) - \chi_a \cdot sin((\lambda_a - 1)\beta)]$$

$$C_{21} = \left(\frac{1}{2}\right)^{\lambda_s + 1} \lambda_s \cdot [cos((\lambda_s + 1)\beta) - \chi_s \cdot cos((\lambda_s - 1)\beta)]$$

$$C_{22} = \left(\frac{1}{2}\right)^{\lambda_a+1} \lambda_a \cdot [sin((\lambda_a+1)\beta) - \chi_a \cdot sin((\lambda_a-1)\beta)]$$

$$C_{31} = \left(\frac{1}{2}\right)^{\lambda_s-2} \lambda_s(\lambda_s+1)(\lambda_s-1) \cdot [cos((\lambda_s+1)\beta) - \chi_s \cdot cos((\lambda_s-1)\beta)]$$

$$C_{32} = \left(\frac{1}{2}\right)^{\lambda_a-2} \lambda_a(\lambda_a+1)(\lambda_a-1) \cdot [cos((\lambda_a+1)\beta) - \chi_s \cdot cos((\lambda_a-1)\beta)]$$

$$F_1 = \frac{1}{2}$$

$$F_2 = \frac{1}{8} - \frac{C_{bw}}{24}$$

$$F_3 = -4C_{bw}$$

In [4] a least square solution for this system was found, see equation B.7 and B.8.

$$\mu_s = \frac{\left(\frac{1}{2}\right)\lambda_a(\lambda_a-1) + C_{bw}}{\left(\left(\frac{1}{2}\right)^{\lambda_s}(\lambda_s+1) \cdot (\lambda_a(\lambda_a-1) - \lambda_s(\lambda_s-1))\right) \cdot [cos((\lambda_s+1)\beta) - \chi_s \cdot cos((\lambda_s-1)\beta))]} \tag{B.7}$$

$$\mu_s = \frac{\left(\frac{1}{2}\right)\lambda_s(\lambda_s-1) + C_{bw}}{\left(\left(\frac{1}{2}\right)^{\lambda_a}(\lambda_a+1) \cdot (\lambda_a(\lambda_a-1) - \lambda_s(\lambda_s-1))\right) \cdot [sin((\lambda_a+1)\beta) - \chi_a \cdot sin((\lambda_a-1)\beta))]} \tag{B.8}$$

C

Derivation Y_f and Y_n for a DS cruciform joint

C.1. Far field factor Y_f

According to [4], the far field factor Y_f for a single edge crack in a DS cruciform joint is defined as:

$$Y_f = Y_{fm} - r_s(Y_{fm} - Y_{fb}) \tag{C.1}$$

With for Y_{fm} and Y_{fb} the following approximations are derived by [31] with an error less than 0.5%:

$$Y_{fm}\left(\frac{a}{t_p}\right) = \sqrt{\left(\frac{2}{\pi}\right) tan\left(\frac{\pi}{2}\cdot\frac{a}{t_p}\right)}\cdot\frac{0.752+2.20\left(\frac{a}{t_p}\right)+0.370\left(1-sin\left(\frac{\pi}{2}\cdot\frac{a}{t_p}\right)\right)^3}{\sqrt{\left(\frac{a}{t_p}\right)}cos\left(\frac{\pi}{2}\cdot\frac{a}{t_p}\right)} \tag{C.2}$$

$$Y_{fb}\left(\frac{a}{t_p}\right) = \sqrt{\left(\frac{2}{\pi}\right) tan\left(\frac{\pi}{2}\cdot\frac{a}{t_p}\right)}\cdot\frac{0.923+0.199\left(1-sin\left(\frac{\pi}{2}\cdot\frac{a}{t_p}\right)\right)^4}{\sqrt{\left(\frac{a}{t_p}\right)}cos\left(\frac{\pi}{2}\cdot\frac{a}{t_p}\right)} \tag{C.3}$$

C.2. Notch factor Y_n

The notch factor fopr a symmetrical welded joint like a DS cruciform joint according to [4] is defined as formulated in equation C.4.

$$Y_n\left(\frac{a}{t_p}\right) = \left(\frac{2}{\pi}\right)\left(\left(1-2r_s\left(1-f_1\right)\right)\cdot f_2 + r_s\left(2f_1-1\right)\left(\left(1-f_1\right)\left(\frac{\pi}{2}\right)-2\left(\frac{a}{t_p}\right)\right)+2r_s\left(\frac{a}{t_p}\right)\right) \tag{C.4}$$

The sub functions $f_1\left(\frac{a}{t_p}\right)$ and $f_2\left(\frac{a}{t_p}=\frac{1}{2}\right)$ are formulated below in equation C.5 and C.6:

$$f_1\left(\frac{a}{t_p}=\frac{1}{2}\right) = \frac{(\lambda_a-\lambda_s)(\lambda_s\lambda_a-2C_{bw})}{\lambda_a(\lambda_a-1)-\lambda_s(\lambda_s-1)}+C_{bw} \tag{C.5}$$

$$\begin{aligned} f_2\left(\frac{a}{t_p}\right) = {} & \left(\frac{a}{t_p}\right)^{\lambda_s-1}\mu_s\left(\frac{\sqrt{\pi}}{2}\right)\frac{\Gamma\left(\frac{\lambda_s}{2}\right)}{\Gamma\left(\frac{\lambda_s+1}{2}\right)}\lambda_s(\lambda_s+1)\cdot(cos((\lambda_s+1)\beta)-\chi_s cos((\lambda_s-1)\beta))+ \\ & \left(\frac{a}{t_p}\right)^{\lambda_a-1}\mu_a\left(\frac{\sqrt{\pi}}{2}\right)\frac{\Gamma\left(\frac{\lambda_a}{2}\right)}{\Gamma\left(\frac{\lambda_a+1}{2}\right)}\lambda_a(\lambda_a+1)\cdot(cos((\lambda_a+1)\beta)-\chi_a cos((\lambda_a-1)\beta))+ \\ & C_{bw}\left(4\left(\frac{a}{t_p}\right)-\frac{\pi}{2}\right) \end{aligned} \tag{C.6}$$

D

Sensor inspection procedure

Monthly inspection

1. Check whether the bonding is intact, i.e. no cracks or loosening of the adhesive layer.

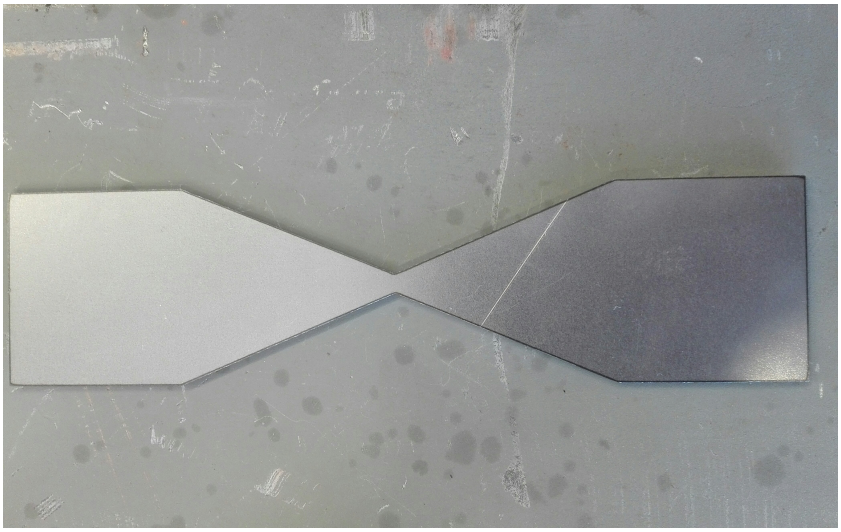

Figure D.84: Intact sensor

2. Check the notches for cracks. One side of the sensor has completely failed if the crack has grown through the complete width.
3. Write the failure date on the concerned side of the sensor and report it to Damen.
4. Keep inspecting monthly for the other sensor in case of a parallel sensor

E

MATLAB script to extract *SN* curves based on TS concept

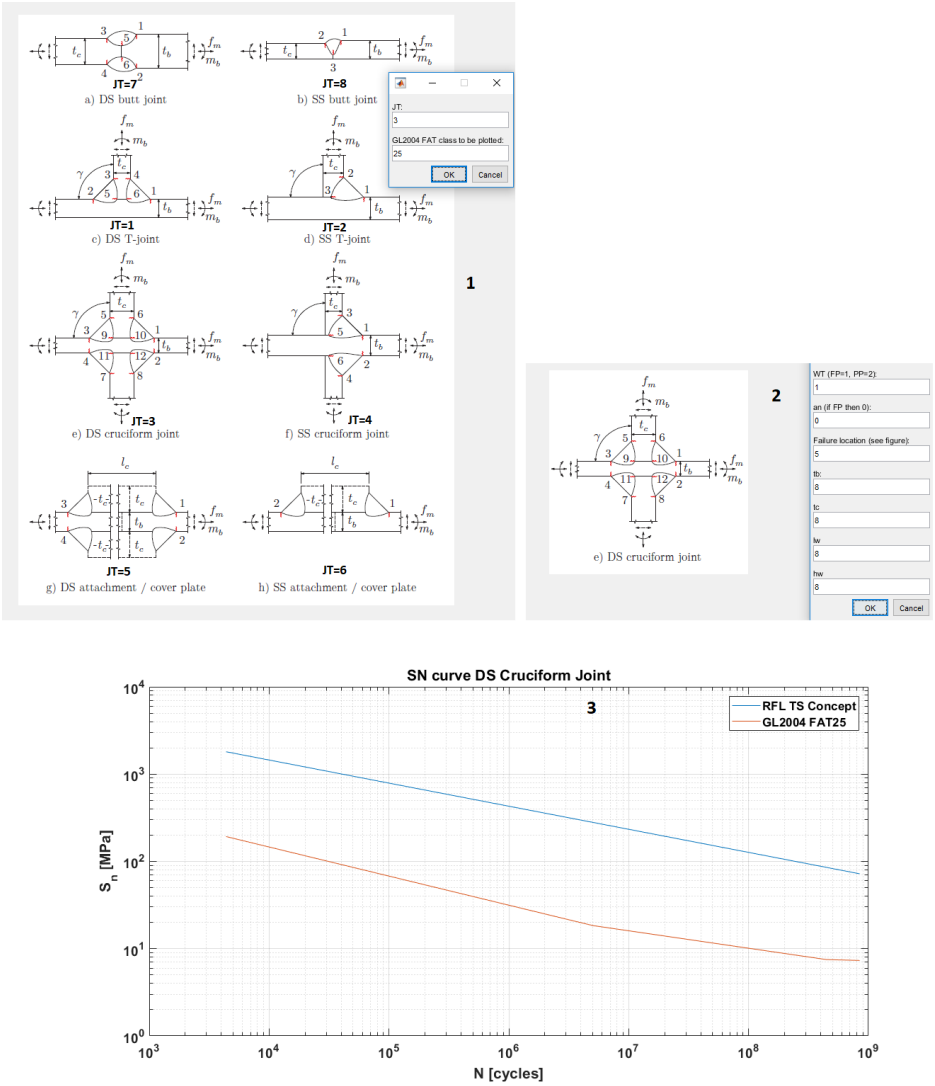

Figure E.86: Screenshots from MATLAB script. 1: To enter the joint type and the relevant GL FAT class. 2: To enter the relevant dimensions of the considered joint. 3: The output, an *SN* curve

F

Commonly applied welded joints

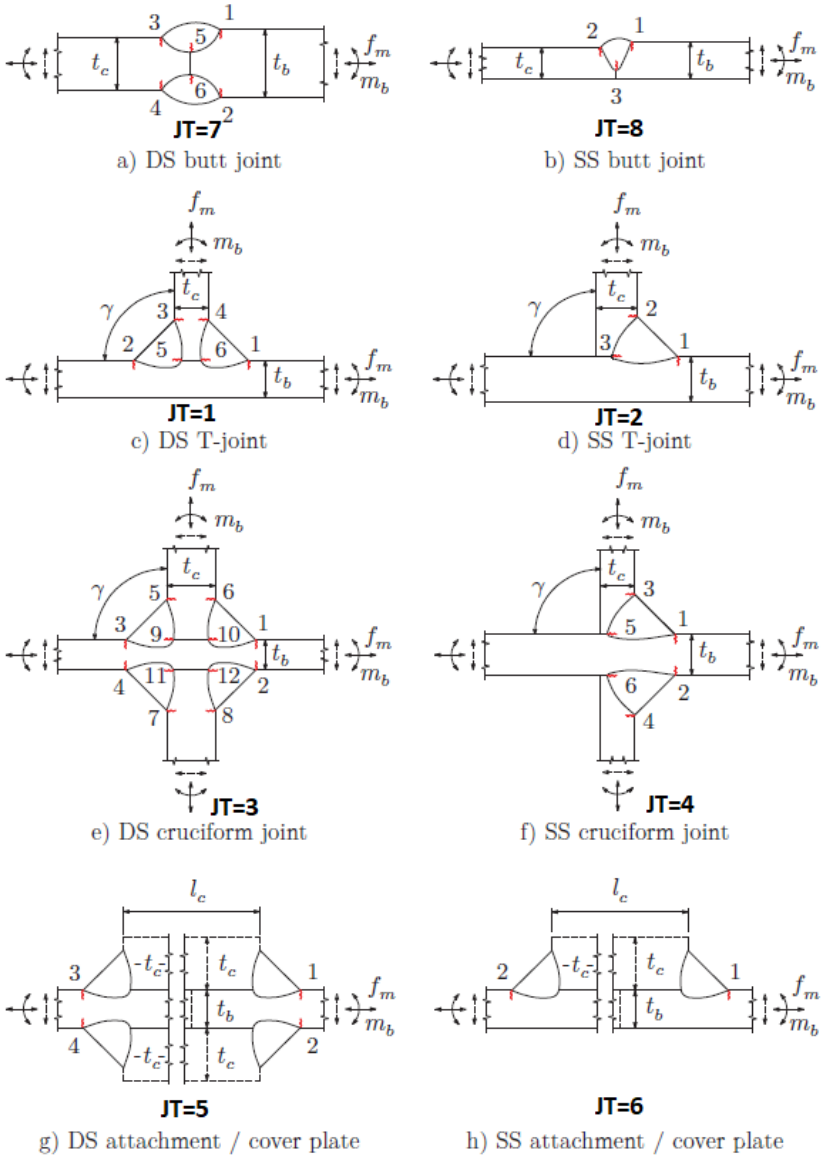

Figure F.88: Commonly applied welded joints implemented in TS concept